THE JOURNAL
OF
CHEMICAL PHYSICS

VOLUME 8 JULY, 1940 NUMBER 7

An Experimental Study of the Near Ultraviolet Absorption Spectrum of Benzene*

W. F. RADLE AND C. A. BECK
Department of Physics, The Catholic University of America, Washington, D. C.

(Received April 23, 1940)

The wave numbers and relative intensities of 500 of the absorption bands of benzene vapor in the 2600A region have been determined. A detailed study has been made of the variation of intensity with temperature of the main band of the *A*, *B*, and *D* progressions. These three bands have been assigned to the ground state, the 606-cm^{-1} and 2×606-cm^{-1} vibrational states, respectively, by Sponer and collaborators. The experimental data are in good agreement with a statistical calculation of the population factors for these states.

INTRODUCTION

THE known electronic spectrum of benzene lies in two regions of the ultraviolet, one at 2600A and the other at 2000A. The latter is the stronger and has been investigated in absorption by Henri[1] and Carr and Stücklen[2] and more recently by Price and Tutte.[3] The last two investigations show that the 2000A region, in reality, consists of two regions, one at 2040A and a very strong one at 1850A.

The 2600A region has been studied in emission,[4] fluorescence,[5] and absorption,[1,6] the latter in both the liquid and vapor state. This band system in absorption is a relatively weak one. In contrast to the diffuse character of the absorption bands in the vapor at 2000A, those in the 2600A region exhibit considerable structure. Henri[1] has published the wave-lengths of about 75 of the stronger bands. Almasy and Shapiro[7] list about 110 bands between 35,346 cm^{-1} and 38,121 cm^{-1} obtained at higher vapor concentrations. Kronenberger[8] has extended the investigation of benzene absorption to the solid phase at -259°C and has measured the wave-lengths of about 250 of the bands.

A theoretical study of the electronic levels of benzene has been made by Hückel,[9] Pauling and Sherman,[10] Sklar,[11] and Goeppert-Mayer and Sklar.[12] They have investigated the nature and

* A dissertation submitted in partial fulfillment of the requirements for the Degree of Doctor of Philosophy (1940) at the Catholic University of America and reproduced here in a partly revised and extended form by the permission of the university authorities.

[1] V. Henri, J. de phys. et rad. (6) **3**, 181 (1922) and *Structure des Molécules* (Hermann, Paris, 1925), p. 108.

[2] E. P. Carr and H. Stücklen, J. Chem. Phys. **6**, 55 (1938).

[3] W. C. Price and W. T. Tutte, Proc. Roy. Soc. **174**, 207 (1940).

[4] J. B. Austin and I. A. Black, Phys. Rev. **35**, 452 (1930).

[5] G. B. Kistiakowsky and A. Nelles, Phys. Rev. **41**, 595 (1932); G. R. Cuthbertson and G. B. Kistiakowsky, J. Chem. Phys. **4**, 9 (1936); C. K. Ingold and co-workers, J. Chem. Soc. p. 912 (1936).

[6] R. Witte, Zeits. f. Wiss. Phot. **14**, 347 (1915); K. Schulz, Zeits. f. Wiss. Phot. **20**, 1 (1920); G. B. Kistiakowsky and A. K. Solomon, J. Chem. Phys. **5**, 609 (1937); A. Ionescu, Comptes rendus Acad. Roum. **2**, 39 (1937).

[7] F. Almasy and C. V. Shapiro, Zeits. f. physik. Chemie **B25**, 391 (1934).

[8] P. Pringsheim and A. Kronenberger, Zeits. f. Physik **40**, 75 (1926); A. Kronenberger, *ibid.* **63**, 494 (1930).

[9] E. Hückel, Zeits. f. Physik **70**, 204 (1931); Zeits. f. Elektrochem. **43**, 752 (1937).

[10] L. Pauling and A. Sherman, J. Chem. Phys. **1**, 606, 679 (1933).

[11] A. L. Sklar, J. Chem. Phys. **5**, 669 (1937).

[12] M. Goeppert-Mayer and A. L. Sklar, J. Chem. Phys. **6**, 645 (1938).

TABLE I.

WAVE NUMBERS (VAC.)	INTENSITY	ASSIGNMENT
36,158	1 (*a*)	
36,174	1 (*a*)	
36,233	1 (*b*)	
36,254	1 (*a*)	
36,317.2	2	$F_0^1; B_{-1}^1$
36,334.6	1	
36,342	1 (*a*)	
36,351	1 (*a*)	
36,387.8	2	
36,413.7	2	
36,478.0	3	$F_0^0; B_{-1}^0$
36,496.2	4	
36,510	1 (*b*)	
36,526	1 (*b*)	
36,538	1 (*a*)	
36,624.7	3	A_{-2}^0
36,657	1 (*a*)	
36,668	1 (*a*)	
36,699	1 (*a*)	
36,750	1 (*a*)	
36,772	1 (*a*)	
36,823.7	2	
36,834	2 (*a*)	
36,841	2 (*a*)	B_0^4
36,857	1 (*a*)	
36,866	1 (*a*)	
36,886	1 (*a*)	
36,899	2 (*a*)	
36,905.9	2	
36,925	1 (*b*)	
36,990.7	8	
37,000.9	8	B_0^3
37,016.1	4	
37,048.1	5	
37,057.3	5	
37,064	5 (*b*)	
37,068	5 (*b*)	
37,071.4	4	
37,076	4 (*a*)	
37,081	4 (*a*)	
37,156.8	25	B_0^2
37,160.4	25	
37,216.7	18	
37,230.2	21	D_0^1
37,234.1	6	
37,237.9	6	
37,289.9	9	
37,296	5 (*b*)	
37,303	7 (*a*)	
37,316	9 (*a*)	
37,321.1	140	B_0^1
37,326.8	12	
37,330.0	4	
37,335	4 (*a*)	
37,350	4 (*a*)	
37,366	4 (*a*)	
37,387.8	7	D_0^0
37,392.9	55	
37,402.4	7	
37,452.5	25	
37,457.3	12	
37,476.1	25	B_0^0
37,481.9	420	
37,489.7	30	
37,498	4 (*a*)	
37,524	7 (*a*)	
37,527.4	4	
37,532.6	4	
37,544	7 (*a*)	
37,568.9	4	
37,611.7	10	
37,616.8	85	A_{-1}^0
37,626.2	4	
37,632	4 (*a*)	
37,640	4 (*a*)	
37,651.4	10	
37,656.5	4	
37,663	4 (*a*)	
37,678	5 (*a*)	
37,714.1	12	
37,766.8	25	
37,795.4	12	
37,814.0	7	
37,822.8	9	
37,836.9	12	
37,878.5	9	
37,915.6	6	
37,926.8	35	H_0^0
37,944.8	7	
37,956.5	18	
37,962.6	12	
37,967.8	25	
37,976	7 (*a*)	
37,981	7 (*a*)	
37,990.8	18	
38,000	5 (*a*)	
38,009	4 (*a*)	
38,021.4	9	
38,029.3	9	
38,043.8	30	
38,053	5 (*a*)	
38,064	5 (*a*)	
38,084.1	55	B_1^2
38,089.4	12	(origin)
38,112.9	30	
38,118.0	25	
38,121.8	25	
38,125.4	18	A_0^3
38,133.2	35	
38,141.3	30	
38,154.0	30	D_1^1
38,171.1	21	
38,182.5	25	
38,190.5	35	
38,204.3	55	
38,210.0	55	
38,245.4	160	B_1^1
38,253	21 (*a*)	
38,281.1	230	
38,285.2	210	A_0^2
38,292.3	170	
38,316.6	130	D_1^0
38,335	35 (*b*)	
38,343.3	190	
38,350.0	140	
38,359.7	250	C_0^1
38,365.2	160	
38,377	25 (*b*)	
38,401.8	55	B_1^0
38,407.0	550	
38,448.4	950	A_0^1
38,452.4	950	
38,478	25 (*a*)	
38,491.2	70	
38,517.5	210	C_0^0
38,523.0	620	
38,529.3	210	
38,562.4	140	
38,580	55 (*b*)	
38,607.5	620	A_0^0
38,612.2	7500	
38,640.2	9	
38,649.0	25	
38,655.0	25	
38,673.0	10	
38,691.5	15	
38,694	25 (*a*)	
38,699.5	12	
38,713	7 (*b*)	
38,718.7	12	
38,728	7 (*b*)	
38,738.1	12	
38,746.2	15	
38,753.1	9	
38,758.3	15	
38,766.9	21	
38,773.1	7	
38,777.7	7	
38,783.1	7	
38,790	9 (*a*)	
38,796.8	9	
38,801.4	9	
38,811	7 (*b*)	
38,828.1	9	
38,839.7	35	
38,851.5	35	
38,867.8	25	
38,870.8	12	
38,875.8	18	
38,880.1	21	
38,883.6	15	
38,891.3	25	
38,914	12 (*a*)	
38,919.9	55	
38,927.0	55	G_0^1
38,929.5	35	
38,943.7	18	
38,952.8	18	
38,967.0	30	
38,985	12 (*a*)	
38,995	12 (*a*)	
38,999.5	25	
39,010	25 (*a*)	B_2^2
39,038.6	170	
39,047.0	25	
39,056	25 (*a*)	A_1^3
39,063	25 (*a*)	
39,073.1	30	
39,082.0	250	G_0^0
39,086.8	250	
39,092.3	25	
39,100.2	25	
39,104.5	25	
39,114.9	35	
39,122	25 (*b*)	
39,124	25 (*b*)	C_1^2
39,134.2	130	
39,138.8	12	
39,147.2	21	
39,159	12 (*b*)	
39,163.1	21	B_2^1
39,168.5	130	
39,173.7	25	
39,204.5	280	A_1^2
39,209.3	230	
39,215.6	140	
39,230.8	55	
39,236.0	150	D_2^0
39,239.4	40	
39,248	25 (*b*)	
39,255.1	170	
39,265.5	170	
39,272.1	140	C_1^1
39,281.4	170	
39,287.7	130	
39,330.6	350	B_2^0
39,371.2	750	A_1^1
39,376.1	510	
39,393	55 (*a*)	
39,398.9	130	
39,408.6	55	E_0^1
39,423.1	160	
39,440.1	160	C_1^0
39,445.3	675	
39,451.0	335	
39,468	55 (*b*)	
39,473	55 (*b*)	
39,487.1	55	
39,529.6	1200	A_1^0
39,534.2	7000	
39,541.2	35	
39,552.2	55	
39,560.8	335	
39,565.3	35	E_0^0
39,568.7	250	
39,571.9	12	
39,577.5	25	
39,604	25 (*a*)	
39,614.4	25	
39,622.2	25	
39,627.6	15	
39,632.1	15	
39,638.2	335	
39,648.0	12	
39,651.2	12	
39,656.4	25	
39,669	12 (*a*)	
39,678	12 (*a*)	
39,685.9	12	
39,689.6	12	
39,697.2	25	
39,706.4	25	
39,715.1	25	
39,765.4	190	
39,774.3	25	
39,783.2	250	
39,793	15 (*a*)	
39,806	12 (*a*)	
39,814	15 (*a*)	
39,836	15 (*a*)	
39,841.5	55	
39,847.3	45	
39,850.7	70	
39,868	21 (*a*)	
39,889.0	15	B'^1_0
39,894.1	55	
39,906.3	21	
39,916.1	15	
39,921.3	15	
39,927.6	12	
39,962.1	120	
39,971.9	70	
39,981.0	40	
39,997	55 (*a*)	

TABLE I.—*Continued.*

WAVE NUMBERS (VAC.)	INTENSITY	ASSIGNMENT	WAVE NUMBERS (VAC.)	INTENSITY	ASSIGNMENT	WAVE NUMBERS (VAC.)	INTENSITY	ASSIGNMENT	WAVE NUMBERS (VAC.)	INTENSITY	ASSIGNMENT
40,004.8	140		40,604.0	25		41,446.5	85		42,658.2	140	
40,010.2	160	G_1^0	40,616.8	25		41,473	30 (*a*)		42,683.1	21	
40,015.4	25		40,627	12 (*a*)		41,478.6	350		42,704	12 (*a*)	
40,023.6	40		40,636.8	25		41,497.2	25		42,800.9	130	B'_3^0
40,039	40 (*a*)		40,648.8	18		41,508	12 (*a*)		42,845.0	130	
40,050.2	190	B'_0^0	40,686.5	170		41,524.1	25		42,872	25 (*a*)	
40,056.2	55		40,696.8	35		41,536.4	25		42,892.1	40	
40,069.6	25		40,704.8	335		41,572.3	15		42,919.0	30	
40,079	25 (*b*)		40,724.5	25		41,576.8	15		42,940	21 (*a*)	
40,084.8	25		40,735.9	25		41,606.6	140		42,954.3	25	
40,090.8	55	B_3^1	40,762	25 (*a*)		41,624.3	325		43,009.3	325	A'_2^0
40,109.1	85		40,770.6	25		41,634	12 (*a*)		43,032.0	85	
40,131.5	230		40,786.4	25		41,648	12 (*a*)		43,056.0	25	
40,137.3	55	A_2^2	40,800.9	25		41,682	25 (*a*)		43,114.8	12	
40,154.4	55		40,812.2	55	B'_1^1	41,700.1	55		43,122.2	12	
40,159.9	210		40,835.4	18		41,718	12 (*a*)		43,199.2	35	
40,177.7	230		40,840.1	25		41,731	25 (*a*)		43,204.2	35	A_5^0
40,186.8	140		40,862.2	12		41,741.0	140		43,215.8	300	
40,193.5	65		40,883.3	30		41,760.9	70		43,235.5	40	
40,202.5	140	C_2^1	40,894.5	30		41,824.1	25		43,245.9	30	
40,208.4	55		40,903.5	55		41,837	12 (*a*)		43,284	18 (*a*)	
40,224.5	25		40,915	25 (*a*)		41,851	12 (*a*)		43,314	15 (*a*)	
40,248.3	160		40,920	25 (*a*)		41,873	12 (*a*)		43,409	21 (*a*)	
40,252.5	160	B_3^0	40,927.3	55		41,884.5	160	B'_2^0	43,461.2	21	
40,261	55 (*b*)		40,930.4	55		41,923.9	160		43,475.8	12	
40,273	55 (*b*)		40,968.5	230	B'_1^0	41,947.0	30		43,540.9	25	
40,286	55 (*b*)		40,978.0	35		41,952.2	30		43,573.7	170	
40,292.8	510		41,002.3	190		41,974.1	140		43,600.9	9	
40,297.7	350	A_2^1	41,014	25 (*a*)	A'_0^1	41,997.0	35		43,623.5	9	
40,313.1	55		41,028.5	55		42,002.3	25		43,716.6	35	
40,319.8	130		41,053.9	55	A_3^2	42,018.9	55		43,765.6	25	
40,327	25 (*b*)		41,075.9	120		42,035.3	35		43,781	12 (*b*)	
40,328.7	35		41,081.7	120		42,088.0	100	A'_1^0	43,791	12 (*b*)	
40,333.2	55		41,099.7	140		42,111.8	70		43,808.9	25	
40,344.7	160		41,107	18 (*a*)		42,129	30 (*a*)		43,836.4	18	
40,361.4	35		41,114.7	35		42,137.6	85	A_4^1	43,929.1	160	A'_3^0
40,366.4	420	C_2^0	41,121.5	35		42,157	25 (*a*)		43,952.9	40	
40,372.0	230		41,128.3	35		42,187	18 (*a*)		44,032.6	12	
40,383.4	55		41,160	25 (*b*)		42,194.6	30		44,133.0	35	A_6^0
40,387.0	55		41,165.3	450		42,204.1	55		44,301.8	5	
40,426	55 (*b*)		41,168.4	30		42,211.8	18		44,319	7 (*a*)	
40,445.6	950		41,173.5	55	A'_0^0	42,221.6	25		44,459	6 (*b*)	
40,450.1	550	A_2^0	41,218.4	350	A_3^1	42,286.6	250		44,488.8	30	
40,456.0	6500		41,239.9	75		42,297.7	950	A_4^0	44,683.0	9	
40,473	140 (*a*)		41,253.9	25		42,318.3	160		44,724.9	8	
40,482.7	335		41,266.6	140		42,328.2	40	E_3^0	44,753	6 (*a*)	
40,489.4	325	E_1^0	41,276.3	35		42,365.4	35		44,847.9	35	A'_4^0
40,492.6	30		41,280.4	35		42,396.9	55		44,869.8	25	
40,509	25 (*a*)		41,285.7	210	C_3^0	42,415.8	18		45,050.4	18	A_7^0
40,525.5	55		41,291.1	65		42,443	17 (*a*)		45,083.2	7	
40,535.0	25		41,303.9	55		42,456	17 (*a*)		45,221.6	4	
40,543	35 (*b*)		41,366.0	375		42,488.2	18		45,402.9	13	
40,550.6	25		41,370.8	375	A_3^0	42,494.4	18		45,766.1	12	
40,558.9	250		41,377.9	3500		42,525.1	25		45,786.5	9	
40,576.8	35		41,399.2	170		42,544.2	110				
40,590	25 (*a*)		41,402.3	170	E_2^0	42,565.4	18				
40,598.1	15		41,409.9	190		42,621.1	55				

value of the electronic terms and Sklar has predicted that the transition responsible for the 2600A region is a forbidden one but, in accordance with the selection rules of Herzberg and Teller, becomes weakly allowed due to the interaction of nontotally symmetrical vibrations of the proper symmetry. This was confirmed in the most recent analysis of the spectrum by Sponer, Nordheim, Sklar, and Teller.[13] They have identified most of the important bands in the

[13] H. Sponer, G. Nordheim, A. L. Sklar, and E. Teller, J. Chem. Phys. **7**, 207 (1939).

system with transitions between vibrational levels whose frequencies are known from the analysis of infra-red, and Raman spectra. The appearance of the bands as a whole is due to two main progressions, a strong one A and a weak one B situated 1126 cm^{-1} from A toward longer wave-lengths. The members of each progression are spaced 923 cm^{-1} apart and extend toward shorter wave-lengths. The origin of the B progression has been disputed. Kistiakowsky and Solomon[14] have determined in absorption the intensities of the first member of each progression at various temperatures. With the exception of the value of the intensity of B_0^0 at $-15°C$ which was rejected because of an assumed lack of temperature equilibrium between the absorption cell and the benzene reservoir, the data show that the intensity of both bands continually decreases with increasing temperature. They interpret this as evidence that the population of the level from which each of these bands starts must be continually decreasing and attributed the behavior, in this case, to the vibrationless ground state and consequently assigned the origin of both bands to this state. This assignment of the B_0^0 band to the vibrationless ground state is in disagreement with the results of Sponer and collaborators, who assign it to a transition from the excited 606 cm^{-1} vibrational level in the ground state. Theoretically, it is evident that the intensity of a band originating in the vibrationless ground state decreases in intensity with an increase of temperature while the intensity of a band starting from an excited vibrational level at first increases with temperature up to a certain point (which might be called an inverting temperature) and then decreases. This is so because the more the temperature is increased, the more molecules leave the ground state, but for the first vibrational state, for example, molecules are at first entering it but later as many leave it for upper states as reach it from the ground state. At even higher temperatures the loss of molecules to higher states is greater than the gain from lower ones. This is especially marked at ordinary temperatures, if there are many close-lying levels lying above due to vibrations and combinations of vibrations and not so many levels below the one in question. This is especially true in the case of benzene.*

Because of the inherent difficulty in the experiment of Kistiakowsky and Solomon, it was decided to repeat the investigation as a second part of this work. The purpose of the first part is to provide a more complete table of wave-lengths of the absorption bands of benzene in the 2600A region.

General Apparatus

All spectrograms were taken with a 5-meter concave aluminized grating spectrograph in the first order, with a dispersion of about 3.4A per mm. The source was an all-quartz hydrogen tube operating from an a.c. transformer at approximately 0.9 ampere. Ballast and control resistances were introduced into the high voltage leads to give greater stability. Under these conditions the tube current did not fluctuate more than one to two percent during an exposure of about six minutes. The absorption cell was 50 cm long and 25 cm in diameter and of fused quartz throughout with the exception of the benzene reservoir which was of Pyrex and connected to the cell by means of a graded seal.

The authors are indebted to Dr. W. T. Ziegler for a very pure sample of benzene having a boiling point range of only 0.01°C.

Part I

Determination of wave numbers and the estimation of relative intensities in the wave number tables

Due to the fact that the absorption bands differ greatly in intensity it was necessary to take exposures at different concentrations of benzene vapor in order to obtain spectrograms suitable for more complete wave-length measurements. The amount of vapor in the absorption cell was controlled by varying the temperature of the side-arm containing a small amount of liquid or solid benzene. An exposure was taken at every 10° C interval as the temperature of the side-arm was varied from $-70°C$ to $50°C$ while the temperature of the absorption cell was kept constant. Adjacent to each exposure was the iron spectrum

[14] G. B. Kistiakowsky and A. K. Solomon, J. Chem. Phys. **5**, 609 (1937).

* Cf. Sponer, etc., reference 13, p. 213.

obtained from an arc operating at 4 amperes on 220 volts d.c.

The plates were measured on a comparator reading to 0.001 mm and fitted with a telescope equipped with interchangeable objectives. The method adopted was to set the comparator single hair parallel to the short wave-length edge of the absorption band such that a little light above the general background illumination was visible between the short wave-length edge of the absorption band and the single hair of the comparator. The accuracy with which the single hair could be set on a band depended on the appearance of the bands. Some were about as sharp as lines, others were broad with a sharp short wave-length edge while a few, designated by (*a*) in Table I exhibited a diffuse character. Some of the latter appeared to be two or more close-lying bands, while others seemed to be broad and washed out and quite different in appearance from the other measured bands. At the concentrations used in these measurements, some of the bands were scarcely visible and are indicated by (*b*). The error for the (*a*) and (*b*) bands is about ± 2 cm^{-1}, while bands with a well-defined edge have a probable error of 1 cm^{-1}, these being given to tenths which may be justified especially for close differences.

In the same table are given the relative intensities estimated from a plate on which many exposures were taken at different concentrations at room temperature. The band that was just visible at the highest concentration was assumed to be of unit intensity. Then for any other band one determined at what concentration it was just visible. From the concentration factor the relative intensity of the band was determined assuming that Beer's law holds and the bands have the same shape.

The assignments of SNST are given to the stronger bands. The relative intensities of the satellites accompanying many of the bands vary in a somewhat erratic manner as one goes through a progression. It is, accordingly, not possible at present to distinguish in an unambiguous manner between the origin of a band and its branches. Hence, in some cases, we have grouped two or three bands together, one of which is almost certainly the origin. For a group of three, a strong central one is presumably the origin.

Part II

The influence of temperature on band intensity

Apparatus.—This investigation required a method of varying the temperature of the absorption cell and maintaining it reasonably constant during an exposure. This was accomplished by surrounding the cell with a jacket consisting of an electrical heating unit and a cooling unit made from $\frac{1}{4}$-inch copper tubing through which alcohol cooled by solid carbon dioxide could be rapidly circulated. The entire assembly was designed to keep the temperature of the absorption cell as uniform as possible at any temperature from -50°C to several hundred degrees centigrade.

Intensity marks were recorded on the plate by means of a rotating sector disk with six equally spaced slots subtending an angle of 40° each. The disk was driven at a speed of 1200 r.p.m. by means of a synchronous motor connected to a reduction gear. The phase of the disk was adjusted with the help of a stroboscope so that a slot appeared in front of the slit of the spectrograph when the hydrogen tube was luminous during each half-cycle. The six intensity marks were obtained by blocking out the slots in succession. Thus the highest intensity mark corresponded to six open slots, the next to five open slots, etc., and to one open slot for the weakest intensity mark.

Procedure

Since the two bands of interest (A_0^0 and B_0^0) differ widely in intensity a different vapor concentration was required for each to give a satisfactory microphotometer trace. For the stronger of the two bands (A_0^0) a side-arm containing solid benzene was kept at -50°C for about thirty minutes and then sealed off from the absorption cell. The first exposure was taken with the absorption cell at -35°C and then at convenient intervals up to and including 250°C. While it was possible to take exposures at higher temperatures, these were avoided because of evidence of photochemical decomposition. In some preliminary work an exposure was taken at 300°C. After several hours a film formed on that part of the window of the absorption cell where

the light from the hydrogen discharge entered. The absorption band of the film extended over the entire region of investigation. For this reason the exposure time was kept as short as possible and the observations were restricted to 250°C and below. As a check, observations were made from low to high temperatures and then repeated, on the same plate, from high to low temperatures. There was no evidence of photodecomposition.

The above procedure was repeated at a higher concentration of benzene vapor, which was necessary for the study of the B_0^0 band. In this case the side-arm was maintained at a temperature of −20°C for some time before it was sealed off from the absorption cell. In this part the temperature of the absorption cell was not allowed to go below −15°C.

Microphotometer traces* were obtained for the A_0^0, B_0^0, and D_0^0 bands. A calibration curve for each absorption band was obtained by plotting the effective absorption coefficient α, obtained from the readings for the six intensity marks, against galvanometer deflections. The effective absorption coefficient α is equal to $\log(1/T)$, where T is defined as the ratio of the transmitted to the incident light. The value of the coefficient α at several points on the microphotometer trace was plotted against ν, the frequency. The area under this curve is proportional to the intensity of the absorption band. This area was obtained by means of graphical integration.** Unfortunately, it represents only approximately the intensity of an absorption band because of the overlapping of neighboring bands especially at the higher temperatures. If, on the other hand, one limits the integration to a fixed frequency interval, there will be some error due to neglect of part of the band. In both cases, the ratios are more reliable than the individual readings.

TABLE II. *Absorption intensity of the B_0^0 band.*

T°C	A_i	A_ρ	A_ρ (M.I.T.)
−15	9.5	9.2	5.9
32	12.4	11.0	8.5
100	14.1	12.9	9.0
150	10.0	10.0	6.0
200	8.1	5.9	4.8
250	5.0	3.8	

TABLE III. *Experimental and calculated intensities.*

T°C	606 (B_0^0) Cal.	606 (B_0^0) Exp. (Aver.)	2×606 (D_0^0) Cal.	2×606 (D_0^0) Exp.	Ground (A_0^0) Cal.	Ground (A_0^0) Exp.
−35					100	100
−15	75	68	23	9		
32	97	89	51	44	69	89
100	100	100	88	68	42	49
150	85	71	100	100	27	39
200	66	52	97	96	17	23
250	48	32	83	58	10	10

Results and Their Interpretation

The results of the intensity measurements on the B_0^0 band are given in Table II in arbitrary units. The first column A_i gives the total area under the α *vs.* ν curve while in the A_ρ columns the integration has been limited to a fixed frequency interval of about 80 cm^{-1}. In the last column, the data were obtained from measurements on the microphotometer traces of another plate with a different microphotometer.† The data clearly show that the intensity of the B_0^0 band has a maximum.

The variation of the intensity of a band with temperature can be calculated from statistical mechanics. Except for overlapping bands, the area of an individual band at different temperatures is proportional to a factor dependent on the Boltzmann distribution at each temperature. Hence we can write for each band area A_i an expression of the form,

$$A_i = \frac{p_i N g_i e^{-(h\nu_i/kT)}}{\sum_k g_k e^{-(h\nu_k/kT)}},$$

where p_i is a proportionality factor which includes the transition probability, g_i the degeneracy of the absorbing state, ν_i its frequency, and N the total number of molecules, the $\sum_k$ to be taken over all vibrations and combinations of vibrations in the ground state. This expression

* The authors wish to express their thanks to Dr. Hibben of the Geophysical Laboratory and to Dr. Johnson and Dr. McAllister of the Smithsonian Institution for their kind assistance and permission to use their Moll recording microphotometers.

** For B_0^0 this included the two longer wave-length members of the group, while for A_0^0 and D_0^0 all given members were taken.

† The traces were recorded on 35-mm film by the recording wave-length microphotometer at the Massachusetts Institute of Technology.

for A_i can be shown to be equal to

$$A_i = p_i N g_i e^{-(h\nu_i/kT)} \Pi_j (1 - e^{-(h\nu_j/kT)})^{g_j},$$

provided the vibrations are simple harmonic as seems to be approximately the case in benzene. The 20 known fundamental frequencies of benzene in the ground electronic state were substituted in the Π_j. The above expression was evaluated for the vibrationless ground state, the 606-cm^{-1} and 2×606 cm^{-1} vibrational states, which are, respectively, the low levels of the A, B, and D progressions.

The results of the calculation for the 606-cm^{-1} vibrational level are compared with the intensity of the B_0^0 band in columns 2 and 3 of Table III (the figures are relative to the value at the temperature in the table for which the intensity is a maximum). In each case the maximum intensity is taken to be one hundred. It is clearly seen that the results are in qualitative agreement with the assignment of the B_0^0 band to the 606-cm^{-1} level by Sponer and collaborators. In columns 4 and 5 the calculated intensities of the 2×606-cm^{-1} level are correlated with the experimental intensity data for the D_0^0 band. The agreement is sufficiently good to verify their assignment of this band to a transition from the 2×606-cm^{-1} vibrational level. The theoretical intensity of ground state transitions at different temperatures are given in column 6. The measurements of the intensity of the A_0^0 band are recorded in column 7. The agreement is an additional confirmation that the A_0^0 band is due to a transition from the vibrationless ground state.*

The authors wish to express their appreciation to Professor H. Sponer and Dr. A. L. Sklar for suggesting the problem and to Professor K. F. Herzfeld for his constant interest and advice.

* The results for the A_0^0 and B_0^0 bands agree fairly well with the trend of those of Kistiakowsky and Solomon. Their discarded point at -15°C is relatively lower than that of the authors.

JULY, 1940 JOURNAL OF CHEMICAL PHYSICS VOLUME 8

The Absorption of Phenyl Mustard Oil in the 4.8μ Region

DUDLEY WILLIAMS
University of Florida, Gainesville, Florida

(Received March 16, 1940)

An intensive study of the 4.8μ band of phenyl mustard oil has shown this band to have three components. Although these components have not been completely resolved, the present work indicates the frequencies involved to be 2130, 2080, and 1950 cm^{-1}. The two highest frequencies have counterparts in the Raman spectrum, but the frequency 1950 cm^{-1} has not been observed by Raman methods. Fermi resonance is discussed as a possible explanation of the observed spectrum. Re-investigation of the spectra of the methyl, ethyl, and phenyl nitriles and isonitriles failed to reveal complexities in the region of 2100 cm^{-1}.

RAMAN studies[1] of isothiocyanates have revealed the presence of two lines of approximately equal intensity in the frequency range in which N≡C frequencies are active. Badger[2] has sought to explain this so-called "splitting of the N≡C frequency" in terms of a Fermi resonance between the N≡C vibration and some other normal vibration of the molecule which is a submultiple of the N≡C frequency. In the spectra of ethyl and isobutyl mustard oils appears a Raman line of frequency of 1070 cm^{-1}, approximately half the 2100-cm^{-1} N≡C frequency. Badger has suggested that further infra-red study of the mustard oils* might be desirable.

[1] Complete bibliography: J. H. Hibben, *The Raman Effect and its Chemical Applications* (Reinhold, 1939).
[2] R. M. Badger, J. Chem. Phys. **5**, 178 (1937).

* *Note:* The formula for phenyl mustard oil or phenyl isothiocyanate generally accepted by the organic chemist is ϕ-N=C=S. However, two alternative structures ϕ-S−N⇄C and ϕ-N$^+$≡C−S$^-$ seem to be more in accord with the spectroscopic evidence. The first of these is similar to the fulminic acid structure suggested by Langmuir. In the present paper the symbol C≡N is used to refer to the bond in the normal thiocyanates and the symbol N≡C to refer to the modification of the bond in the mustard oils.

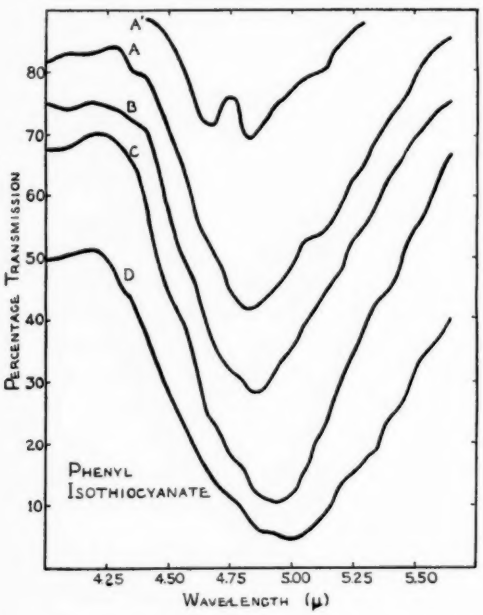

FIG. 1. The transmission of phenyl isothiocyanate in the 4.8μ region. Transmission determinations were made at intervals of 0.01μ.

The object of the present investigation was to obtain pertinent information on the infra-red spectrum of the phenyl compound. Previous infra-red studies[3,4] have revealed the presence of a broad, intense band with maximum absorption near 4.8μ in the mustard oil spectra but, in general, have failed to detect any complexities in band structure.[5] Therefore, the first part of the present work concerned itself with an intensive study of the 4.8μ absorption with a view to detecting the presence of any "splitting" similar to that observed in the Raman spectrum; the second part of the work involved a search for approximate submultiples of the N≡C frequency. The prism spectrometer employed has been described in an earlier publication;[6] the only variation which has been made is the substitution of an Eppley copper-constantan thermopile for the receiver used previously. Fluorite cell windows were used in the 4.8μ region, and rock-salt windows were employed in the region 8μ–15μ. Owing to the intense absorption near 4.8μ, it was necessary to use extremely thin films of the mustard oil. A number of different cells were used, cell thicknesses ranging from the thinnest film obtainable by pressing the fluorite plates together (probably about 0.005 mm) to a maximum thickness of 0.03 mm.

The transmission curves obtained are shown in Fig. 1, curves *A*, *B*, *C*, and *D* being arranged in order of increasing cell thickness. It may be seen from this figure that the absorption maximum shifts from 4.85μ in curve *A* to 5.00μ in curve *D*, an apparent decrease in frequency with increasing cell thickness. It will also be noted that the observed absorption band is unsymmetrical; in curve *A*, for example, there is strong evidence for a side band at 5.15μ and a suggestion of a depression in the curve at 4.70μ. The observed transmission curves can be explained by the superposition of these absorption bands with maxima near 4.7μ, 4.8μ, and 5.1μ. This was done by graphical methods for the curves shown in Fig. 1 and for curves representing the transmission of other cells of intermediate thickness. Such a procedure entails certain inherent difficulties, since there is no satisfactory method of accurately determining cell thicknesses in work of this type and since band shapes for the components must be chosen arbitrarily. The *relative* thicknesses of the cells were determined by a comparison of their transmissions in other spectral regions. The use of different band shapes for the components yielded slightly different values for the wave-lengths of the individual maxima but showed the absorption coefficients of the components near 4.7μ and 4.8μ to be approximately equal and much greater than the coefficient of the third component near 5.1μ.

Since even the thinnest obtainable cells of the liquid showed such intense absorption that the components could not be resolved, it was decided to study the transmission of a solution of phenyl mustard oil in the inert solvent carbon tetrachloride. The results for a ten-percent solution (cell thickness 0.01 mm) are shown in curve *A'*. Here the high frequency bands are separated, the maxima occurring at 4.68μ and 4.82μ. However, in this curve, the third band near 5.1μ appears

[3] W. W. Coblentz, *Carnegie Institution of Washington Publication No. 35* (1905), p. 60.
[4] W. Gordy and D. Williams, J.Chem. Phys. **4**, 85 (1936).
[5] *Note:* The only exception is Coblentz' curve for the allyl compound, which has a maximum at 4.5μ in addition to the broad band near 4.8μ.
[6] R. Taschek and D. Williams, J. Chem. Phys. **6**, 546 (1938).

only as an inflection point in the transmission curve.

From a comparison of the transmission curves for the liquid and for the carbon tetrachloride solutions, it thus appears that the broad 4.8μ band previously reported is actually complex. The most satisfactory values for the wave-lengths of the components as obtained by the above methods are 4.68μ, 4.82μ, and 5.12μ. Incomplete resolution of the components probably tends to cause the high frequency maximum to appear at slightly longer wave-lengths and the other two maxima appear at shorter wave-lengths than would be the case if higher resolution were possible. The 4.68μ and 4.82μ components probably correspond to the observed Raman lines, while the weaker 5.12μ band has no counterpart in the existing Raman data.

In the search for sub-multiples of the N≡C frequency the transmission of liquid phenyl isothiocyanate was studied as far as 15μ. The results obtained are in such close agreement with the early work of Coblentz that publication of the curves appears needless. One intense band was observed at 14.6μ which was not reported by Coblentz, as his measurements stopped at 14μ; otherwise, no new bands were observed. One might expect the band arising from the vibration involved in the Fermi resonance proposed by Badger to be comparable in intensity with the N≡C band. The only intense bands observed were at 10.8μ, 13.3μ, and 14.6μ. In addition to the intense bands, several rather weak bands were observed at 8.7μ, 9.3μ, and 10.0μ; these appear as depressions of five or ten percent in a transmission curve showing ninety percent absorption at 4.8μ.

Table I gives a comparison of the infra-red and Raman spectra of phenyl mustard oil. The data are in only fair agreement. The discrepancy in the frequencies near 2100 cm^{-1} may be attributed to lack of complete resolution in the infra-red work, but the lack of agreement in the case of 1260 and 1150 cm^{-1} is difficult to explain. The infra-red frequencies of 1950, 1075, and 925 cm^{-1} are apparently inactive in the Raman spectrum. The frequencies 1075, 1000, and 685 cm^{-1} seem to approach sub-multiple relationship more closely than any other observed frequencies. However, the relationship is only approximate. It should also be noted that the 1075- and 1000-cm^{-1} frequencies are only weakly active in the infra-red and probably would not be expected to produce the effect suggested by Badger. Thus, it would seem that the 685-cm^{-1} frequency arises from the vibration most likely to produce any resonance phenomena involved in the 4.8μ band. This frequency has been identified as arising from a vibration in which the C−S bond is active.[7]

The results of the present work on phenyl mustard oil may be summarized as follows: (1) The absorption near 4.8μ has been shown to consist of three overlapping bands.[8] (2) There are three approximate sub-multiple frequencies which might be involved in the Fermi resonance suggested by Badger.

Hibben[7] has suggested that, if Fermi resonance is a valid explanation of the "splitting" of the N≡C frequency in mustard oils, splitting should also be observed in the case of the organic cyanides and isocyanides, since sub-multiples of the N≡C frequency are found in the Raman spectra of these compounds. This splitting has not been observed in Raman work. In the

TABLE I. *A comparison of the infra-red and Raman data for phenyl mustard oil.*

Present Infra-Red Study		Raman Data[1]
Band Position (μ)	Frequency cm^{-1}	Frequency cm^{-1}
3.25	3070	3063
—	—	2772
4.68	2130	2172
4.82	2080	2100
5.12	1950	—
6.25	1600	1590
6.70	1490	1488
7.95	1260	1244
8.70	1150	1168
9.30	1070	—
10.0	1000	1003
10.8	925	—
13.3	750	752
14.6	685	689
		621
Infra-red Data		494
		354
		245

[1] K. W. F. Kohlrausch, *Der Smekal-Raman Effekt* (Springer, 1931).

[7] Reference 1, pp. 282–283.

[8] *Note:* Transmission measurements were made on methyl and ethyl mustard oils and some indications of complexities in 4.7μ region were found. However, since the components could not be separated, it seems inadvisable to publish any data until a study can be made with a spectrometer of higher resolving power.

present work attempts were made to detect possible complexities in the C≡N and N≡C infra-red bands of methyl, ethyl, and phenyl compounds. None of the observed bands showed any complexity. Hence, although a Fermi resonance mechanism may be involved in the mustard oil vibrations, it is not active in these closely related compounds.

JULY, 1940 JOURNAL OF CHEMICAL PHYSICS VOLUME 8

Spectroscopic Evidence for Hydrogen Bonds: Effects of Chelation on the Carbonyl Frequency[1]

WALTER GORDY,*
Mendenhall Laboratory of Physics, Ohio State University, Columbus, Ohio

(Received April 25, 1940)

The vibrational band characteristic of the carbonyl linkage was measured for *o*-hydroxyacetophenone, *o*-methylaminobenzoate, *o*-methylsalicylate, *o*-hydroxybenzaldehyde and for compounds similar to these but lacking an adjacent proton-donor group. Chelation through hydrogen bonding was found to shift the C=O band to longer wave-lengths by about 0.15μ to 0.20μ, or 40 cm^{-1} to 53 cm^{-1}, and to increase its intensity. Similar effects were observed for the carbonyl band of the enol forms of acetylacetone, ethyl malonate, ethyl acetoacetate. The magnitude of the effects of hydrogen bonding on the carbonyl band shows that energy changes in the proton-acceptor groups cannot be neglected in the computation of the energy of the hydrogen bond from spectroscopic data. The results also show that measurements on the proton-acceptor group can often be used as criteria for the presence of hydrogen bonding when experimental difficulties prevent accurate measurements of the effects on the vibrational band of the proton-donor group. Smaller effects were noted for ethylenic linkages of some of these compounds.

THE usual method of studying hydrogen bonding by means of infra-red absorption spectroscopy is to observe the effects of the bonding on the vibrational band of the group which donates the proton. It has been shown, however, that the linkage produces measurable effects on the group to which the proton is donated,[2] and that such effects can be used as criteria for the presence of hydrogen bonding in certain instances where experimental difficulties make measurements on the proton-donor group uncertain.

More measurements of the effects of hydrogen bonding on the proton-acceptor group are needed as an aid to quantitative calculation of the energy of the hydrogen bond from spectroscopic data. There have been several attempts[3] to discover a mathematical formula or relation between the energy of the hydrogen bond and the shift in the vibrational frequency of the proton-donor group. The results presented here indicate that the variation in the dissociation energy of the proton-acceptor group is appreciable and that it cannot be neglected in even an approximate computation of the energy of the hydrogen bond from spectroscopic data.

The carbonyl group is one of the most important and widely occurring among organic compounds. In previous papers of this series[1] it was shown that the carbonyl oxygen of aldehydes, ketones and esters accepts protons from alcohols, phenol, HCl and other proton-donor molecules to form hydrogen-bonded complexes. The association of the carboxylic acids comes about through the donation of the acid proton to the carbonyl group.[2b] Hydrogen bonding to a carbonyl group is responsible for numerous cases

* Now at Mary Hardin-Baylor College, Belton, Texas.

[1] This paper is a continuation of a series on hydrogen bonding. Other articles in the series are: J. Chem. Phys. **8**, 170 (1940); **7**, 93, 99, 163, 167 (1939); **6**, 12 (1938); J. Am. Chem.Soc. March (1940); **60**, 605 (1938). The last reference gives references to earlier papers.

[2] (a)W. Gordy, Phys. Rev. **50**, 1151 (1936); J. Am. Chem. Soc. **60**, 605 (1938); (b) R. H. Gillette and F. Daniels, J. Am. Chem. Soc. **58**, 1139 (1936); M. M. Davies and G. B. B. M. Sutherland, J. Chem. Phys. **6**, 755 (1938).

[3] R. M. Badger and S. H. Bauer, J. Chem. Phys. **5**, 839 (1937); J. J. Fox and A. E. Martin, Proc. Roy. Soc. (London) **A162**, 419 (1937); G. B. B. M. Sutherland, J. Chem. Phys. **8**, 161 (1940).

of chelation,[4] and the carbonyl group probably participates in the hydrogen bonding which takes place in the proteins.[5] The results reported in the present paper show how the infra-red measurements on this group can be used for the study of chemical interactions in which the group participates.

The instrument used is of the type described by Strong and Randall;[6] the particular adaptations and procedures used in this laboratory have been explained in other publications.[1] The cell windows were of fluorite. The absorbing layer was maintained at a constant thickness, 0.0015 cm.

Discussion of Results

In Fig. 1 is shown the spectrum of *o*-hydroxyacetophenone as compared with that of acetophenone, which is similar but does not have an OH group adjacent to the carbonyl group, as does *o*-hydroxyacetophenone. In acetophenone the carbonyl frequency appears at 5.96μ, whereas in *o*-hydroxyacetophenone it is shifted to 6.17μ, and its intensity is increased.

Figure 2 shows the effects of an adjacent NH_2 or OH group on the carbonyl frequency of an ester group. In methylbenzoate the carbonyl frequency appears at 5.82μ. When, however, an NH_2 group is adjacent to the carbonyl group, as in *o*-methylaminobenzoate, or an OH group is adjacent, as in *o*-methylsalicylate, the carbonyl frequency is shifted to 5.96μ and 5.98μ, respectively. A similar disturbance takes place when the carbonyl frequency is that of an aldehyde. Fig. 3 gives a comparison of the carbonyl frequency of *o*-hydroxybenzaldehyde with that of benzaldehyde. The shift in the frequency is about 0.21μ, or 57 cm^{-1}.

In all of the above compounds the bands found at about 6.3μ are characteristic of the benzene ring, and may, if resonance effects are neglected, be regarded as arising from a C=C linkage. For *o*-hydroxyacetophenone and *o*-hydrobenzaldehyde the carbonyl frequency is not well separated from this frequency of the benzene ring. In these cases there is likely to be considerable coupling which probably causes the shift in the C=O band to be greater than it would otherwise be. The overlapping of the two bands prevents an accurate determination of their centers. In *o*-methylaminobenzoate and *o*-methylsalicylate the frequencies are sufficiently separated to allow more accurate determination of their centers, and hence these cases probably give a better estimate of the effect of intramolecular hydrogen bonding on the carbonyl frequency. In the latter cases there is a shift of about 0.05μ to higher frequencies in the C=C band of the benzene ring. Resonance in the benzene ring has the effect of lowering the C=C frequency which would be expected from a normal Kekulé structure. Consequently, if conjugation resulting from chelation tends to decrease the resonance in the benzene ring, this would explain the shift to shorter wave-lengths in the benzene ring frequency. There are other evi-

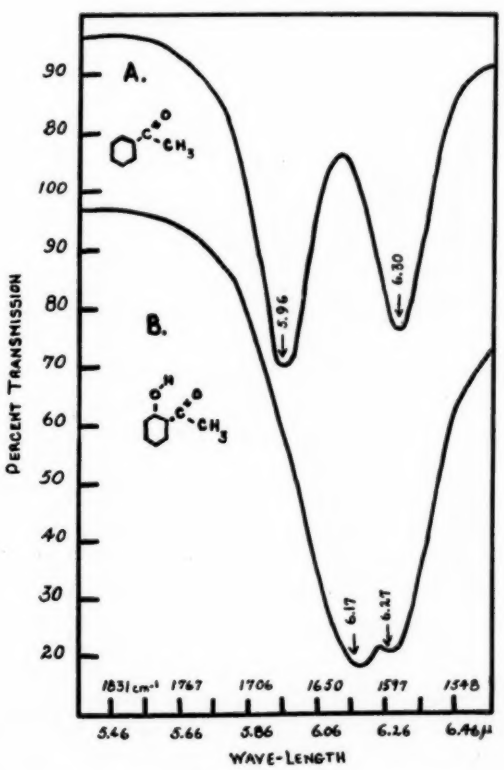

Fig. 1. Transmission of 0.0015-cm layer. A. Acetophenone. B. *o*-Hydroxyacetophenone.

[4] M. L. Huggins, J. Org. Chem. **1**, 407 (1936); E. N. Lassettre, Chem. Rev. **20**, 259 (1937).

[5] G. A. Albrecht and R. B. Corey, J. Am. Chem. Soc. **61**, 1087 (1939); L. Pauling and C. Niemann, J. Am. Chem. Soc. **61**, 1860 (1939).

[6] J. Strong and H. M. Randall, Rev. Sci. Inst. **2**, 585 (1931).

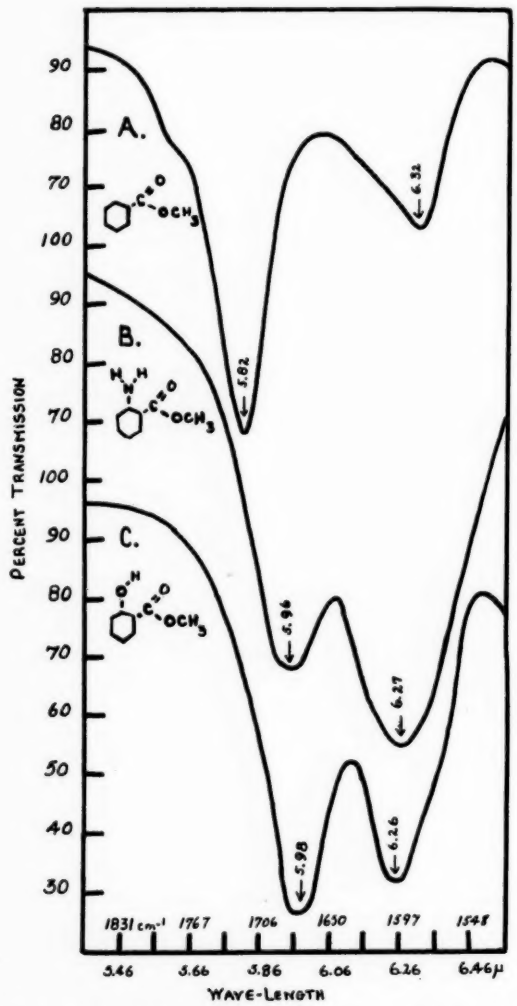

FIG. 2. Transmission of 0.0015-cm layer. A. Methylbenzoate. B. *o*-Methylaminobenzoate. C. *o*-Methylsalicylate.

dences for the decrease of resonance in the benzene ring by chelation.[7]

From chemical data acetylacetone in the liquid state is thought to exist about eighty percent in the enol form and about twenty percent in the keto form.[8] Spectroscopic data offer evidence that in the enol form a hydrogen bond links the carbonyl group to form a ring:[9]

$$\begin{array}{l} \quad\quad O-H\cdots O \\ \quad\quad\quad | \quad\quad\quad \| \\ CH_3-C=CH-C-CH_3. \end{array}$$

[7] L. Pauling, *Nature of the Chemical Bond* (Cornell University Press, 1939), p. 313; W. Baker and O. M. Lothian, J. Chem. Soc. 628 (1935); 274 (1936).

[8] Conant and Thompson, J. Am. Chem. Soc. **54**, 4044 (1932).

[9] R. Freymann, J. de phys. et rad. **10**, 1 (1939).

From the above noted results of intramolecular hydrogen bonding on the C=O group one would expect the carbonyl frequency of the enol form to be shifted to the longer wave-lengths and to be increased in intensity. Apparently this is what happens. See Fig. 4. The enol form, however, has an ethylenic linkage the absorption of which makes the data difficult of interpretation. The immediate environment of the carbonyl groups of the keto form of acetylacetone is the same as that of the carbonyl group of acetone. Consequently a comparison curve of pure acetone was run. The minimum in the transmission curve of acetylacetone, which occurs at 5.84μ, the position of the C=O acetone band, is no doubt due to the absorption of the keto form. The broad band, with a center at about 6.22μ, is probably a superposition of the C=O band of the enol form and the C=C band of this form, which would be expected to occur in the region of 6.2μ. The rather large shift of the C=O band is

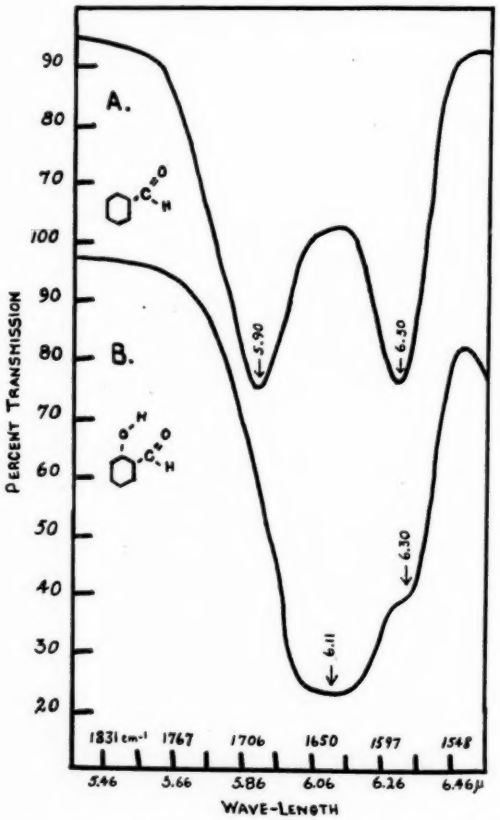

FIG. 3. Transmission of 0.0015-cm layer. A. Benzaldehyde. B. *o*-Hydroxybenzaldehyde.

doubtless caused partly by conjugation with the C=C linkage and partly by hydrogen bonding.

Figure 5 gives a comparison of the absorption in the region of 5.36μ to 6.56μ of ethyl acetate with ethyl malonate and ethylacetoacetate. In addition to the carbonyl absorption occurring at about 5.75μ, the latter two compounds have weak bands in the region of 6.12μ. These bands appear in the region in which an ethylenic linkage would be expected to absorb. Since they are not found in the curve for ethyl acetate, they are likely due to the C=C absorption of the enol form or to a superposition of this linkage with the C=O, shifted by conjugation and hydrogen bonding. Their small intensity shows that very

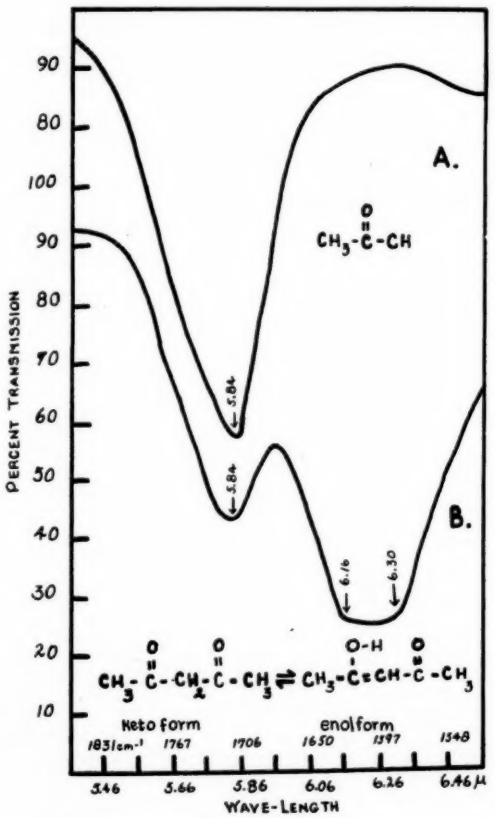

FIG. 4. Transmission of 0.0015-cm layer. A. Acetone. B. Acetylacetone.

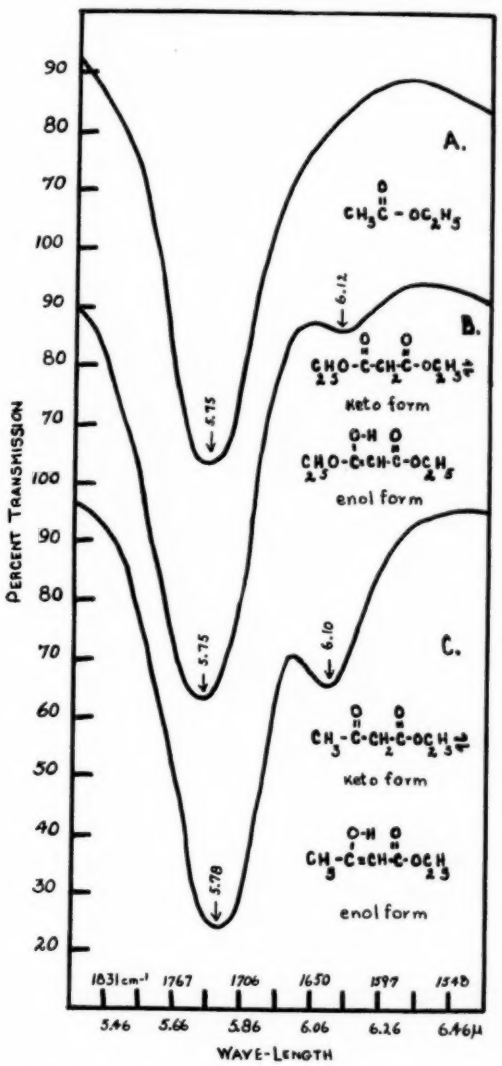

FIG. 5. Transmission of 0.0015-cm layer. A. Ethyl acetate. B. Ethyl malonate. C. Ethylacetoacetate.

little of the enol form is present and that ethyl malonate enolizes much less than ethylacetoacetate.

The author wishes to express his thanks to Professors Alpheus W. Smith and Harald H. Nielsen for their support and interest in this work, and to Dr. Spencer C. Stanford for his helpful discussion.

Raman Spectra of Amino Acids and Related Compounds

V. Deuterium Substitution in the Amino Group[1]

JOHN T. EDSALL AND HERBERT SCHEINBERG
Department of Physical Chemistry, Harvard Medical School, Boston, Massachusetts

(Received April 15, 1940)

Raman Spectra are reported for $CH_3 \cdot ND_2$, $CH_3 \cdot ND_3^+$, $^+D_3N \cdot ND_3^+$ and $^+D_3N \cdot ND_2$. Comparison with the spectra of the corresponding compounds containing no deuterium reveals three classes of frequencies: (1) Those arising from the methyl group are unchanged within the experimental error by deuterium substitution in the amino group. (2) The amino and ammonium group frequencies are higher in the H than in the D compounds by a factor of 1.33 to 1.36. Among these a characteristic $-ND_3^+$ valence vibration is found near 2180 cm^{-1}, corresponding to an $-NH_3^+$ vibration near 2970. These frequencies are broad and rather faint, and are lower by several hundred wave numbers than the corresponding sharp intense lines arising from the uncharged $-NH_2$ and $-ND_2$ groups. The principal deformation frequency of the NH_3^+ and NH_2 groups appear to be near 1620; the corresponding frequency of the $^-ND_3^+$ and $-ND_2$ groups is near 1200. (3) Other frequencies are changed by a factor of less than 1.3 when deuterium is substituted for hydrogen in the nitrogen. The most intense lines in this group are the C−N and N−N stretching frequencies near 1000 cm^{-1}, which show a decrease of 20 to 50 cm^{-1} on deuterium substitution. Some calculations, based on a very simple model, were made for these frequencies, but they did not quantitatively explain the observed results.

STUDIES on the Raman spectra of compounds containing amino and ammonium groups have left uncertain the nature of some of the frequencies found. In a number of instances, such uncertainties may be removed by a study of molecules in which the hydrogen of the $-NH_2$ or $-NH_3^+$ group has been replaced by deuterium. This paper reports the effect of such a replacement on the spectra of methylamine and its hydrochloride, and of the two hydrochlorides of hydrazine. The results serve to identify several frequencies hitherto uncertain, especially those associated with the electrically charged $-NH_3^+$ group, and also reveal the remarkable constancy of the methyl group frequencies, and their independence of deuterium substitution in an adjoining amino group.

EXPERIMENTAL

The experimental technique employed in exciting the Raman spectra has been described in the earlier papers of this series.[2–5] The deuterium-substituted compounds were studied in a small Raman tube of somewhat less than 3 cc capacity; the spectra obtained with this were fully as satisfactory as those obtained using larger tubes.

As in previous studies[6] a filter solution consisting of paranitrotoluene (2 percent) and rhodamine 5 GDN Extra, dissolved in alcohol,[7] was found extremely valuable. This filter transmits Hg 4358A freely, while removing almost completely all other mercury lines (except the yellow lines, which do not interfere) and greatly diminishing the continuous background at 4600A and beyond. The concentration of rhodamine employed was 0.02 g per liter of solvent if the liquid to be photographed was optically clear. The concentration was increased in some cases to as much as 0.05 g per liter, for the study of liquids containing suspended particles which could not easily be removed. Under the action of light, this filter solution slowly declines in its power to transmit Hg 4358A; it should therefore be changed after each run. A stock solution (2.5 g/liter) of the rhodamine dye in alcohol will keep well in the dark for some weeks. The filter solution may then be readily prepared from this by dilution with alcohol and addition of paranitrotoluene.

[1] Some of the data here presented have already been briefly discussed in a review by J. T. Edsall, *Cold Spring Harbor Symposia in Quantitative Biology* **6**, 40 (1938).
[2] J. T. Edsall, J. Chem. Phys. **4**, 1 (1936).
[3] J. T. Edsall, J. Phys. Chem. **41**, 133 (1937).
[4] J. T. Edsall, J. Chem. Phys. **5**, 225 (1937).
[5] J. T. Edsall, J. Chem. Phys. **5**, 508 (1937).
[6] J. T. Edsall and E. B. Wilson, Jr., J. Chem. Phys. **6**, 124 (1938).
[7] This solution was contained in a cylindrical filter tube 30 mm in diameter, interposed between the mercury arc and the Raman tube.

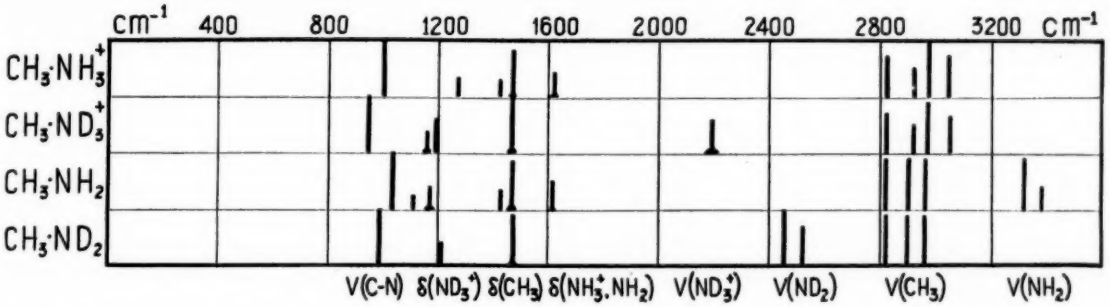

FIG. 1. Raman spectra of methylamine and methylammonium ions. The symbols V and δ indicate the region in which the valence and deformation frequencies, respectively, of the various groups are found.

The polarization measurements here reported on Raman lines were made with the aid of "Polaroid" by the method already described.[6]

PREPARATION OF MATERIALS

Methylamine hydrochloride was obtained from the Eastman Kodak Company, and twice recrystallized from alcohol and ether. Chloride found 52.5 percent, calculated 52.5 percent.

Hydrazine dihydrochloride was obtained from Eastman, and used without further purification.

Hydrazine monohydrochloride was prepared from the dihydrochloride by prolonged heating at 140°, until HCl ceased to be evolved, and was twice recrystallized from concentrated aqueous solution by addition of alcohol and ether. Melting point 86–89° (not very sharp); value reported in the literature is 89°. Probably a small amount of the dihydrochloride was still present; this was also indicated by the very faint presence in the Raman spectrum of the line at 1036 cm^{-1}, characteristic of the dihydrochloride. Otherwise the Raman spectrum of the material was identical with that already reported[3] on another sample prepared by a quite different method.

Deuterium substitution in the amino or ammonium group was effected by dissolving the substances described above in 99.65 percent deuterium oxide, removing the water by evaporation in vacuum over phosphorus pentoxide, and repeating the operation two or three times. Calculation showed that the D/H ratio for the hydrogen of the amino group should be close to or greater than 100 to 1 after this treatment; and the Raman spectrum showed no lines or bands characteristic of H_2O, or N−H linkages, in the solutions so prepared. Hydrazine dihydrochloride, however, gives off some HCl while being dried in vacuum, and it was necessary to add some HCl (in D_2O) to the final solution in deuterium oxide, used for obtaining the Raman spectrum, in order to reconvert it entirely into the dihydrochloride.

CH_3ND_2, dissolved in D_2O, was obtained from CH_3ND_3Cl by addition of NaOD in D_2O. The process was carried out in a small distilling apparatus, made entirely of glass, and the CH_3ND_2 was then distilled directly into the Raman tube. A solution of $CaCl_2$ in water, at about −15°C, was circulated through the outer

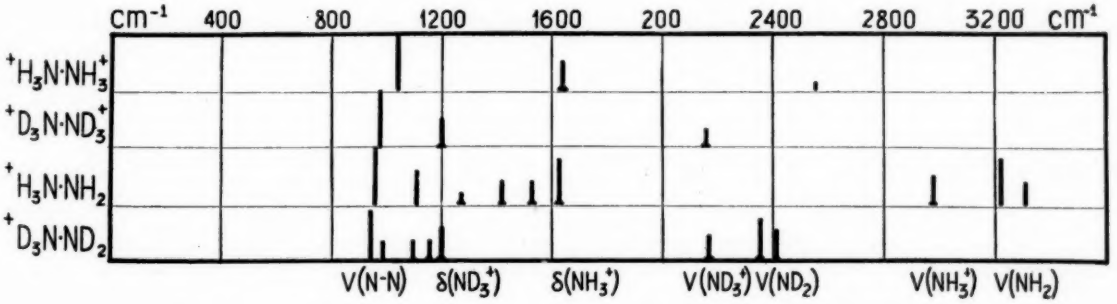

FIG. 2. Raman spectra of the ions derived from hydrazine. Symbols as in Fig. 1.

jacket of the condenser continuously throughout the distillation; and the Raman tube and the upper unjacketed portion of the condenser tube were surrounded with solid CO_2. (This should be removed from the condenser tube in the latter part of the distillation, when the temperature of the distillate begins to rise markedly—otherwise D_2O will freeze in the condenser and block it.) The spectrum obtained from CH_3ND_2 in D_2O showed a very faint line at 3360, presumably arising from an N−H vibration, and indicating a slight contamination with H_2O, this being the only compound studied which gave spectroscopic evidence of such contamination. Even in this case, however, the ratio of H to D was probably 1 to 20 or less.

Discussion

The data obtained are listed in Table III and represented graphically in Figs. 1 and 2.

The observed frequencies may be divided into three classes: (1) the methyl group frequencies, which are practically unaffected by deuterium substitution in the amino group; (2) the amino or ammonium group frequencies, which increase by a factor of 1.33 to 1.36 on replacing D by H in these groups; (3) other frequencies, which change by a smaller factor than 1.3, and involve the structure of the molecule as a whole more intimately than do the other two classes of frequencies.

Table I. *Characteristic frequencies of the amino and ammonium groups in some simple ions and molecules.*

CH_3ND_2	CH_3NH_2	Ratio
1212	1614	1.332
2450	3322	1.356
2527	3382	1.338
$CH_3ND_3^+$	$CH_3NH_3^+$	
1190	1620	1.361
2190	[2980]	1.36
$C(ND_2)_3^+$	$C(NH_2)_3^+$	
2374	3212	1.353
2433	3290	1.352
$CO(ND_2)_2$	$CO(NH_2)_2$	
1201	1604	1.335
2421	3235	1.336
2506	3385	1.351
2603	3496	1.343
$^+D_3N \cdot ND_2$	$^+H_3N \cdot NH_2$	
1198	1632	1.362
2176	2963	1.362
2354	3197	1.358
2410	3286	1.363

Note: The values for $C(NH_2)_3^+$, $CO(NH_2)_2$, and the corresponding deuterium components are taken from J. W. Otvos and J. T. Edsall, J. Chem. Phys. 7, 632 (1939).

Methyl group frequencies.—Comparison of the spectra of CH_3NH_2 and CH_3ND_2 shows that four strong lines—1470, 2825, 2904 and 2965—are, within the limits of experimental error, unchanged in position or intensity by the deuterium substitution. Ample evidence has long been available to indicate the association of these frequencies with the $-CH_3$ group. It could scarcely have been predicted, however, that alteration in the mass of an adjoining group should have a negligible influence on the value of these frequencies.

Besides the intense depolarized methyl group frequency at 1470 in CH_3NH_2 and CH_3ND_2—a line which is also intense in infra-red absorption—a much weaker line at 1428 appears in the Raman spectrum of CH_3NH_2.[4] The same frequency has been found by Cleaves and Plyler in the infra-red spectrum,[8] and has been interpreted by them as a parallel C−H deformation vibration. It is probable that this line is also present in the CH_3ND_2 spectrum, but it could not be made out with certainty on account of its faintness and of the presence of a more intense continuous background than was present in the spectrum of CH_3NH_2.

The situation is similar in the ions $CH_3 \cdot NH_3^+$ and $CH_3 \cdot ND_3^+$, which have five strong frequencies in common—1466, 2835, 2910, 2975 and 3040. It is clear, therefore, that all these lines arise from the methyl group, and the previous suggestion[4] that one or two of them do not must be abandoned. It is probable, however, as indicated later in this discussion, that a weak diffuse frequency near 2980 arises from the $-NH_3^+$ group in $CH_3 \cdot NH_3^+$, but is completely covered up by the very intense line of the same frequency arising from the methyl group. A weak line at 1426—presumably associated with the methyl group—is found in $CH_3NH_3^+$; a corresponding line may well be present in $CH_3ND_3^+$, but could not be identified with certainty.

The presence of four lines above 2800 cm^{-1}, all associated with the methyl group, calls for comment. Kirby-Smith and Bonner[9] have ob-

[8] A. P. Cleaves and E. K. Plyler, J. Chem. Phys. 7, 563 (1939).

[9] J. S. Kirby-Smith and L. G. Bonner, J. Chem. Phys. 7, 880 (1939).

served four lines in this region in the Raman spectrum of gaseous methylamine, and have interpreted them in terms of a double resonance interaction with one or both of the frequencies at 1426 and 1470 cm^{-1}. A similar interpretation probably applies here; we should favor the second hypothesis suggested by Kirby-Smith and Bonner, involving interaction of both 1426 and 1470 with the C−H vibrations near 2900.

The three frequencies near 2825, 2900 and 2970 are closely similar in CH_3NH_2, $CH_3NH_3^+$ and the corresponding compounds with deuterium attached to the nitrogen. The frequency near 2970, however, must represent a different mode of vibration in the amine and in the ammonium ion, since in CH_3NH_2 it is depolarized and in $CH_3NH_3^+$ it is very highly polarized. The depolarized line at 3040 appears only in the ammonium ions and not in the amines.

Amino and ammonium group frequencies.—On the basis of relative intensities and of shift in frequency on deuterium substitution, certain lines can be clearly allocated to these groups. The ratio of fundamental frequencies for the diatomic radicals N−H and N−D should—assuming completely harmonic vibrations—be 1.38. The ratio of N−H to N−D frequencies in the molecules studied in our investigations is given in Table I. The values obtained range from 1.33 to 1.36. The valence vibrations involving the N−H linkage in the uncharged amino group, lying between 3200 and 3500 cm^{-1}, are unmistakable, as are the analogous vibrations arising from the N−D linkage, which are found between 2350 and 2600 cm^{-1}. Polarization measurements on CH_3ND_2 indicate that the lower N−D valence vibration at 2450 is polarized, and the higher one, at 2515, is probably depolarized. Thus these two lines correspond, respectively, to the two lines at 3320 (*P*) and 3380 (*D*) in CH_3NH_2.[10]

The N−H valence vibrations in gaseous methylamine[9] lie at 3360 and 3470. The much lower values found in the liquid are presumably due to dipole interaction and hydrogen bond formation. There is no significant difference, however, between the values found for these frequencies in pure liquid methylamine and in its aqueous solution.[4]

The valence vibrations of the $-NH_3^+$ group in aqueous solution are difficult to detect, partly because they are broad and rather faint, but chiefly because they often coincide with the C−H valence vibrations which are also present in all organic ammonium compounds. Among substances containing an $-NH_3^+$ group but no carbon atom, the $+H_3N\cdot NH_2$ ion, in aqueous solution, gives a broad, moderately strong line at 2983 cm^{-1}; and the $^+H_3N-OH$ ion gives one at 2741 and another, more intense, at 2953.[4] All these lines are most readily interpreted as arising from the $-NH_3^+$ group. This interpretation has been greatly strengthened by the work of Ananthakrishnan[11] on the Raman spectra of crystals of ammonium halides and sulfates, hydroxylamine and hydrazine hydrochloride and sulfate, and glycine. NH_4Cl and NH_4Br give three frequencies near 2800, 3030 and 3130. Crystals of hydrazine dihydrochloride and of glycine give a series of weak frequencies between 2500 and 3200 cm^{-1}. These must arise primarily from the charged ammonium groups. They are profoundly influenced, however, by the nature of the crystal lattice and the interionic forces in it, since the sulfates of the ammonium, hydroxylammonium, and hydrazinium ions show very few and very weak lines in this range, in marked contrast to the corresponding chlorides.[12] Hydrazine dihydrochloride in solution in water likewise shows little or no trace of the many frequencies in this region found in the crystal.

The effect of deuterium substitution on the ammonium group throws further light on one of its characteristic valence vibrations. Every compound containing the $-ND_3^+$ group shows a very broad Raman line of rather low intensity between 2160 and 2200 cm^{-1}. This holds for $CH_3ND_3^+$, $^+D_3N\cdot ND_3^+$, $D_2N\cdot ND_3^+$, and glycine, $^+D_3N\cdot CH_2\cdot COO^-$ (unpublished measurements). The correlation appears unmistakable. If the mean value of this frequency (2180) is

[10] The polarization of the strongest lines in the Raman spectrum of CH_3NH_2 has been determined by J. Cabannes and A. Rousset, Ann. de physique **19**, 270 (1933).

[11] R. Ananthakrishnan, Proc. Ind. Acad. Sci. (A)**5**, 76, 87, 200 (1937).

[12] The effect of interionic forces in the crystal lattice on the vibrational frequencies is illustrated by the behavior of the principal valence vibration of the N−O bond in the hydroxylammonium ion. In the chloride, this is a single sharp line at 999 cm^{-1}; in the sulfate, it breaks up into a doublet at 1000 and 1012 (reference 11, p. 90).

multiplied by the factor 1.36 (see Table I), the corresponding $-NH_3^+$ vibration is calculated to be 2970, in close agreement with the values actually found for the $^+H_3N\cdot NH_2$ and $^+H_3N-OH$ ions. Almost any compound containing a methyl group gives a very powerful Raman line of nearly the same frequency, which will completely conceal the rather weak diffuse line arising from the $-NH_3^+$ group.

The $-NH_3^+$ group valence vibrations are broader, fainter and of lower frequency than those arising from the $-NH_2$ group. The $-NH_3^+$ lines are very similar in general appearance to the hydroxyl frequencies found in the alcohols when examined in the liquid state; whereas the $-NH_2$ frequencies are sharp and intense like the corresponding C−H vibrations.[13]

Broad diffuse lines of moderate intensity in the neighborhood of 1625 are found in the spectra of $CH_3NH_3^+$, CH_3NH_2, $^+H_3N\cdot NH_3^+$, $H_2N\cdot NH_3^+$ and other compounds containing the $-NH_2$ or $-NH_3^+$ group. In the compounds for which polarization measurements have been made, they appear to be depolarized, and probably arise from a deformation frequency of the NH_2 or $-NH_3^+$ group, comparable to the 1470 frequency of the methyl group. The corresponding deuterium compounds all show a similar broad line near 1200, the ratio of the two frequencies being that characteristic for N−H and N−D frequencies. This assignment of the 1625 line in CH_3NH_2 has already been made by Cleaves and Plyler[8] and by Owens and Barker[14] on the basis of infra-red studies. The corresponding line at 1618 in the Raman spectrum of liquid hydrazine (and at 1585 in the infra-red absorption of hydrazine vapor) has been given the same interpretation by Goubeau.[15]

The deformation frequency of liquid H_2O lies at 1640, and that of D_2O at 1210. Comparison studies with pure water, however, showed that the lines of similar frequency observed in aqueous solutions of the amino compounds were far too intense to be attributed only, or even chiefly, to the solvent.

TABLE II. *Effect of deuterium substitution on the* C−N, C−C *and* N−N *frequencies.*

MOLECULE OF ION	FREQUENCY	$1/\mu$	f(DYNE−CM$^{-1}\times10^{-5}$)
H_3C-NH_2	1034	0.1290	4.86
H_3C-ND_2	995	0.1223	4.74
$H_3C-NH_3^+$	995	0.1225	4.63
$H_3C-ND_3^+$	947	0.1167	4.50
$^+H_3N-NH_3^+$	1036	0.1176	5.37
$^+D_3N-ND_3^+$	979	0.1000	5.60
$^+H_3N-NH_2$	965	0.1212	4.54
$^+D_3N-ND_2$	943	0.1056	4.93
H_3C-CH_3	993	0.1334	4.33
D_3C-CD_3	852	0.1110	3.83

The C−N and N−N frequencies.—All the compounds studied show a powerful polarized line near 1000 cm^{-1}, undoubtedly associated primarily with stretching of the C−N or N−N bond. In all cases this frequency is lower in the deuterium than in the corresponding hydrogen compound. If the vibrations are assumed to be harmonic, and the CH_3, NH_2 and other groups are treated as if they were atoms of the same mass, force constants for the C−N and N−N bonds may be calculated from the formula $f=0.05863\mu\nu^2$, where ν is the observed frequency in cm^{-1} and μ is the reduced mass. The values obtained are given in Table II.

In methylamine and the methylammonium ion, the apparent force constant diminishes when D is substituted for H on the nitrogen; that is, the diminution in frequency is greater than would be expected, assuming the simplest possible model and no change in force constants as a result of deuterium substitution. A deviation in this direction might be expected because the actual vibration is not a pure stretching in molecules of this type, but also involves some degree of bending, in which the increased inertia of D as compared with H atoms will exert an additional depressing effect on the frequency, beyond what would be expected if the molecule were regarded as entirely rigid except for the

[13] In the spectrum of $CH_3ND_3^+Cl^-$ in D_2O, it was noticed that the band near 2520, characteristic of D_2O, was much more intense relative to the band near 2370 than was the case in the spectrum of pure D_2O. The interpretation of this observation remains uncertain. No corresponding effect could be definitely detected in the spectrum of $CH_3NH_3^+Cl^-$ in H_2O; but the very broad diffuse character of the H_2O bands would make such a change far more difficult to observe then in D_2O.

[14] R. G. Owens and E. F. Barker, J. Chem. Phys. **8**, 229 (1940).

[15] J. Goubeau, Zeits. f. physik. Chemie **45B**, 237 (1940).

TABLE III. *Observed Raman spectra. (The notation employed here is the same used in references 2, 3, 4 and 5.)*

1. Methylamine, CH_3NH_2 in water. This spectrum has already been reported.[4] Studies on a new preparation in the small Raman tube used for the deuterium compounds gave no lines not previously reported.

2. Methylamine-d_2, CH_3ND_2 in D_2O. 4.4 moles per liter, by titration. $\Delta\nu$: 995 (7) (*k, i, e*); 1214 (3*b*) (*k, e*); 1473 (5*b*) (*k, e*); 2450 (6) (*k, e*); 2527 (4*b*) (*k, e*); 2824 (4) (*k, e*); 2903 (4*b*) (*k, i, e*); 2969 (5*b*) (*k, i, e*); 3364 (0) (*k*).
Polarization measurements (6) indicated that the lines at 995, 2452, 2824, 2903 and 3364 were strongly polarized; those at 1214, 1473, 2527 and 2969 were nearly completely depolarized.
The line at 3364 presumably arises from an N−H vibration (see discussion in text).

3. Methylammonium chloride, $CH_3NH_3^+Cl^-$ in H_2O (44 percent solution) $\Delta\nu$: 998 (8) (*k, i, g, f, e*); 1271 (2*b*) (*k, e*); 1426 (1) (*k, e*); 1466 (6) (*k, e*); 1620±40 (3*b*) (*k, e*); 2831 (4) (*k, e*); 2904 (3) (*k, e*); 2973 (7) (*k, i, e*); 3041 (5) (*k, i, e*).
This spectrum is nearly identical with that reported in reference 2, except for the lines at 1426 and 1620, which were not then reported (the latter being omitted, although visible on the plates, because it was then attributed to water; it is, however, far too intense to be so explained).
For polarization measurements on some of the lines in $CH_3NH_3^+Cl^-$, see reference 4.

4. Methylammonium-d_3 chloride. $CH_3ND_3^+Cl^-$ in D_2O (36 percent solution, by weight). $\Delta\nu$: 947 (10) (*k, i, e*); 1158 (1*b*) (*k, e*); 1190 (2*b*) (*k, e*); 1466 (7) (*k, e*); 2193 (2*vb*) *k, e*); 2840 (4) (*k*); 2907 (3) (*k*); 2976 (8) (*k, i, e*); 3048 (6) (*k. i. e*).

5. Hydrazinium dichloride, $[^+H_3N\cdot NH_3^+]Cl^-_2$ in H_2O. This spectrum has already been reported;[4] a repetition gave no new feature.

6. Hydrazinium-d_6 dichloride, $[^+D_3N\cdot ND_3^+]Cl^-_2$ in D_2O (25 percent solution by weight, +1.6 *N* DCl). $\Delta\nu$: 828 (0?) (*k, e*); 945 (2*b*) (*k, e*); 979 (4*b*) (*k, e*); 1199 (2*vb*) (*k, e*); 2160 (0*vb*) (*e*); 2390 (D_2O) (*k, e*); 2503 (D_2O) (*k, e*).
The only line in this spectrum which can be ascribed with complete certainty to the ion $^+H_3N\cdot NH_3^+$ is that at 979; the lines at 1199 and 2160 almost certainly arise from this ion also; 828 (a doubtful line) and 945 probably arise from the ion $^+D_3N\cdot ND_2$ (see spectrum No. 8 below, and the discussion of the hydrazine ions in reference 4). 2390 and 2503 appear as in pure D_2O.

7. Hydrazinium monochloride, $Cl^-\ ^+H_3N\cdot NH_3$ (33 percent solution in H_2O). $\Delta\nu$: 962 (8) (*k, e*); 1033 (0) (*e*); 1107 (6) (*k, e*); 1424 (1*b*) (*k, e*); 1533 (1*b*) (*k, e*); 1632 (4*b*) (*k, e*); 2963 (2*vb*) (*k*); 3197 (6*b*) (*k*); 3286 (4*b*) (*k*).
The line at 1033 probably arises from a trace of the ion $^+H_3N\cdot NH_3^+$. The weak line at 1274, previously reported (4), was not observed, but there seems no reason to doubt its reality, as the present spectrum was somewhat less intense. In all other respects the present spectrum is virtually identical with that previously reported.

8. Hydrazinium-d_5 monochloride. $Cl^-\ ^+D_3N\cdot ND_2$ (33 percent by weight in D_2O). $\Delta\nu$: 838 (1/2*b*) (*e*); 943 (4) (*k, e*); 989 (1) (*k, e*); 1098 (1/2) (*k, e*); 1158 (1/2) (*e*); 1198 (1) (*k, e*); 2176 (1*vb*) (*k, e*); 2354 (2) (*k, e*) 2410 (1) (*k, e*).
The line at 2354 practically coincides with the center of a D_2O band; but the intensity and sharpness of the line differentiates it clearly from the D_2O band. The D_2O band near 2500 cm^{-1} was also, of course, plainly visible in the spectrum.

C−N bond. The measurements of Stitt[16] for the corresponding frequency in C_2D_6, as compared with C_2H_6, indicate that this deviation is even more marked in ethane than in methylamine or the methylammonium ion (Table II).

The results in the two hydrazine ions are quite different, however. The shift in frequency on substituting D for H is *less* than would be expected for the simple harmonic diatomic model; thus the apparent force constant is greater for the D than for the corresponding H compound, and the explanation offered above would entirely fail to account for the facts. The deviation in this case, however, is in the direction that would be expected if the vibrations were markedly anharmonic.[17] Thus the observed data appear compatible with the view that the anharmonicity of this vibration is greater in methylamine and its ion than in ethane, and greater in the hydrazine ions than in methylamine. In other words the anharmonicity would be least for the compound containing two $-CH_3$ groups, greatest for the compounds containing two $-NH_2$ or $-NH_3^+$ groups, and intermediate for those containing one group of each type. Whether such an interpretation would adequately explain the facts is a question that must await a more searching and detailed analysis.

Other frequencies.—For the frequencies listed in the spectra in Table III, other than those already discussed, we have no interpretation to offer. Attention should be directed, however, to the two broad frequencies of low intensity at 1424 and 1533 in $^+H_3N\cdot NH_2$. The spectrum of $^+D_3N\cdot ND_2$ shows two lines, very similar in appearance, at 1098 and 1158. The ratio for the H and D compounds is 1.297 for the two lower frequencies, and 1.324 for the two higher ones. If it is justifiable to assume a correspondence between the modes of vibration involved, this would indicate that both frequencies represent vibrations involving chiefly the amino and ammonium groups as such, with little displacement of the heavy molecular framework.

[16] F. Stitt, J. Chem. Phys. **7**, 297 (1939).
[17] K. W. F. Kohlrausch, *Der Smekal-Raman Effekt: Ergänzungsband 1931–1937* (Berlin, 1938), pp. 124–126.

Infra-Red and Raman Spectra of Polyatomic Molecules

XII. Methyl Acetylene*

BRYCE L. CRAWFORD, JR.
Sterling Chemistry Laboratory, Yale University, New Haven, Connecticut

(Received April 27, 1940)

The infra-red absorption of methyl acetylene gas has been studied between 2.5 and 25μ; the Raman spectrum of the liquid has been measured. A complete vibrational analysis is given, and the thermodynamic properties of the gas, between 250° and 1000°K, are tabulated. A normal coordinate treatment has been carried out, in which all force constants were determined *a priori* from other molecules. The ten fundamentals are calculated with an average error of 1.1, and a maximum error of 2.3 percent.

THE study of the vibrational frequencies of methyl acetylene was undertaken in order that the results might aid in unraveling the spectrum of the more complicated dimethyl acetylene molecule.[1] The Raman spectrum alone served to locate the fundamentals of methyl acetylene,[2] well enough for this purpose, and the investigation of the infra-red spectrum was deferred. This has now been carried out, and we here present the complete data on this molecule.

The most interesting result of the present study is the success of the normal coordinate treatment. The force constants used were determined completely *a priori*, being transferred from other molecules of similar structure, or (in one case) calculated by averaging other force constants; the agreement of the frequencies thus calculated with the observed fundamentals is more than satisfactory.

TABLE I. *The Raman spectrum of liquid methyl acetylene.*

FREQ., cm^{-1}	CHARACTER*	ASSIGNMENT
333	10, *b*, *D*	*E* Fund.
642	4, *b*, *D*	*E* Fund.
926	6, *P*	A_1 Fund.
1035	0, —	*E* Fund.
1380	2, *D*?	A_1 Fund.
1444	2, —	*E* Fund.
2125	12, *P*	A_1 Fund.
2735	1, —	$1380^2=2760$ (A_1)†
2866	3, —	$1444^2=2888$ (A_1+E)†
2927	8, *P*	A_1 Fund.†
2975	2, —	*E* Fund.
3300	3, —	A_1 Fund.

* *b*=broad; *P*=polarized ($\rho<6/7$); *D*=depolarized ($\rho=6/7$).
† Resonance among these three levels.

EXPERIMENTAL[3]

The methyl acetylene was supplied by Professor G. B. Kistiakowsky; it had been prepared for use in his hydrogenation calorimeter, and was extremely pure.[4] The Raman spectrum of the liquid material was studied using the apparatus previously described,[5] using Hg 4358A excitation. The results have been reported previously,[2] and the agreement with the earlier work of Glockler and Davis[6] pointed out. We give here a microphotometer trace, Fig. 1, and a summary of the observed shifts, together with the assignments, Table I.

The infra-red absorption of the gas was studied from 2.5 to 25μ. The spectrometer has been previously described;[5] fluorite, rocksalt, and KBr prisms were used in the appropriate spectral regions. The frequencies of the transmission minima are listed in Tables II and III, and the transmission curves given in Figs. 2 and 3.

While the frequencies of the observed minima in the 1450 cm^{-1} region are given in Table III, we attribute little significance to these values. By analogy with the methyl halides, we should expect a perpendicular band, with a branch

* Presented to the Division of Physical and Inorganic Chemistry of the American Chemical Society at Cincinnati, April, 1940.

[1] B. L. Crawford, Jr., J. Chem. Phys. **7**, 555 (1939).
[2] B. L. Crawford, Jr., J. Chem. Phys. **7**, 140 (1939).

[3] The experimental work reported here was carried out at Harvard University, during the author's tenure of a National Research Fellowship in Chemistry.
[4] J. B. Conn, G. B. Kistiakowsky and E. A. Smith, J. Am. Chem. Soc. **61**, 1868 (1939).
[5] H. Gershinowitz and E. B. Wilson, Jr., J. Chem. Phys. **6**, 197, 247 (1938); J. T. Edsall and E. B. Wilson, Jr., J. Chem. Phys. **6**, 124 (1938).
[6] G. Glockler and H. M. Davis, J. Chem. Phys. **2**, 881 (1934).

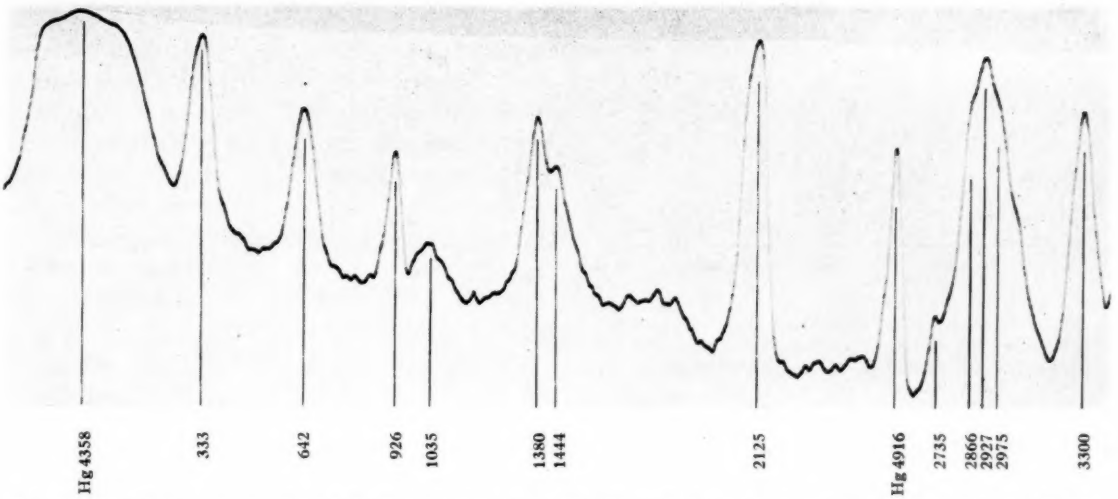

FIG. 1. Microphotometer tracing of the Raman spectrum of liquid methyl acetylene. Frequency shifts are marked in cm^{-1}; all marked lines are excited by Hg 4358.

spacing of about 11 cm^{-1}, to appear in this region. However, the resolution of the spectrometer (fluorite prism) was certainly insufficient to give the true rotational structure of the band, and the partial resolution obtained is of little value in studying a band of this complexity, which is also overlaid by other bands.

The parallel character of the bands at 926, 1187, and 1260 cm^{-1} is nicely shown; the formulas of Gerhard and Dennison[7] give an expected doublet spacing of 21.7 cm^{-1}, with a negligible Q branch, for a parallel band of methyl acetylene. The doublet band at 1110 cm^{-1} is not resolved so clearly, due to the lower resolving power of the rocksalt prism which had to be used at this frequency.

The peak at 418 cm^{-1} is rather doubtful; the increasing effect of stray radiation at the extreme long-wave limit of the spectrometer may give rise to artifacts. However, the existence of a band at approximately 400 cm^{-1} cannot be doubted.

The faint shoulders at the following frequencies are also uncertain: 652, 1623, 2074 cm^{-1}.

FUNDAMENTAL FREQUENCIES

Symmetry and frequency types

The methyl acetylene molecule has the symmetry C_{3v}; it follows[8] that there will be ten distinct frequencies, of which five will belong to the A_1 class (nondegenerate) and five to the E class (doubly degenerate). All vibrations are permitted to appear in both the Raman and the infra-red. Raman lines arising from A_1 vibrations may be polarized; those arising from E vibrations will be depolarized. The A_1 infra-red bands will be of the parallel type; the E bands, of the perpendicular type. Consideration of the various bond frequencies to be expected leads to the division shown in Table IV.

The "expected frequencies" given in Table IV are estimates obtained by analogy with other molecules. The values for the three C−H stretching and the C≡C stretching frequencies are derived from the methyl halides and the acetylene molecule, and need no comment. The magnitudes of the two C−H bending frequencies, near 1400 cm^{-1}, and of the CH_3 rocking frequency, near 1000 cm^{-1}, were estimated by a rather crude interpolation in the series of methyl halide frequencies; the C_2H group, of mass 25, was regarded as intermediate between fluorine, of mass 19, and chlorine, of mass 35. The C−C stretching frequency should be not too far from that in ethane, 993 cm^{-1}, although the presence of the triple bond may be expected to affect this frequency somewhat. The bending of the acetylenic hydrogen should have a frequency between those of the similar vibrations in C_2H_2, 605 and 730 cm^{-1}. The other low lying bending frequency

[7] S. L. Gerhard and D. M. Dennison, Phys. Rev. **43**, 197 (1933).

[8] See, for example, J. E. Rosenthal and G. M. Murphy, Rev. Mod. Phys. **8**, 317 (1936).

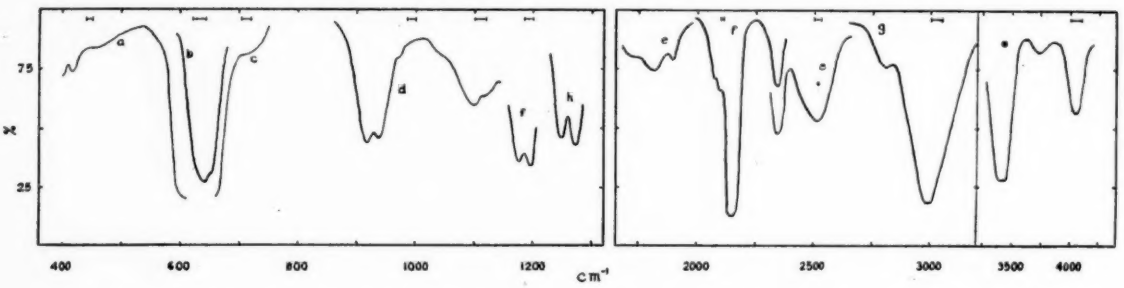

FIG. 2. Transmission curve of methyl acetylene gas, from 400 to 1300 and from 1700 to 4250 cm^{-1}. Path length, 30 cm. Slit widths are indicated near the top of the plot. KBr prism: *a*, 705 mm; *b*, 21 mm. NaCl prism: *c*, 705 mm; *d*, 352 mm. CaF_2 prism: *e*, 705 mm; *f*, 352 mm; *g*, 101 mm; *h*, 21 mm.

TABLE II. *The observed infra-red frequencies of methyl acetylene, with assignments. Frequencies in cm^{-1}.*

FREQ. OBS.	UNCERTAINTY	INT.*	ASSIGNED	FREQ. CALC.	SYMMETRY†
418	2	*w*?	1041–642	399	A_1+E
			1380–(971)	409	A_1+E
454	10	*vw*	1380–926	454	A_1
642	1	*vs*	Fund.	642	E
652	2	*m*?	333[2]	666	A_1+E
720	15	*w*	1041–333	708	A_1+E
			1380–642	738	E
916	2				
(926)		*s*	Fund.	926	A_1
937	2				
971	5	*w*	642+333	975	A_1+E
1041	5	*w*	Fund.	1041	E
1099	4				
(1110)		*m*	1444–333	1111	A_1+E
1120	7				
1176	1				
(1187)		*ms*	2151 – (971)	1180	A_1+E
1197	1				
1247	2				
(1260)		*vs*	642[2]	1284‡	A_1+E
1272	2				
(see Table II)			(Fund.	1380	A_1)
			(Fund.	1444	E)
1515	4	*m*	2151 – 642	1509	E
1623	7	*vw*?	926+1041	1624	A_1+E
			−333		
1721	8	*vw*	1380+333	1713	E
1815	5	*w*	2151 – 333	1818	E
1895	5	*w*	642[3]	1926‡	A_1+E
2074	7	*w*?	1041[2]	2082	A_1+E
(2088)					
2101	7	*w*	642+1444	2086	A_1+E
2151	4	*s*	Fund.	2151	A_1
2342	12	*ms*	2995 – 642	2353	A_1+E
			2151+333	2484	E
2515	20	*ms*	1041+1444	2485	A_1+E
			3430 – 926	2504	A_1
2809	50	*mw*	1380+1444	2824	E
2995	40	*vs*	Fund.	2995	E
3430	50	*s*	Fund.	3430	A_1
3750	60	*w*	various		
4050	60	*m*	combinations		

* *w* = weak; *m* = medium; *s* = strong; *v* = very. Bands marked with (?) are of doubtful reality.
† Only the symmetries of the infra-red active components are given.
‡ This very reasonable assignment for the 1260 cm^{-1} band implies a large anharmonic factor for the 642 cm^{-1} fundamental. For the second overtone, (1260) + 642 gives a value of 1902 cm^{-1}.

should lie between the 213 and the 371 cm^{-1} frequencies of dimethyl acetylene.

Vibrational analysis

Four of the A_1 and three of the E fundamentals may be assigned at once. The polarized character of the Raman shifts at 926, 2125, and 2927 cm^{-1} marks them as arising from A_1 vibrations, and their intensities show them to be fundamental frequencies. In the infra-red, two of these frequencies appear at 926 and 2151 cm^{-1}, the parallel-type structure being resolved in the former band. We may take these infra-red (gas-phase) values for the fundamental frequencies. The frequency near 2927 cm^{-1}, is overlaid in the

TABLE III. *Frequencies of observed transmission minima in the 1450 cm^{-1} region, in cm^{-1}. Uncertainty of each is about 4 cm^{-1}.*

PEAK NUMBER*	FREQUENCY	Δ
1	1348	
		14
2	1362	
		10
3	1372	
		13
4 (*br*)	1385	
		18
5 (*sh*)	1403	
		16
6	1419	
		12
7	1431	
		15
8	1446	
		18
9 (*sh*)	1464	
		12
10	1476	
		12
11	1488	
		27
12	1515	

* *br* = broad; *sh* = shoulder.

infra-red by the band at 2995 cm^{-1}; we must therefore take the Raman value for the fundamental. The intensity of the Raman shift at 2866 cm^{-1} indicates the usual Fermi resonance between the first overtone of the 1450 cm^{-1} frequency and the 2900 cm^{-1} fundamental; the true value of the latter will therefore lie between 2866 and 2927 cm^{-1}. We rather arbitrarily take 2910 cm^{-1} for this fundamental.

The assignment of the 3430 cm^{-1} infra-red band to the C−H′ stretching fundamental needs little comment. The large difference between the infra-red value and that of 3300 cm^{-1} obtained in the Raman (liquid-phase) experiments indicates a profound effect of the intermolecular fields on this C−H′ bond.

In the E class, we may assign the two low frequency Raman lines at 642 and 333 cm^{-1} to the C≡C−H′ and the C≡C−CH_3 bendings, respectively; the 642 cm^{-1} frequency appears unshifted in the infra-red. The infra-red band at 2995 cm^{-1} may be assigned to the perpendicular C−H stretching in the methyl group; this fundamental appears in the Raman at 2975 cm^{-1}.

The frequencies of the three remaining vibrations are less certain. There can be little doubt that the Raman shifts at 1380 and 1444 cm^{-1} correspond to the A_1 and E C−H bending vibrations, respectively; unfortunately the complexity of the 1450 cm^{-1} band in the infra-red, partially resolved by the spectrometer, is such that we cannot get more accurate values for these frequencies. Accordingly, we have accepted the Raman values. The infra-red band we assign to the combined absorption of the two fundamental vibrations (1380 and 1444 cm^{-1}), together with the combination tone $1041+333=1374(A_1+A_2+E)$, components of which may interact with both of the fundamentals. We make no attempt to analyze the partially resolved "structure" of this band.

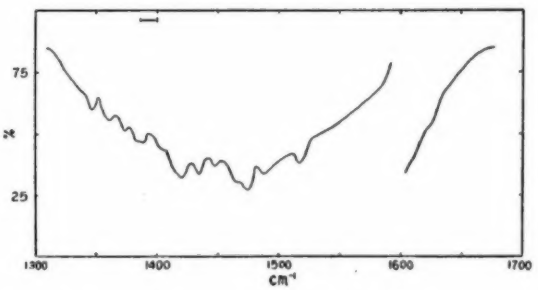

FIG. 3. Transmission curve of methyl acetylene gas, 1300 to 1700 cm^{-1}. Path length, 30 cm; CaF_2 prism; pressures of 101 and 705 mm. Effective slit width, 14 cm^{-1}.

In looking for the remaining fundamental frequency, the perpendicular CH_3 rocking vibration, we may be guided by the analogy with the methyl halides. The Raman shift at 1035 cm^{-1} is a reasonable choice; this vibration appears in the infra-red as a weak band at 1041 cm^{-1}. It must be pointed out that this band may quite well be assigned to a difference tone, 1380−333=1047 cm^{-1}; its weakness would be consistent with this assignment. On the other hand, the little knowledge we have about infra-red vibrational intensities would lead us to expect the CH_3 rocking fundamental to be weak in absorption; this vibration in the methyl halides gives quite weak

TABLE IV. *Types of vibration in methyl acetylene.*

TYPE	A_1	E	EXPECTED FREQUENCY
C−H′ stretching*	1	0	*ca.* 3300
C−H stretching	1	1	2900–3000
C≡C stretching	1	0	*ca.* 2000
C−H bending, ⊥	0	1	1475
C−H bending, ∥	1	0	1350–1400
CH_3 rocking	0	1	*ca.* 1000
C−C stretching	1	0	*ca.* 1000
C≡C−H′ bending*	0	1	*ca.* 600
C≡C−C bending	0	1	*ca.* 300
Totals	5	5	
Activity†	*R, P*: *IR*, ∥	*R, D*: *IR*, ⊥	

* H′ refers to the acetylenic hydrogen as distinguished from the methyl hydrogens.
† *R* = Raman-active; *P* = may be polarized ($\rho \leq 6/7$), *D* = depolarized ($\rho = 6/7$). *IR* = infra-red-active: ∥ = parallel bands, ⊥ = perpendicular bands.

TABLE V. *The fundamental frequencies of methyl acetylene, observed and calculated in cm^{-1}.*

	OBS.	CALC.	ERROR, PERCENT	FORCE CONSTANTS INVOLVED
A_1	926	925	−0.1	K_C, k_{CA}, $k_{C\gamma}$
	(1380)*	1402	+1.6	H_α, H_β, $h_{\alpha\beta}$, $k_{C\gamma}$
	2151	2137	−0.7	K_A, k_{CA}, $k_{H'A}$
	(2910)*	2905	−0.2	K_H
	3430	3331	−2.9	$K_{H'}$, $k_{H'A}$
E	(333)*	332	−0.3	H_φ, $h_{\varphi\theta}$
	642	656	+2.3	H_θ, $h_{\varphi\theta}$
	1041	1040	−0.1	H_β
	(1444)*	1475	+2.1	H_α, H_β, $h_{\alpha\beta}$
	2995	3021	+0.9	K_H

* These values are taken from Raman measurements on the *liquid* state.

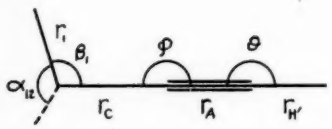

FIG. 4. Potential energy variables for methyl acetylene. Dotted line indicates projection of r_2, r_3 on the plane of the paper. Equilibrium values of α_{ij}, β_i, are all 109° 28′, the tetrahedral angle.

infra-red bands.[9] The other infra-red bands between 800 and 1300 cm^{-1}, excepting the 971 cm^{-1} shoulder, are all of the parallel type. Thus, while the evidence that this fundamental lies at 1041 cm^{-1} is weak, we must either accept this frequency or postulate that the fundamental is overlaid. We have adopted the former course, supported somewhat by the excellent check with the calculated value for this frequency (see below).

The other bands in the infra-red spectrum give no conclusive evidence either for or against the doubtful points of the above analysis. Using the fundamentals listed in Table V, we have assigned the various observed bands as shown in Table II. In this table, only the most reasonable assignments for each hand are given. The frequencies for all active binary combinations, including difference tones with a lower level below 1000 cm^{-1}, were calculated. Of 62 "predicted bands" lying between 400 and 3000 cm^{-1}, all but 9 either appeared or lay beneath some other band; it does not seem worth while to publish this list of predicted bands.

The assignment of the 1187 cm^{-1} parallel band is not very satisfactory; it seems unlikely that a difference tone arising from a combination level at 971 cm^{-1} should give a moderately strong band. However, such a band cannot be pronounced impossible on the basis of present information about infra-red intensities.

Normal coordinate treatment

The factors of the secular equation for methyl acetylene are closely related to those for dimethyl acetylene;[1] the approximate factoring technique effectively reduced the A_1 factor from a quintic to one cubic and two linear equations, and the E factor from a quintic to one quartic and one linear equation. The neglected interactions amounted to at most 1.2 percent of the frequency, and were included in the final calculations where they were appreciable.

The potential energy expression used was of the modified valence-force type. The potential arising from methyl-group distortions was based on that used by Stitt for ethane,[10] and was found to be satisfactory for dimethyl acetylene:[1]

$$2V_1 = K_H \sum_3 (\Delta r_i)^2 + H_\alpha r_1^2 \sum_3 (\Delta\alpha_{ij})^2 + H_\beta r_1^2 \sum_3 (\Delta\beta_i)^2 + h_{\alpha\beta} r_1^2 \sum_6 (\Delta\beta_i)(\Delta\alpha_{i,\ i\pm1}) + k_{C\alpha} r_1 \sum_3 (\Delta r_C)(\Delta\alpha_{ij}) + k_{C\beta} r_1 \sum_3 (\Delta r_C)(\Delta\beta_i).$$

Here $i=1, 2, 3$; the number of terms in each summation is indicated. The bond distances and valence angles are shown in Fig. 4. Since $k_{C\alpha}$ and $k_{C\beta}$ always appear as $(k_{C\alpha}-k_{C\beta})=k_{C\gamma}$, there are only five constants in this part of the potential. The values used in ethane[10] and dimethyl acetylene[1] were used (see Table VI).

The potential for other distortions was based on Colby's work on C_2H_2[11] and on dimethyl acetylene:[1]

$$2V_2 = K_C(\Delta r_C)^2 + K_A(\Delta r_A)^2 + K_{H'}(\Delta r_{H'})^2 + k_{CA}(\Delta r_C)(\Delta r_A) + k_{H'A}(\Delta r_{H'})(\Delta r_A) + H_\varphi r_C^2(\Delta\varphi)^2 + H_\theta r_{H'}^2(\Delta\theta)^2 + h_{\varphi\theta} r_C r_{H'}(\Delta\varphi)(\Delta\theta).$$

TABLE VI. *Force constants in methyl acetylene.*

CONSTANT	TYPE	VALUE (10^5 DYNES/CM)
K_H	C−H stretching, CH_3	4.79*
H_α	HCH bending, CH_3	0.46*
H_β	HCC bending, CH_3	0.55*
$h_{\alpha\beta}$	interaction, CH_3	+0.02*
$k_{C\gamma}$	interaction, CH_3	−0.47*
K_A	C≡C stretching	15.587†
$K_{H'}$	C−H′ stretching	5.850†
$k_{AH'}$	interaction	+0.056†
H_θ	C≡C−H′ bending	0.2096†
K_C	C−C stretching	5.183‡
k_{CA}	interaction	+0.44‡
H_φ	C≡C−C bending	0.155‡
$h_{\varphi\theta}$	interaction	+0.145§

* Ethane: reference 10.
† Acetylene: reference 11.
‡ Dimethyl acetylene: reference 1.
§ See text: $h_{\theta\theta}=+0.1567$, $h_{\varphi\varphi}=+0.134$.

[9] W. H. Bennett and C. F. Meyer, Phys. Rev. **32**, 888 (1928).

[10] F. Stitt, J. Chem. Phys. **7**, 297 (1939).

[11] W. F. Colby, Phys. Rev. **47**, 388 (1935). The constants given in Table VI have been recalculated on the basis of our equilibrium bond distances; see footnote 20 of reference 1.

In the dimethyl acetylene molecule, a large interaction was found between the two C−C bonds; on this basis, one might expect a similar interaction term, of the form $[k_{CH'}(\Delta r_C)(\Delta r_{H'})]$, to be necessary here. However, since the C−C and the C−H′ vibrations have widely different frequencies, and since the two bonds are not directly connected, this interaction was omitted.

All but one of the force constants can be transferred directly from similar bond structures in ethane,[10] dimethyl acetylene,[1] or acetylene itself.[11] The remaining constant, $h_{\varphi\theta}$, expresses the interaction between the C≡C−C and C≡C−H′ bendings; this structure has not been previously encountered. However, the interaction between the two C≡C−C bendings in dimethyl acetylene, $h_{\varphi\varphi}$, and that between two C≡C−H′ bendings in acetylene, $h_{\theta\theta}$, are known; $h_{\varphi\theta}$ was taken to be the mean of these two values.

The equilibrium bond distances were assumed to be:[12] C−H, 1.093, C−H′, 1.057, C−C, 1.462, C≡C, 1.204A, with tetrahedral angles in the CH_3 group.

The frequencies calculated in this way are compared with the observed values in Table V. The agreement is quite good; when it is remembered that the force constants were obtained purely from bond-structure considerations, and were not adjusted in any way to the observed frequencies, the comparison is most gratifying. The agreement for the 642 cm^{-1} E fundamental could be improved by adjusting the interaction constant $h_{\varphi\theta}$.

Thermodynamic Calculations

The fundamentals of Table V were used, together with the molecular structure data,[12] to calculate by standard statistical methods the virtual entropy, the free energy function, and the specific heat of methyl acetylene in the hypothetical perfect gas state at one atmosphere pressure. The universal constants were taken from the *International Critical Tables;* the molecular weight of the compound was taken as 40.03, and the symmetry number as 3. The moments of inertia are 5.1525 and 96.894 (10^{-40} g cm^2). The normal boiling point is 250.0°K.[4] The resulting thermodynamic values are given in Table VII.

Table VII. *Thermodynamic properties of methyl acetylene, perfect gas at 1 atmos. pressure, in cal./mole degree. Constants from the International Critical Tables.*

T, °K	S^*	$-(F^0-H_0^0)/T$	C_p^*	$+(F^0/T)$
250.0	56.87	47.09	11.12	+136.89
298.16	59.31	48.87	12.54	105.39
400.	63.98	52.14	15.40	62.85
600.	71.91	57.44	19.85	19.22
800.	78.68	61.93	23.19	−4.44
1000.	84.58	65.86	25.74	−19.86

Since these values depend entirely upon the correctness of the vibrational assignment, it is difficult to estimate the uncertainty. However, the most uncertain frequency is that at 1041 cm^{-1}; a change of 100 cm^{-1} in this frequency would affect the entropy and the free energy function by less than 0.5 percent, and the heat capacity by less than 2 percent, at the most unfavorable temperatures of Table VII.

Rossini has given[13] the value 44,309±240 cal./mole for the heat of formation of gaseous methyl acetylene at 298.16°K. From this we obtain the value $\Delta H_0^0 = 45{,}995$ cal./mole for methyl acetylene gas. This value has been used to calculate the free energy of methyl acetylene as given in the last column of Table VII; the elements in their standard states *at 0°K* are assigned zero energy, according to the system used by Rodebush in the *International Critical Tables* and recently recommended by Aston.[13] The heat content H^0, referred to this energy zero, is easily obtained from the entropy and free energy.

In concluding, I wish to thank Professor G. B. Kistiakowsky for his kindness in supplying the methyl acetylene used; and to express to Professor E. B. Wilson, Jr., who suggested this study to me, my appreciation of the continued interest he has shown in the work.

[12] G. Herzberg, F. Patat and H. Verleger, J. Phys. Chem. **41**, 123 (1937); L. Pauling, H. D. Springall and K. J. Palmer, J. Am. Chem. Soc. **61**, 927 (1939).

[13] Cincinnati meeting of the American Chemical Society, April, 1940.

The Concentration of C^{13} *

CLYDE A. HUTCHISON,† DAVID W. STEWART AND HAROLD C. UREY
Department of Chemistry, Columbia University, New York, New York

(Received April 22, 1940)

The chemical exchange method has been applied to the separation of the isotopes of carbon. Various exchange reactions have been tested, using counter-current flow in packed fractionation columns, and of these, the exchange between hydrogen cyanide gas and a solution of sodium cyanide in water has been found to be most efficient. In this exchange, the isotope of carbon of atomic weight 13 (ordinarily present to the extent of 1.06 percent) is concentrated in the gas phase. Suitable conditions for the exchange have been determined, and a satisfactory apparatus has been devised. Using two fractionation units in a cascade arrangement, sodium cyanide, containing carbon of 25 atom percent C^{13}, has been produced at a rate of 2.5 grams per day. This corresponds to a transport of 0.15 grams of C^{13} per day. In all, more than 20 grams of carbon, containing 25 percent of C^{13}, and additional quantities of less concentrated material, have been obtained in this way.

INTRODUCTION

IN this paper we report the extension of chemical methods for the separation of isotopes to the concentration of the carbon isotope of atomic weight 13. The possibility of the use of such methods was first pointed out by Urey and Greiff[1] who calculated isotopic equilibria for gaseous exchange reactions involving isotopes other than hydrogen. For effective separation of isotopes it is necessary that a two-phase system be devised and three varieties of such two-phase systems have been used up to the present time. The first of these, involving gaseous and liquid phases, has been used for the concentration of the oxygen isotopes by simple distillation and for the concentration of nitrogen and sulfur isotopes by chemical exchange. Using two liquid phases, Lewis and MacDonald[2] effected a considerable concentration of the lithium isotope of mass 6, and Taylor and Urey[3] using a liquid-solid exchange reaction have effected some concentration of the rarer lithium, potassium and nitrogen isotopes.

Roberts, Thode, and Urey[4] have reported a considerable concentration of C^{13} by the use of a gas-liquid exchange reaction, and have pointed out how the process could be extended. This has now been accomplished, and with certain modifications in the original method, a considerable quantity of carbon has been prepared containing 25 percent of C^{13}, instead of the normal concentration of 1.06 percent.

TWO-PHASE EXCHANGE REACTIONS INVOLVING THE CARBON ISOTOPES

A considerable number of possible exchange reactions suitable for the separation of the carbon isotopes have been studied in this laboratory and have been partly reported in the literature. These various studies were made, for the most part, with a fractionation column packed with Fenske glass spirals, though the Pegram column[5] was used in some cases. In general this column was fed at the top with total reflux at the bottom, though in two experiments the column was fed at the bottom and reflux was from the top. The results of such studies are summarized in Table I.

Carbon dioxide in exchange with bicarbonate ion in solution would be by far the most desirable exchange reaction from many points of view. The reaction, however, is very slow, and hence it is not suitable for these counter-current methods. The enzyme *carbonic anhydrase* does catalyze the reaction and some separation was secured by using it, but it was quite evident that it would be impossible to effect any very great fractionation unless a more suitable catalyst could be found.

* Publication assisted by Ernest Kempton Adams Fund for Physical Research of Columbia University.

† Present address, Department of Chemistry, University of Buffalo, Buffalo, New York.

[1] H. C. Urey and L. J. Greiff, J. Am. Chem. Soc. **57**, 321 (1935).

[2] G. N. Lewis and R. T. MacDonald, J. Am. Chem. Soc. **58**, 2519 (1936).

[3] T. I. Taylor and H. C. Urey, J. Chem. Phys. **6**, 429 (1938).

[4] I. Roberts, H. G. Thode and H. C. Urey, J. Chem. Phys. **7**, 137 (1939).

[5] J. R. Huffman and H. C. Urey, Ind. Eng. Chem. **29** 531 (1937).

TABLE I.

LIQUID PHASE	GAS PHASE	METHOD OF REFLUX	COLUMNS USED	SEPARATION OBTAINED (FOLD INCREASE IN C^{13} CONC.)
Aqueous solution of $KHCO_3$	CO_2	Addition of acid at bottom	35-ft. Pegram column	None[a]
Aqueous solution of $KHCO_3$ plus enzyme catalyst	CO_2	Addition of acid at bottom	35-ft. Pegram column	1.28 (45 hr.)[a]
Liquid CH_3OH	CH_3OH	Boiling at bottom	35-ft. Pegram column	Practically none[b]
Acid cuprous chloride solution of CO	CO	Boiling at bottom	25 ft. of $\frac{3}{8}$" packed column	1.69[b]
Acetone solution of C_2H_2	C_2H_2	Heating at bottom	25 ft. of $\frac{3}{8}$" packed column	1.19 (at −80°C)[b]
Acetone solution of CO_2	CO_2	Heating at bottom	5.6 ft. of $\frac{3}{8}$" packed column	None[b]
Liquid HCOOH	HCOOH	Boiling at bottom	5.6 ft. of $\frac{3}{8}$" packed column	None (1.5 hr.)[b]
Aqueous solution of $CH_3NH_2 \cdot HCl$	CH_3NH_2	Addition of NaOH at bottom	10 ft. of $\frac{3}{8}$" packed column	None[c]
Aqueous solution of HCN	HCN	Solution of HCN in water at top	25 ft. of $\frac{3}{8}$" and 40 ft. of 1" packed columns	0.9[c]
Aqueous solution of NaCN	HCN	Addition of NaOH at top	25 ft. of $\frac{3}{8}$" packed columns	6.7[c]

[a] H. C. Urey, A. H. W. Aten, Jr. and A. S. Keston, J. Chem. Phys. **4**, 622 (1936).
[b] H. C. Urey, G. A. Mills, I. Roberts, H. G. Thode and J. R. Huffman, J. Chem. Phys. **7**, 138 (1939).
[c] Previously unpublished.

Many types of catalysts have been tried, but without success. Catalysts suggested by Roughton and Booth,[6] including phosphate buffers, sulfites, and acetates showed little effect in the columns. This work has been extended, with similar results by Mills.[7] Acetone solutions of carbon dioxide and acetylene were tried without appreciable fractionation, indicating that the simple process fractionation factor differs but slightly from unity, for in these cases the rate of solution of the gas in the solvent is rapid. Cuprous chloride solutions of carbon monoxide and acetylene gave considerable indication that they might be used if no more suitable methods could be devised. The separation was not large, but would have been sufficient to produce carbon satisfactory for isotopic tracing. Exchange reactions involving solutions of methylamine hydrochloride and methylamine gas, and a simple solution of hydrogen cyanide in water and hydrogen cyanide gas gave very slight separation, as did also the distillation of formic acid and methyl alcohol. In the case of methyl alcohol, considerable separation of the oxygen isotopes resulted, but almost no separation of the carbon isotopes. In the methylamine exchange, there was some concentration of N^{15}. In view of these disappointing experiments we turned to the use of sodium cyanide solution exchanging with hydrogen cyanide gas for the purpose of separating the isotopes of carbon. This method was one of the first considered but had not been favored because of the discouraging polymerization of hydrogen cyanide in the presence of sodium cyanide and the highly poisonous character of hydrogen cyanide.

The reactions for hydrogen cyanide exchange are

$$HC^{12}N + C^{13}N^- = HC^{13}N + C^{12}N^- \quad K = 1.026$$
$$HCN^{14} + CN^{15-} = HCN^{15} + CN^{14-} \quad K = 1.003.$$

The equilibrium constants for these reactions

[6] F. J. W. Roughton and V. H. Booth, Biochem. J. **32**, 2049 (1938).
[7] G. A. Mills and H. C. Urey, J. Am. Chem. Soc. **62**, 1019 (1940).

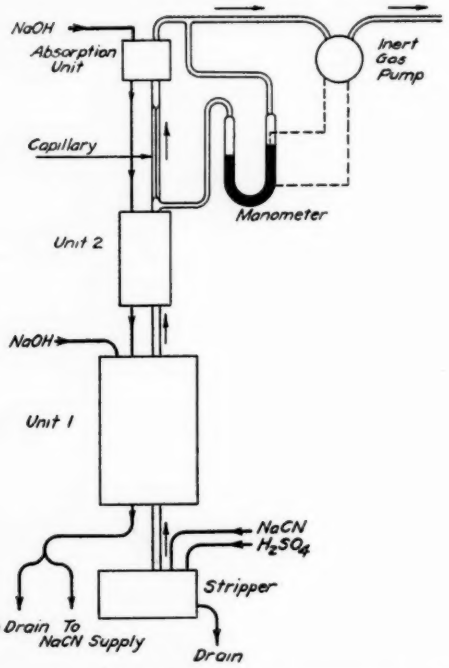

FIG. 1. Countercurrent system for the concentration of C^{13}.
——— liquid flow; ═══ gas flow;
- - - - - electrical connection.

were calculated using the known vibration frequencies of the HCN and CN^- molecules, and assuming that the ratio of the distribution functions for the cyanide ions in solution can be calculated by formulae applicable to the gaseous ions. The equilibrium constants calculated are given with the equations. The fractionation factor for the hydrogen cyanide-cyanide ion exchange for C^{12} and C^{13} is calculated to be about as favorable as that found in the case of the separation of the nitrogen isotopes using the ammonium ion-ammonia exchange reaction, for which $K=1.023$ (experimental).[8] In the case of carbon, however, the rare isotope concentrates in the gas phase instead of in the liquid phase as was true in the nitrogen experiments. The calculations for the cyanide exchange indicate that N^{15} will be concentrated to a much smaller extent than C^{13}. Actually, it is found that the N^{15} concentrates very slightly in the liquid phase.

APPARATUS

Because of the poisonous character of hydrogen cyanide it was deemed unwise to operate all three units of the cascade used in the nitrogen separation. A diagram of this apparatus appears in the paper by Thode and Urey.[8] Such operation would require a large amount of a solution of hydrogen cyanide to be present continuously in a building devoted to university instruction. We have, therefore, modified the two smaller units of the nitrogen apparatus for the separation of the carbon isotopes. In this case it is necessary that the feed of raw material be supplied at the bottom of the larger unit, instead of the top, and that reflux occur partially at the top of the larger, and totally at the top of the smaller unit. Quite obvious modification of the previous apparatus can be made. Fig. 1 shows schematically the system that was used.

The feed consisted of solutions of sodium cyanide and sulfuric acid pumped simultaneously into the reaction vessel at the bottom of the larger unit, which we shall call Unit 1. The hydrogen cyanide was boiled from the solution in a copper pot with a stripping column and the solution of sodium sulfate and excess sulfuric acid was pumped to waste, this pumping being regulated by means of a contact and relay in order to maintain a constant level in the refluxing boiler. The sodium cyanide solution flowing from the bottom of Unit 1 was divided into two parts by a suitable rubber tube pump,[8] one-half being pumped to waste and the other being returned to the supply of sodium cyanide so that it was used again, decreasing the amount of cyanide required. Sodium hydroxide was pumped into the top of Unit 1 at a fixed rate and also into the top of Unit 2 at a rate about one-fifth as great. A gas connection was made from the top of Unit 1 to the bottom of Unit 2 and sodium cyanide flowing from the bottom of Unit 2 was pumped continuously to the top of Unit 1. Final reflux of all hydrogen cyanide was made at the top of Unit 2. This arrangement permitted Unit 2 to use as starting material the concentrated product from the top of Unit 1.

The pressure was maintained at a constant value at the foot of the apparatus by a regulator which controlled the addition of sodium cyanide and sulfuric acid.

The fractionation units used in this apparatus are referred to as No. 1 and No. 2, and are the same as those designated as No. 2 and No. 3 in

[8] H. G. Thode and H. C. Urey, J. Chem. Phys. **7**, 34 (1939).

the apparatus used for the separation of nitrogen by Thode and Urey.[8] Rubber tubing pumps of the type described by these authors have been used throughout the apparatus. For small rates of flow, these have proved to be the most reliable of any pumps that we have used.

It was necessary to arrange for a continuous removal of inert gas from the top of the second unit. Air dissolved in the solutions constantly entered the apparatus and if it should accumulate at the top, it would gradually fill up the entire system and hence stop the flow of hydrogen cyanide gas upward through the columns. On the other hand, the removal of the air from the top of Unit 2 must be made in such a way that no hydrogen cyanide is lost since this would constitute a forward flow, and would represent a serious loss of heavy material, and if too large would prevent a building up of high concentrations at this point. Fig. 1 shows how this was accomplished. The hydrogen cyanide flowed from the top of Unit 2 through a capillary to the auxiliary absorbing unit. Sodium hydroxide was first pumped to the absorbing unit and then pumped from the bottom of this unit to the top of Unit 2. As long as flow is maintained through the capillary a pressure is maintained across a manometer with a contact actuating a gas pump. If inert gas builds up in the top of the auxiliary absorbing unit, the rate of flow of hydrogen cyanide through the capillary will decrease. This breaks the contact in the manometer and starts the vacuum pump which removes the inert gas from the top of the absorbing unit. This causes rapid absorption of hydrogen cyanide again and re-establishes the contact in the manometer, thus stopping the pump. This method has worked satisfactorily for long periods without serious difficulty. A trap containing a solution of silver nitrate was used to recover any traces of hydrogen cyanide which might be pumped off with the inert gas.

Details of Operation

3.3N sodium cyanide solution and 4.0N sulfuric acid were fed into the apparatus at the foot of Unit 1 from the two tubes of a double rubber tube pump. At the top of Unit 1, 4.7N sodium hydroxide solution was added at the rate of 9.0 cc per minute. At the top of the absorption unit sodium hydroxide solution was added at the rate of 2.0 cc per minute. The sodium hydroxide feed pumps were driven by governor controlled motors. In the case of all other pumps in the apparatus, the rate was not critical.

The chief difficulty encountered during the first operation of the apparatus was caused by the polymerization of hydrogen cyanide. The polymer of this substance is well known. It is a dark brown solid which plugged the columns and caused a marked lowering of the critical flooding rate of flow. Sodium sulfite added to the sodium hydroxide feed solutions was first used to cut down the rate of polymerization.[9] However, it was later found that sodium sulfide was much more effective for this purpose, under the conditions of operation of the apparatus. No serious difficulty was experienced from this source when the sodium hydroxide feed solutions were made 0.2M in sodium sulfide. In the last run of 27 days only small amounts of black polymer appeared in Unit 1.

If complex cyanides which do not exchange with cyanide ion should be formed at the top of our units, they would constitute a constant forward flow, for they would pass through the columns unchanged and be pumped to waste at the bottom of Unit 1. Experiments on the exchange between ferrocyanide ions and cyanide solutions showed that the rate of exchange was very small, and hence it was deemed advisable to use iron free sodium hydroxide. Solutions of such material were kindly supplied to us by the Michigan Alkali Company in rubber lined drums, the sodium hydroxide containing, according to the company's analysis, 0.3 part per million of iron, and correspondingly small amounts of other heavy metals which might form complex cyanides. Iron free sodium sulfide was conveniently prepared by absorption of hydrogen sulfide in the iron free alkali.

It will be seen by reference to Table I that the concentration of C^{13} produced by hydrogen cyanide gas flowing against an aqueous solution of hydrogen cyanide is very small. Hence it was desirable to keep the pressure in the apparatus as low as possible, in order that the amount of

[9] U. S. Patents, No. 1,856,606 and No. 1,950,899. We are indebted to the E. I. DuPont deNemours & Co. for permission to use these patents.

hydrogen cyanide dissolved in the liquid phase should be as small as possible. This pressure could not, however, be made less than a certain minimum value at the foot of Unit 1, where the pressure was controlled, because of the pressure drop through the packed columns. A satisfactory operating pressure at the foot of Unit 1 was found to be 12.5 cm of Hg.

Samples for analysis, and the C^{13} produced were withdrawn from the apparatus by attaching an evacuated bulb of suitable size at the top of Unit 2. Analyses were made with the mass spectrometer, as in the work previously reported. The hydrogen cyanide withdrawn from the apparatus was burned with oxygen over copper oxide and platinized asbestos, the water formed was frozen out, and the resulting carbon dioxide was used in the mass spectrometer. The ratio of the peaks due to $C^{12}O_2$ and $C^{13}O_2$ was determined.

As a safety measure, an auxiliary manometer was attached to the system and so adjusted that a contact was made if the pressure exceeded the working pressure by more than 3 cm of Hg. From this contact, a relay operated to interrupt the power supplied to the whole apparatus in case of a break in any of the columns or connections.

Results

In steady operation, under the most favorable conditions of pressure and rates of flow, the two units reached equilibrium after about twelve days. The approach to the maximum concentration was approximately linear when the isotope ratio was plotted against time. During this period, no material was drawn off and the C^{13} transported was used to build up the concentration of the working hold up in the columns. At equilibrium, the carbon at the top of Unit 1 contained 4.7 atom percent of C^{13}, and that at the top of Unit 2 contained about 26 atom percent of the heavier isotope. Depending upon the exact rate at which material was then withdrawn, the concentration in the final product varied from 22 to 25 percent C^{13}.

After a number of preliminary experiments, the apparatus was kept in operation during two runs of 58 and 27 days, respectively. In the first of these runs, several upsets occurred after equilibrium had been attained so that normal production was reached for only 26 days. In the second run, equilibrium was attained in twelve days. Following this, a steady rate of production was maintained for fifteen days, after which the run ended. During most of this time, 0.150 gram of C^{13} (in NaCN containing 23 percent C^{13}) were produced per day. In all, from the preliminary and final experiments, 80 grams of sodium cyanide were obtained with the maximum C^{13} concentration. This corresponds to about 5 grams of C^{13}. In addition, much larger quantities of sodium cyanide, with C^{13} concentrations ranging downward to twice the normal abundance, were obtained as drainings from the columns at the end of the several experiments.

The hold up in the columns was determined in a separate experiment. Sodium hydroxide solution ($4.7N$) was fed to the columns at the usual rate, and the number of equivalents of alkali determined by draining and rinsing the columns and titrating with acid. In the forty feet of 1″ column the working hold up was found to be 5.1 moles of cyanide; in the 25 feet of $\frac{3}{8}$″ column, the amount was 0.65 mole. Since the concentration of C^{13} increases exponentially along the columns, it was possible to find, by integration, the number of moles of C^{13} present in the apparatus at equilibrium. This amount was 0.209 mole, which is an excess of 0.149 mole over the ordinary concentration of C^{13}. Since this excess was accumulated over a period of twelve days, the transport of the apparatus was 0.0124 mole per day, or 0.161 gram of C^{13} per day. This may be compared with the value of 0.150 gram of C^{13} per day, which was the actual rate of production in the last run.

As Huffman and Urey[5] have shown, the rate of transport, T, is given very nearly by the expression

$$T = wN(\alpha - 1),$$

where w is the total flow in the column, N is the mole fraction of C^{13} in the original material, and α is the simple process fractionation factor. Using this equation, an experimental value for α is found to be 1.012_6. This is considerably lower than the value predicted by theory, and no completely adequate explanation can be offered for the discrepancy. The problem of the theory of such columns will be considered further by Dr. K. Cohen.[10]

[10] K. Cohen, J. Chem. Phys., in press.

To decrease the time required for the system to reach equilibrium would require a smaller hold up in the columns. This could be obtained by using a larger number of units in the cascade, each changing the concentration by a smaller amount than in the present apparatus, and each decreasing in cross section in proportion to the liquid flow through that unit. Calculations indicate that if five units, instead of two, were used, the time required would be reduced from twelve to five days.

Such a decrease in time required for the attainment of the maximum concentration is important since the slow polymerization will finally require interruption of the process, and this more rapid attainment of the steady state should make possible a larger production of material of maximum concentration.

We are indebted to the Michigan Alkali Company for the iron free sodium hydroxide used in this work. Dr. Karl Cohen and Mr. C. E. Miller shared in the operation of the apparatus, and during the final runs, A. Ackerman, L. Tenenbaum, and B. Weinstock also assisted in its operation.

JULY, 1940 JOURNAL OF CHEMICAL PHYSICS VOLUME 8

Ultrasonic Velocity in Carbon Dioxide and Ethylene in the Critical Region

CARL M. HERGET*
Rowland Physical Laboratory, The Johns Hopkins University, Baltimore, Maryland
(Received May 8, 1940)

Measurements of the velocity of ultrasonic waves in carbon dioxide and ethylene are presented; the velocity was obtained while the gas was allowed to follow a p–v isothermal. For carbon dioxide the pressure range is 5 to 98 atmospheres at temperatures of 28.0°, 30.0°, 31.0°, 32.0°, 33.0°, 35.0° and 38.0°C. For ethylene the pressure range is 35 to 75 atmospheres at temperatures of 9.7°, 18.7° and 23.0°C. For both gases, as pressure increases, the velocity decreases, falls to a sharp minimum, and then rises steeply on the high pressure side of this minimum. The minima have a discontinuity of slope for isothermals below the critical isothermal, which persists for a limited temperature range above the critical temperature. Above this range the curves become continuous in slope through the minimum. The curve log p *vs.* $1/T$ for the minima is linear through the critical point and, below the critical point, coincides within experimental error with standard vapor pressure data. Some calculations of ratio of specific heats near the critical point are included.

THE velocity of sound in gases near the critical state has been a neglected factor in the study of critical phenomena, largely because of practical difficulties only recently overcome by the development of ultrasonic technique. Hodge[1] in his work in this laboratory on ultrasonic velocity in gases as a function of pressure, included carbon dioxide vapor but stopped just short of the critical point. Spakovskij[2] made measurements in the critical range in carbon dioxide, apparently with audible sound. His reported results, while qualitatively correct in most cases, suffer in the higher pressure ranges both from inaccuracies and sparseness.

The present paper is a report of results obtained by ultrasonic interferometry on carbon dioxide and ethylene at pressures and temperatures including the neighborhood of the critical state. For CO_2 the pressure range is from 5 to 98 atmospheres between temperatures of 28°C and 38°C, and for ethylene pressures from 35 to 75 atmospheres and temperatures 9.7, 18.7, and 23.0°C. In extending the previous ultrasonic work of this laboratory at moderately high pressures, velocities have been determined with the screw interferometer[1] for carbon dioxide and ethylene and the fixed path interferometer[3] was

---

* Now at the Russell Sage Institute of Pathology, New York City.

[1] A. H. Hodge, J. Chem. Phys. **5**, 974 (1937).

[2] V. Spakovskij, Comptes rendus de l'Acad. Sci. URSS **3**, 31 (1934).

[3] J. C. Hubbard and I. F. Zartman, Rev. Sci. Inst. **10**, 382–386 (1939).

used to supplement the work on ethylene.[4] Thermodynamic data calculated in connection with these velocities will be more fully presented in a later paper.

The crystal sources were very large as compared with acoustic wave-length, thus providing a field of plane waves unaffected by diffraction. The interferometers were kept in an oil bath of a temperature easily controlled by a mercury thermal regulator to within ± 0.02°C of a predetermined value. Frequent readings of the bath temperature were taken during a run as a check.

The crystal was driven by the usual method of placing it in parallel with the condenser of a resonant LC circuit, the inductance of which picked up oscillations from a Dow electron-coupled oscillator. A vacuum thermocouple in the LC circuit, with its resultant e.m.f. fed to a galvanometer, allowed current changes in the circuit to be followed. The method of arriving at velocities of sound from these current changes has been amply given[5,6] and will not be repeated here.

The frequency of the driving oscillator was checked by comparison of its fundamental or harmonics with those of commercial broadcast stations. Calibration of the frequency was made some time during each run; there was never cause to discard a set of data because of frequency difficulties. Indeed, no frequency check showed a difference of more than 500 cycles from any other, and most of the calibrations obtained were within 200 cycles of each other. This means a maximum variation in frequency of ± 0.1 percent.

The pressure of the gas was measured by means of a gauge which was tested at the National Bureau of Standards and found to be accurate to within ± 0.5 percent over its entire range. It was graduated in intervals of 10 pounds and the reading could be estimated to about ± 1.0 pounds. While in much of the region studied variation of velocity with pressure is small, and hence a comparatively large tolerance of error in gauge readings is permissible, this is not the case in the immediate neighborhood of the critical point where relatively small pressure changes may produce large or even enormous changes in acoustic velocity. The use of the pressure gauge in this region was therefore supplemented by a method of producing easily inferred small changes of pressure by allowing small measured quantities of the gas to escape from the system.

The carbon dioxide was obtained from a commercial "bone-dry" tank, reputedly 99.5 percent pure. No attempt was made to purify the gas further, except that the valve was opened and the first pound or two of gas was blown off. It was then tested for water vapor by flowing a known volume of the gas, as determined by a flowmeter, through an absorption tube of magnesium perchlorate trihydrate. The carbon dioxide was found to contain slightly less than 0.09 percent water vapor.

The ethylene was of commercial "anaesthesia" grade, probably 99.7 percent pure since it was revealed that at the time the cylinder was bought the purity of the product was higher than the 99.5 percent imposed on this grade. An attempt was made to get rid of residual water vapor and carbon dioxide by cooling the cylinder in cracked ice and salt, and opening the valve until the first few pounds of pressure had been spent. The remainder of the gas was then used without any chemical analysis.

In determining velocities, the procedure was as follows: Gas from the tank was allowed to flow through the chamber until it was thoroughly washed out, after which the exit valve was closed. The bath was cooled about 10° below room temperature and interferometer chamber and gas tank were opened to one another. After sufficient time, dictated by experience, the interferometer chamber was sealed off by means of a needle valve and the bath heated to the desired temperature. By this means pressures higher than those of the gas in the tank could be obtained. After the bath had reached the desired temperature, about an hour was allowed for thermal equilibrium to be established. As is well known from the results of screw interferometry, current reaction peaks, in the absence of strong absorption, are of such sharpness as to be sensibly influenced by changes of temperature smaller than can be detected except by the most delicate

[4] C. M. Herget, Rev. Sci. Inst. **11**, 37–39 (1940).
[5] J. C. Hubbard, Phys. Rev. **38**, 1011 (1931); **41**, 523 (1932); **46**, 525 (1934).
[6] R. S. Alleman, Phys. Rev. **55**, 87 (1939).

means. A very delicate test, then, as to whether equilibrium conditions obtained, was to set the reflector of the interferometer at a nodal position, and observe whether, upon waiting, the reaction peak remained at that reflector setting. If it did, thermal equilibrium was considered attained. Three nodal settings of the reflector near the crystal, and three with the reflector some ten to twenty wave-lengths farther away from the crystal were recorded, along with both temperature and gas pressure. Then the gas was allowed slowly to flow out until the pressure had dropped to the next desired point, equilibrium was again established, and the process repeated. In the best of cases, this procedure gave three wave-length readings for a given pressure which checked with each other to within 2×10^{-5} cm or better than one part in 3000; at other times, due to conditions to be discussed, the agreement was not so good.

Since the frequency was known, this determination of the wave-length allowed the velocity to be computed.

One of the first things which became apparent was the behavior of the quartz crystals under pressure. As pressure was increased, the crevasse became broader and more shallow, and began to be overlapped by neighboring crevasses. This introduced a structure into the reaction peaks, so that they no longer gave simply the rise and fall of a single crevasse, but were influenced also by neighboring crevasses. Since each component in the reaction peak corresponded to a slightly different frequency from any other, this meant that the maximum might shift its position along the reaction peak as the piston advanced from position to position and introduce an error into the determination of the wave-length. This is undoubtedly the cause of the disagreement in wave-length determinations referred to above; however, care was taken to use only crevasses which showed a minimum of such effect and the errors introduced in the velocity readings by this cause were still much smaller than 0.5 percent, the limit set by the pressure gauge.

A third source of inaccuracy entered just at the critical point of both of the gases investigated. Here a state of confusion, doubtless produced by the well-known density fluctuations near the critical point in the chamber was evidenced by unsteadiness of reaction peaks, much more marked in ethylene than in carbon dioxide. In addition, the ethylene at its critical point showed a high scattering of sound, making it impossible to obtain any evidence of the sound field at distances from the crystal of more than five or six wave-lengths. Over the entire range of the results presented the accuracy is within 0.05 percent, except at the minimum of the velocity-pressure curve through the critical point, where the velocities for carbon dioxide are to be considered to have an error of ±2.0 percent, and for ethylene ±3.5 percent. This region of larger errors extends about one-quarter atmosphere either side of the minimum in each case.

At the higher pressures, some crevasses became entirely wiped out, and movement of the piston gave the "liquid" type of reaction. In these cases, the velocities were determined according to the treatment usual with liquids.[7,8]

The velocities determined are given in Tables I, II and III. It will be observed that the velocity curves have a cusp-like minimum in the critical region and below it. In the latter case a discontinuity of slope as well as of velocity values might be expected at change of state, but only a discontinuity of slope was observed. The trend of velocity with increase of pressure, with temperature as the parameter, is shown in the graphs (Figs. 1 and 2). Although the absolute accuracy of the pressure was limited by the gauge to ±0.5 percent, as was previously stated, the readings in a series are believed to be consistent with one another to about ±0.05 atmosphere.

It therefore becomes of interest to know with greater resolution the shape of the minima of the curves, and especially to determine whether or not the discontinuity of slope extended to temperatures above the critical temperature. Accordingly, a series of determinations at 32.2°C was taken of velocity *versus* volume of CO_2 removed from the interferometer, this latter quantity serving in place of gauge pressure readings, as by this means it was possible to measure variations due to pressure changes less than could be observed by the gauge. This gives a much expanded picture in the region of the

[7] Hubbard and Loomis, Phil. Mag. (7) **5**, 1177 (1928).
[8] F. E. Fox, Phys. Rev. **52**, 973 (1937).

TABLE I. *Carbon dioxide.*

FREQUENCY KILOCYCLES	VELOCITY METERS/SEC.	PRESSURE ATMOSPHERES	FREQUENCY KILOCYCLES	VELOCITY METERS/SEC.	PRESSURE ATMOSPHERES
Temperature, 28.0°C					
266	317.6	77.50	287.5	186.2	68.27
266	310.7	77.17	226	188.9	68.00
266	303.2	75.95	266	192.9	67.04
287.5	301.4	75.86	266	193.3	66.90
287.5	291.2	74.39	266	197.4	65.61
287.5	278.6	73.60	266	199.3	65.12
287.5	251.9	70.49	266	203.6	63.50
266	242.8	70.00	266	214.2	57.79
266	226.9	69.18	266	226.1	49.35
287.5	(225)	68.95	266	239.4	37.80
287.5	184.0	68.65	266	255.3	20.59
226	186.9	68.27	266	265.3	8.76
Temperature, 30.0°C					
285.5	324.8	85.60	266	183.3	71.09
285.5	303.9	81.20	266	186.5	70.62
285.5	261.9	76.41	266	188.4	70.50
285.5	222.8	72.81	276.5	190.4	70.21
285.5	209.9	72.53	291	190.1	70.21
266	186.4	72.01	266	189.6	70.18
283	187.2	72.01	291	208.4	63.22
260.2	189.7	71.93	266	220.5	55.13
266	186.4	71.86	266	238.5	38.41
266	187.6	71.86	266	246.7	31.80
287.3	182.0	71.79	266	249.6	28.72
266	177.2	71.71	266	257.9	26.03
266	177.4	71.62	266	264.9	10.73
Temperature, 31.0°C					
266	329.3	88.10	266	210.4	63.10
266	310.0	84.98	266	211.9	62.40
266	286.0	81.18	285.5	213.6	60.58
267.9	291.4	80.85	266	219.8	57.72
266	239.0	76.27	266	234.8	45.14
266	223.5	75.19	285.5	239.7	39.97
266	210.7	74.60	266	240.4	39.49
274.1	203.6	73.95	266	245.6	33.17
274.1	172.0	73.48	266	247.8	31.73
274.1	158.3	73.25	266	250.9	28.47
266	150.1	73.17	266	254.3	24.94
274.1	157.3	73.16	266	254.7	24.13
274.1	168.8	73.09	266	256.3	21.61
274.1	173.9	72.96	266	259.2	17.39
274.1	178.0	72.81	266	261.5	14.54
266	182.8	72.48	266	264.6	12.43
266	200.7	68.22	266	265.4	10.19
Temperature, 32.0°C					
287.5	340.2	93.00	266	172.7	74.58
266	315.6	88.40	266	173.4	74.41
266	279.3	81.60	266	191.7	72.39
266	261.7	80.38	266	214.9	61.32
266	243.3	78.65	266	233.8	46.70
287.5	225.8	77.21	266	241.0	39.59
266	219.3	77.19	266	247.1	33.17
266	197.8	76.04	266	248.5	31.73
266	182.7	75.79	266	254.6	25.01
266	170.7	75.44	266	255.2	24.87
287.5	177.4	75.20	266	255.6	23.51
266	154.8	75.10	266	257.5	21.68
287.5	156.1	75.02	266	259.5	18.55
266	167.9	74.99	266	262.1	14.54
287.5	169.6	74.58	266	264.2	12.50

TABLE I.—*Continued.*

FREQUENCY KILOCYCLES	VELOCITY METERS/SEC.	PRESSURE ATMOSPHERES	FREQUENCY KILOCYCLES	VELOCITY METERS/SEC.	PRESSURE ATMOSPHERES
Temperature, 33.0°C					
266	323.0	92.85	266	206.2	68.35
266	300.6	88.00	266	216.1	62.29
268	292.7	87.41	266	228.7	51.75
266	264.7	82.92	285.5	231.1	48.89
266	205.9	78.17	266	240.1	41.80
266	193.9	77.68	266	249.3	31.67
266	187.3	77.40	266	252.5	28.41
266	170.6	77.20	266	254.7	25.01
266	167.8	76.78	266	255.5	24.95
266	166.9	76.64	266	258.2	21.41
266	172.1	76.40	266	257.9	21.34
266	182.5	75.87	266	260.6	17.39
266	182.7	75.49	266	263.8	13.11
266	197.3	72.30	266	264.9	12.50
266	206.3	68.40	266	266.2	11.14
			266	270.4	5.97
Temperature, 35.0°C					
266	331.8	99.58	266	184.2	78.58
266	313.9	95.71	266	187.6	77.99
266	300.4	93.06	266	189.2	77.56
266	267.9	87.79	266	196.7	75.61
266	221.6	83.14	266	198.5	75.59
266	212.0	82.17	266	204.2	72.48
266	196.3	81.30	266	211.2	67.93
266	187.5	80.77	266	218.1	62.87
266	183.3	80.43	266	213.7	51.84
266	181.0	80.16	287.5	239.2	42.19
266	179.7	79.67	266	241.4	42.19
266	180.2	79.48	266	249.0	33.17
266	179.2	79.48	266	251.4	31.26
266	180.4	79.41	266	267.3	11.14
Temperature, 38.0°C					
266	249.4	99.63	266	192.1	83.87
266	261.3	92.65	266	193.0	82.40
266	215.4	87.61	266	196.3	80.87
268.1	209.1	87.00	274.2	198.4	80.72
267.9	194.0	85.28	268.1	201.4	79.13
266	193.5	85.21	266	207.5	74.63
267.8	192.3	85.07	266	212.3	71.83
267.9	192.2	84.70	266	224.3	62.22
274.2	193.4	84.70	274.3	232.3	53.90
273.2	192.3	83.40	275.2	243.0	42.88
			266	247.7	37.65
268.1	193.0	83.33	266	268.0	11.14

minimum. The points plotted in this way could be interpreted either as falling on a smooth curve or on a curve having discontinuous slope at the minimum. However, very careful gauge readings had been taken in the run, and when the velocity was plotted against pressure instead of against volume change, the points indicated that there was a discontinuity in slope at the gaseous side of the minimum. Fig. 3 shows these results along with a magnified portion of the

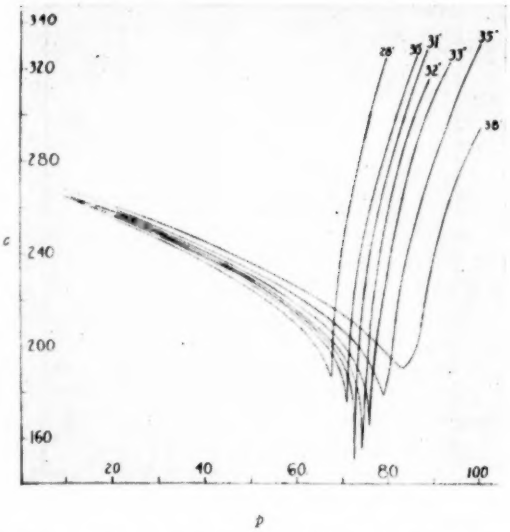

FIG. 1. Trend of ultrasonic velocity (c) in meters per second with pressure (p) in atmospheres above atmospheric, for carbon dioxide at the various temperatures indicated.

minimum of the critical velocity-pressure isothermal.

The minima of sound velocity occur at temperatures and pressures which below the critical point, as would be expected, fall on the p, t equilibrium curve of liquid-vapor. Above the critical point the temperatures and pressures of the

TABLE II. *Ethylene. Frequency—274.1 kilocycles.*

VELOCITY METERS/SEC.	PRESSURE ATMOSPHERES	VELOCITY METERS/SEC.	PRESSURE ATMOPSHERES
Temperature, 9.7°C			
348.5	58.48	165	51.06
318.0	56.97	162	51.06
309.0	55.30	160	50.98
298.6	54.59	193.0	50.76
290.0	53.97	202.8	50.65
280.8	53.41	222.0	49.16
263.0	52.95	239.1	45.21
225.0	51.67	247.6	42.47
196.2	51.26	265.3	35.27
Temperature, 18.7°C			
335.4	71.77	234.1	61.44
325.6	70.55	232.4	61.13
322.8	70.38	229.3	60.37
311.5	69.19	228.7	59.62
306.5	68.48	229.6	58.81
300.3	67.79	230.6	58.19
275.5	65.61	236.8	55.06
254.8	63.62	247.2	50.71
246.5	62.90	261.5	43.65
240.4	62.22	276.8	35.68

TABLE III. *Ethylene. Temperature, 23.0°C.*

FREQUENCY KILOCYCLES	VELOCITY METERS/SEC.	PRESSURE ATMOSPHERES	FREQUENCY KILOCYCLES	VELOCITY METERS/SEC.	PRESSURE ATMOSPHERES
274.1	249.9	66.78	598.0	253.1	51.84
274.1	246.3	66.18	298.0	257.4	49.69
274.1	242.1	65.00	274.1	261.1	47.58
274.1	240.3	64.38	598.0	261.5	47.43
274.1	237.7	62.88	598.0	266.4	44.60
274.1	237.2	61.67	598.0	271.1	41.92
274.1	238.4	61.06	274.1	272.1	41.34
274.1	240.7	59.50	598.0	273.6	40.58
274.1	244.2	56.98	598.0	276.1	39.19
598.0	249.0	54.19	598.0	278.6	37.67
274.1	256.1	52.80	274.1	281.6	35.74

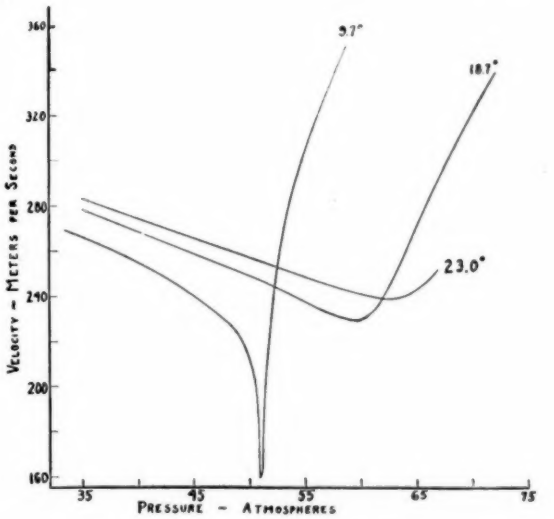

FIG. 2. Trend of ultrasonic velocity with pressure for ethylene at the temperatures indicated.

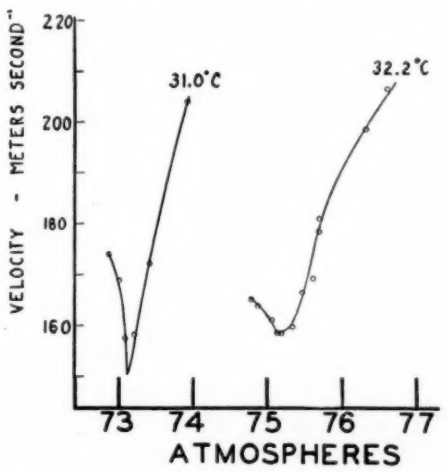

FIG. 3. Large scale plot of two velocity-pressure curves in the immediate neighborhood of the minimum.

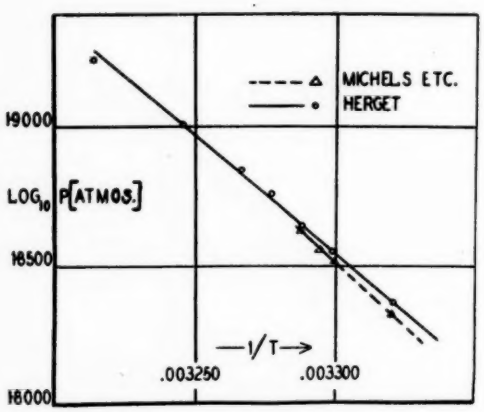

FIG. 4. Log of pressure (in atmospheres) at which minimum occurs in velocity of sound plotted against the reciprocal of the temperature at which the velocity was taken.

sound velocity minima form a natural continuation of the same curve, as predicted from thermodynamics by Eucken.[9] This becomes evident on inspection of Fig. 4. Interest in this subject has been greatly enhanced by the recent work of Professor J. E. Mayer[10] and his students, who have approached it from the point of view of statistical mechanics. Fig. 5 shows two isotherms of the ratio of specific heats of CO_2 calculated from the values of sound velocity and the *pv* data of Amagat.[11] These are included as an illustration of the marked deviations of such

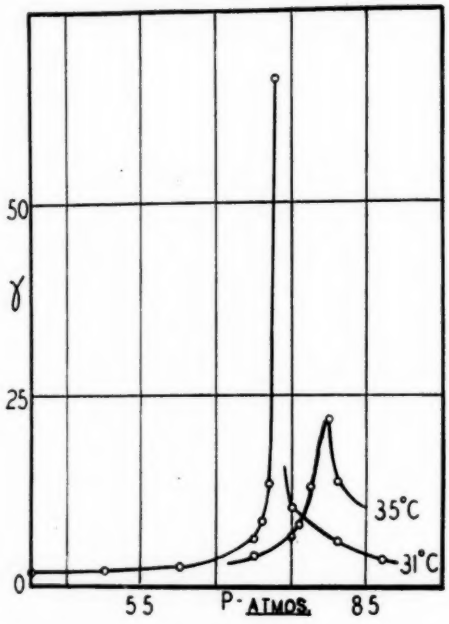

FIG. 5. Plot of ratio of specific heats (γ) *vs.* pressure in atmospheres for carbon dioxide for 31°C and 35°C.

quantities at the critical point and near it. A detailed consideration of the bearing of the results of this paper upon the thermodynamic properties of CO_2 and ethylene will be given in a forthcoming paper.

The author wishes to express his thanks to Professor J. C. Hubbard, under whose direction the work was done, to Professor A. H. Pfund for valuable suggestions, and to Professor J. E. Mayer for many helpful discussions.

[9] A. Eucken, Physik. Zeits. **35**, 708 (1934).
[10] S. F. Harrison and J. E. Mayer, J. Chem. Phys. **6**, 101 (1938).
[11] For method of calculation see J. C. Hubbard and A. H. Hodge, J. Chem. Phys. **5**, 978 (1937).

The Reactions of Methyl Radicals with Benzene, Toluene, Diphenyl Methane and Propylene

HUGH S. TAYLOR AND JOHN O. SMITH, JR.
Frick Chemical Laboratory, Princeton University, Princeton, New Jersey

(Received March 5, 1940)

The reactions of methyl radicals with benzene, toluene, diphenyl methane and propylene to yield methane have been studied in the temperature range of 100–260°C. With toluene the activation energy is 5.6 kcal. and with propylene 3 kcal. Diphenyl methane shows a reactivity corresponding to these low values while the experiments with benzene, as well as earlier work with ethylene, indicate much higher activation energies of methane formation. The activation energies obtained have been correlated with earlier data on reactions with saturated hydrocarbons, with thermal data indicative of the strength of individual C–H bonds, with similar data from the interaction of atomic sodium with halide compounds, with concepts of the organic chemist on bond strengths and with some experimental data on pyrolysis of toluene. It is concluded that, contrary to accepted views, there may be marked differences in C–C and C–H bond strengths among the various hydrocarbons studied.

WE have extended our earlier investigations on the reactions of methyl radicals with various saturated paraffin hydrocarbons[1] to another group of hydrocarbons including benzene, toluene, diphenyl methane and propylene. Our previous work indicated that the activation energies of the reactions of methyl radicals with ethane, neopentane, butane and isobutane were, respectively, 8.3, 8.3, 5.5 and 4.2 kcal., based on an assumed activation energy $E=0$ for ethane formation by radical recombination. We associated these differences in activation energy with the similar differences in the bond energies of primary, secondary and tertiary C–H bonds in saturated paraffins indicated by the data of Kistiakowsky and his colleagues[2] on the heats of hydrogenation of the substituted ethylenes.

Our choice of new reactants for study was obviously dictated by a desire to ascertain the influence of a double bond on the reactivity of the hydrogens on carbon atoms involved in the double bond or adjacent thereto. Various earlier researches and especially the recent work of Taylor and Jungers[3] had indicated a much smaller methane formation from the reaction of methyl radicals with ethylene than obtains with the saturated hydrocarbons. Also, it is known from a variety of observations in organic chemistry, that the presence of a double bond in the molecule appears to produce an alternation of strength throughout the molecule, so that in a compound such as

$$\mathrm{CH_3}-\overset{2'}{\mathrm{CH_2}}-\overset{1'}{\mathrm{CH}}=\overset{1}{\mathrm{CH}}-\overset{2}{\mathrm{CH_2}}-\mathrm{CH_3},$$

the carbon-carbon bond (1 or 1′) next to the double bond is strong, the next (2 or 2′) is weak and so on.[4] If this view can be extended to the strength of the C–H bonds in a hydrocarbon system then the primary C–H bonds in propylene and also in toluene should be weak. The reactions of methyl radicals with such hydrocarbons should reveal such a condition. The interest attaching to the investigation was heightened by the investigation recently reported by Hein and Mesée[5] concerning the pyrolysis of the toluene molecule when investigated by the Paneth-F. O. Rice low pressure technique with mercury mirrors. It was shown by these authors that, of the three possible radical products of such a pyrolysis, phenyl +methyl, tolyl+H, and benzyl+H, the latter practically exclusively occurs, since only dibenzyl mercury could be found among the products.

EXPERIMENTAL DETAILS

The apparatus employed and the mode of procedure were as described in the earlier communication. Mercury dimethyl vapor at 40 mm

[1] J. O. Smith and H. S. Taylor, J. Chem. Phys. **7**, 390 (1939).
[2] E.g., J. B. Conn, G. B. Kistiakowsky and E. A. Smith, J. Am. Chem. Soc. **61**, 1873 (1939).
[3] H. S. Taylor and J. C. Jungers, Trans. Faraday Soc. **33**, 1353 (1937).
[4] For an extended discussion, with literature, see O. Schmidt, Zeits. f. Elektrochem. **39**, 976 (1933).
[5] F. Hein and H. I. Mesée, Naturwiss. **26**, 710 (1938).

pressure, photolyzed with ultraviolet radiation, was the source of methyl radicals and these were produced at the working temperatures recorded below in presence of ~200 mm of the reactant vapor. The products were examined as in the earlier work for methane and, where possible, for ethane. So far as the present work is concerned no importance attaches to the nature and extent of other products. In all these experiments a constant intensity of illumination entered the reaction system. It is evident, however, that varying fractions of this incident radiation were consumed in methyl radical production owing to the variations in the light absorption of the hydrocarbon reactant. Since we are concerned with temperature coefficient of methane production rather than with absolute rate of reaction this factor is of less significance.

Experimental Results

The data obtained in the investigation with toluene, benzene, diphenyl methane and propylene are summarized in Table I. For comparison purposes two experiments with nitrogen and one with hydrogen as the other reactant are also included. The values of k recorded indicate the rate of production of methane and of ethane, respectively, in cc at N.T.P. per minute.

A plot of log $k_{CH_4}-1/T$ for toluene gave a straight line with a slope corresponding to an activation energy of 5.6 kcal. if the activation energy of ethane formation is zero and the reaction studied is $CH_3+C_6H_5CH_3=CH_4+R$. This value is to be contrasted with the values of 8.1 and 8.3 kcal. obtained previously with ethane and neopentane. This indicates that the adjacent double bond in the benzene ring has an effect equivalent to a loosening of the CH bonds in the methyl group of the toluene to the extent of 2.5 kcal. The C−H bonds in the methyl of toluene thus appear to behave approximately as the secondary C−H bonds in a saturated hydrocarbon such as butane which showed an activation energy of 5.5 kcal.

The low yield of methane with benzene as the reactant is shown in Experiments 5–8. The quantities of methane involved are so small that they are heavily influenced by experimental error and are therefore unsuited to calculations

Table I. *Photochemical decomposition of mercury dimethyl in presence of various reactants.*

Reactant	Expt. No.	T°K	$k_{CH_4}\times10^3$	$k_{C_2H_6}\times10^3$	ΔP
Toluene	1	376	5.4	24.2	
	4	432	14.5	20.6	
	2	469	25.2	22.9	
	3	522	42.0	12.0	
Benzene	8	385	1.97	43.2	
	7	430	4.33	37.0	
	5	473	4.46	37.6	
	6	520	10.2	49.0	
Diphenyl methane	20	478	26.1	1.0	
	19	538	43.9	1.91	
Propylene	18	383	8.83	—	124[a]
	17	430	14.82	—	214
	15	480	19.25	—	605
	16	539	28.6	—	—
Nitrogen	11	480	13.7[b]	90.1	
	13	482	19.1[b]	104.3	
Hydrogen	12	480	193.5	93.1	

[a] The decrease in pressure is given in cc at N.T.P. per minute $\times10^3$. It may be assumed to be a measure of propylene polymerization.
[b] The methane was determined in these cases by oxidation to carbon dioxide and measurement as such.

of activation energy. The low values indicate qualitatively, however, a much higher activation energy for the interaction with methyl radicals to form methane especially as the ethane yields point to higher methyl radical concentrations than with toluene. The methane yield in benzene is of the same order of magnitude per unit of ethane produced as with nitrogen. It probably arises in major part from interaction of methyl with mercury dimethyl.

With diphenyl methane as the reactant the methane formation is as great as with toluene under comparable conditions while the ethane formation is considerably less. This points to a still lower activation energy than 5.6 kcal. for the process. No value is given because only two measurements were made, but it is of interest to note that the methane yields exceed those of propylene at comparable temperatures.

The plot of log $k_{CH_4}-1/T$ for the reaction with propylene gives a good straight line corresponding to an activation energy of 3.1 kcal. This is the lowest energy of activation that we have found in the whole range of hydrocarbons studied. The ease of methane formation with propylene in contrast to the difficulty with ethylene indicates that it is the hydrogens of

the methyl group in the propylene which are reacting. The data suggest that these bonds behave as though less firmly bound than the C−H bonds in ethane since the activation energy of the reaction is 8.1−3.1=5 kcal. less.

The data with propylene also indicate once more the efficiency of radicals in the initiation of polymerization processes. This is clearly seen from the data in the final column of Table I. The ratios $\Delta P/k_{CH_4}$, both expressed in cc at N.T.P. per minute$\times 10^3$ are, respectively, 14, 14 and 31 at 383, 430 and 480°K. These would represent actual chain lengths if the polymerization were initiated by the formation of an allyl radical and methane from propylene and methyl. The low activation energy of methane formation revealed in this case indicates that ethane formation from methyls will be correspondingly low. No matter therefore what the nature of the initiation of the polymerization process may be there is clearly an excess of propylene disappearing over the maximum amount of methyl radicals introduced.

The large yield of methane in presence of hydrogen confirms earlier results of the same nature, all indicative of a chain mechanism of methane formation in this case. As was found earlier by Cunningham and Taylor this increased methane formation is secured without decrease in ethane production.

General Discussion

The results obtained with benzene and toluene provide a quantitative basis for the observations of Hein and Mesée concerning the formation of benzyl radicals by the low pressure pyrolysis of toluene. The presence of the phenyl substituent in the toluene molecule lowers the activation energy of the reaction 2.5 kcal. below that with a primary C−H bond in a paraffin saturated hydrocarbon, while the activation energy of the reaction with the C−H bonds in benzene is greater than that with an aliphatic hydrocarbon. It is the C−H bonds in the methyl group in toluene which are the weak linkages involved in free radical formation, and the weakness is to be ascribed to the influence of the adjacent double bond.

This double bond influence is most marked in the reaction with propylene where the decrease in observed activation energy over the primary bond in saturated hydrocarbons amounts to 5 kcal. It is obvious that in any free radical mechanism involving saturated hydrocarbons, reaction of the radical with propylene would be faster than that with either primary, secondary, or tertiary C−H bonds in the saturated molecule. Such interaction would yield, as Rice and Polly[6] have pointed out, the allyl radical. The weakness of the allyl-H bond here indicated as compared with the C−H bonds in the saturated molecules implies a correspondingly decreased efficiency as a chain link in such chain decomposition processes. The radical would have a longer life and would have greater opportunity to disappear by collision with itself or other radical to produce diallyl or a substituted propylene, respectively. The formation of this latter would have a net effect of breaking two radical chains and of producing an olefine of approximately equal efficiency with propylene as a chain breaking agent. The formation of diallyl would have the net effect of breaking one chain per propylene, the diallyl probably having a further efficiency as chain breaker by reason of its C−H bonds on the carbon atoms in the β position to the two double bonds.

With ethylene such conditions do not immediately obtain. The strong C−H bonds in this compound imply a lesser reactivity with methyl radicals to form methane than with the saturated hydrocarbons. Association of ethylene and alkyl radicals generates a higher alkyl radical. It is not surprising therefore that Echols and Pease[7] found no inhibitory influence of ethylene and a marked influence of propylene on the thermal decomposition of *n*-butane. Our data suggest that benzene should exercise no inhibitory influence in such processes but that toluene and diphenyl methane should have an effect, less pronounced than that of propylene.

It is of great interest that these determinations of activation energies of reaction of methyl with both unsaturated and saturated hydrocarbons parallel entirely the results obtained by Polanyi and his collaborators in their studies of the

[6] F. O. Rice and O. L. Polly, J. Chem. Phys. **6**, 278 (1938).

[7] L. S. Echols and R. N. Pease, J. Am. Chem. Soc. **61**, 1024 (1939).

interaction of sodium vapor with a variety of organic halides.[8] In these quite different reactions they also find an increase in the rate of reaction and decrease in activation energy on passage from primary to secondary to tertiary carbon. In both sets of experiments decrease in activation energy is found for compounds with a carbon double bond in a position once removed from the atom linkage attacked and an increase in activation energy or retardation of reaction rate if the reacting atom is directly attached to the double-bonded carbon atom. The actual experimental data in both the Polanyi experiments and our own indicate that differences in activation energies amounting to as much as 10 kcal. obtain in the extreme cases involving the slowest and the most rapid rates for the given process. The activation required depends upon the nature of the carbon compound in which the bond occurs and on the location of the bond in the compound.

The differences in activation energy between ethylene and propylene on the one hand and between benzene and toluene on the other may be associated with the resonance characteristics of the allyl and benzyl radicals produced, from propylene and toluene, respectively, by withdrawal of a hydrogen atom. It has been estimated[9] that the resonance energy of the allyl radical amounts to 15.4 kcal. so that this energy would separate the potential energy surface of the radical-methane product from that which would obtain with a nonresonating radical-methane product from another hydrocarbon reaction as, for example, that between methyl and ethylene. A similar energy difference, due to resonance, of the activated complexes in the two reactions would account fully for the differences in methane formation observed. Similar differences between the well-known resonating structure, the benzyl radical, and that of phenyl would account for the differences in reactivity between toluene and benzene. For the same reason, the reactivity of methyl radicals towards diphenyl methane ought to be greater than that towards toluene, as actually found.

The interpretation of the experimental data with respect to the unsaturated and aromatic hydrocarbons on the basis of resonance energy of the activated complexes and the radicals produced rather than on the basis of bond strengths of the compounds studied raises the question as to whether the data on the reactivities of the primary, secondary and tertiary C−H groupings in the saturated hydrocarbons might not be similarly interpreted. In these cases the radicals formed, e.g., ethyl, butyl, isobutyl, are not ordinarily regarded as resonating structures. The differences in activation energies observed, amounting to 4 kcal. between ethane and isobutane are of a lower order of magnitude than those observed between ethylene and propylene. By attributing these differences of activation energy to differences of stability due to resonance effects between such radicals as ethyl and isobutyl, one could retain the Pauling principle of C−H bond energies practically identical in magnitude in the saturated hydrocarbons. The thermochemical data of Kistiakowsky and his co-workers do however suggest that differences in bond energies up to but not exceeding those found in our earlier work may exist in such systems.

A more difficult problem is involved, however, in the application of resonance to the comparative rates of formation of methane from the interaction of methyls with ethane and ethylene. The greater reactivity of ethane would suggest that there was a much greater resonance in the activated complex $[CH_3-C_2H_6]$ than in that of $[CH_3-C_2H_4]$. It is not at once evident why this should be so. The alternative is that the C−H bond strength in ethylene is stronger than that in ethane. This conclusion is in accord with classical views in organic chemistry. It is deriving support from the work now in active prosecution which interprets the restricted rotation in a molecule such as ethane in terms of the effect of the methyl radical on the adjacent C−H bonds, tending to weaken these. The same processes of reasoning would lead to a strengthening of the C−H bonds in ethylene. As already emphasized the problem is not peculiar to C−H systems but extends, as in the work of Polanyi, to the carbon-halogen linkages in various homologous groups of organic compounds.

[8] For a convenient summary of these data, see M. Polanyi, *Atomic Reactions* (Williams and Norgate, London, 1932), Section 3, pp. 49–50.

[9] J. E. Lennard-Jones and C. A. Coulson, Trans. Faraday Soc. **35**, 811 (1939).

A Chemical Detector for Molecular Beams

J. H. SIMONS AND J. GLASSER
School of Chemistry and Physics, The Pennsylvania State College, State College, Pennsylvania

(Received March 13, 1940)

A thin film of tellurium has been found satisfactory for a detector plate for atomic hydrogen, oxygen, chlorine, and bromine and offers promise for organic free radicals. By a method of intensification with the use of positive development a high sensitivity is obtained. The technique of the preparation, use, and development of this detector is given. A list of possible uses of this detector is included.

CHEMICAL detectors for molecular beams have been used for atomic hydrogen,[1] atomic oxygen,[2] and for other purposes. As the chief disadvantage of a chemical detector is its low sensitivity, a means of intensifying the image is important. Images formed by condensation from beams of copper, silver, gold, nickel, iron, lead, and thallium have been intensified by wet physical development methods.[3] A chemical detector has advantages in that it is selective for one type of particle in a mixed beam, and the image is permanent and can be removed from the apparatus and photographed.

We have found that a film of tellurium would serve as a detector for beams of atomic hydrogen, oxygen, chlorine, and bromine, the image being formed by the removal of the metal. Intensification of the plate by physical development enabled invisible films to be used; the sensitivity was, thereby, greatly increased.

Tellurium is a particularly useful substance for the detecting film as it forms compounds such as the hydride, oxide, chloride, and bromide which are more volatile than the element. It also forms volatile organic compounds. The film is readily formed by vaporization of the element and condensation on the target plate. A distinct and particularly useful property is the fact that the film is not deactivated by molecular oxygen, water vapor, etc., so that it can be exposed to the laboratory atmosphere. It is known that films of lead, antimony, zinc, and cadmium[4] are deactivated by oxygen when used for organic radicals. The tellurium film can be intensified by a positive development using a silvering solution.

TECHNIQUE

The glass slit systems were made in two ways. For use with hydrogen atoms from a hot wire source it was made by pinching a glass tube over a supported nichrome ribbon and then dissolving the metal with hot hydrochloric acid.[1] For the other experiments it was made in the following manner. Two flat circular disks of glass 1 mm thick were ground with a V notch along a diameter until the depth of the V was one-half the thickness of the disk. Each disk was then broken and the two broken edges were ground together to make a flat smooth fit. One semicircular piece was then placed in a frame and a slit ground in it in the middle of the straight edge with another piece of flat glass. A microscope was used for observation. The two halves of the disk were then placed together on the flat ground end of a glass collar and carefully sealed. The collar was ring sealed in a piece of glass tubing. The other slit was made in a similar manner. To line up the slits the ends of the tubes containing them were first ground flat. These ends were then placed together and rotated until the slits were in line as determined optically. Clamped in this position they were carefully sealed. The dimensions of the slits were 0.05×2.5 mm and 0.5 mm thick. They were 5.5 cm apart, and the second slit was 5.0 cm from the detector.

For the electrodeless discharge source of atoms a 1-k.v.a. 25,000-v transformer was used. It consumed 10 to 20 amp. from a 110-v 60-cycle power supply and was coupled to a spark gap of air-cooled zinc electrodes. For the hot wire

[1] Phipps and Taylor, Phys. Rev. **29**, 309 (1927).
[2] Kurt and Phipps, Phys. Rev. **34**, 1357 (1929).
[3] Esterman and Stern, Zeits. f. physik. Chemie **106**, 399 (1923). Gerlach, Ann. d. Physik **76**, 179 (1925).
[4] Paneth and Lautsch, Ber. **64**, 2708 (1931).

source of hydrogen atoms a tungsten filament was heated by current from storage batteries. The 1.6 amp. gave a temperature of approximately 2800°K.

The detecting chamber is shown in Fig. 1. The tellurium furnace is made of a small piece of 10-mm glass tubing. It has a 2-mm opening in the front and is about 3 cm long. It is wound with eight turns of 10-mil tungsten wire. The wire is imbedded in a glass capillary and sealed onto the tubing as it is wound. It is necessary to enclose the heating wire in glass as tellurium reacts with hot metals. The plateholder is carried on a ground joint so that it can be turned to face either the tellurium furnace or the slit system. This joint also enables a number of images to be formed on one plate. The plate is a circular 18-mm microscope cover glass held in a metal (nickel) holder which clamps on the end of the glass carrier.

The tellurium film was made in the following manner. With the pressure in the detecting chamber about 10^{-6} mm Hg and the plate facing the furnace, a direct current from storage batteries at 0.2 amp. below the operating current was supplied to the furnace for ten minutes. The operating current (about 3 amp.) was then used for the required time. The furnace was allowed to cool for at least ten minutes before the plate was turned and exposures made. The operating current was such as would produce a barely visible film in thirty minutes. A two-hour distillation at the operating current produced a film on the plate the weight of which was of the order of magnitude of 10^{-6} gram. As a two-minute distillation produced a film which could be developed, it is evident that the two-minute film is of atomic dimension in thickness. The permanency of a very thin film (2 min.) is shown in that one was exposed to the laboratory atmosphere for 24 hr. and then evacuated for 2 hr. It developed normally. If an appreciable quantity of tellurium oxide had been formed it would have been removed by the evacuation, and the plate would not have developed.

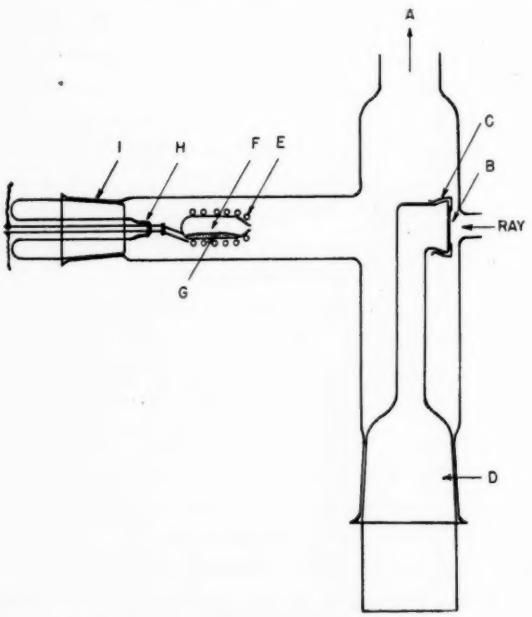

FIG. 1. Detecting chamber. (*A*) connection to pumping system, (*B*) glass plate, (*C*) plateholder, (*D*) ground joint, (*F*) tellurium furnace, (*E*) heating element (*G*) powdered tellurium, (*H*) press seal, (*I*) ground joint.

The developing solution used to intensify the tellurium film is the one recommended by Odell[5] for the physical development of photographic plates. The plate was removed from the detecting chamber, placed in a small holder made of glass rod, and immersed in a freshly made developing solution. The development was watched and, when satisfactory (15 to 60 minutes), the plate was removed, washed with distilled water, and placed on edge to drain and dry.

For hydrogen, oxygen, and chlorine the gases were introduced into the system from commercial cylinders through a capillary leak so adjusted that the pressure in the fore-slit system was approximately 0.1 mm Hg, that in the collimating chamber about 10^{-4} mm and in the detecting chamber about 10^{-6} mm. For the electrodeless discharge source of hydrogen and oxygen atoms 0.6- or 3.0-percent water was added to the elementary gases by bubbling them through a water trap. The chlorine was bubbled through sulfuric acid.

DETECTION OF IMAGES

Hydrogen atoms

Studies were made of the sensitivity of the detector using hydrogen atoms from the hot wire source. Tellurium films varied from faintly visible

[5] Odell, *The New Photo-Miniature, Physical Development* (Tenant and Ward, 1935).

(30 minutes distillation time) to very thin (2 minutes). Exposure times varied from 15 to 0.5 minutes. Fig. 2 shows a plate with a 5-minute distillation time and 15- and 5-minute exposures. The image from a 0.5-minute exposure on a 2-minute plate could still be readily observed and photographed. The technique can probably be extended to increase further the sensitivity.

Control tests were made with hydrogen flowing but the filament cold and with the filament hot but no hydrogen flowing. Negative results showed that neither molecular hydrogen nor radiation from the filament were responsible for the image. The dimensions of the images agreed closely with those calculated from the geometry of the slit system.

Under a microscope the clean, developed images obtained from short exposures appeared to contain some particles of deposited silver. The number of particles increased with shorter exposures. Photomicrographs were made of the images and the number of particles contained in a given area were counted. Although a simple linear relationship did not exist between particle count and exposure time, it is feasible that this method could be used for quantitative measurements of beam intensity.

The hydrogen atoms probably reacted with the tellurium to form tellurium hydride which evaporated from the surface. There is, however, the alternate possibility that the heat generated in the formation of molecular hydrogen on the surface evaporated the tellurium. This explanation does not appear likely as it has been reported that atomic hydrogen does not remove either lead or bismuth mirrors,[6] and tellurium is not much more volatile than these metals.

Compared to other chemical detectors for atomic hydrogen under similar conditions the developed tellurium plate is many fold more sensitive.

With hydrogen atoms from an electrodeless discharge source images were readily obtained on developed plates. These were observed when the hydrogen contained either 0.6- or 3.0-percent water and in some cases when no water was added.

[6] Rice and Rice, *The Aliphatic Free Radicals* (The Johns Hopkins Press, 1935).

FIG. 2.

Oxygen atoms

Clean images produced by oxygen atoms were readily obtained on developed plates with ten-minute exposures. As equally good images were obtained with either 0.6- or 3-percent water vapor in the oxygen; the images could not be produced by atomic hydrogen from the trace of water. In addition, exposure times were too short to detect such a small percentage of hydrogen atoms. Images were not obtained when the oxygen was flowing but the discharge not operating, even when the discharge bulb was heated to 400°C externally. This shows that molecular oxygen at this temperature is not effective, and this temperature is above that experienced when the discharge is operating.

Chlorine atoms

When exposures were made with chlorine atoms on visible films (over 30 minutes distillation time), the images were optically more dense than the surrounding film, whereas, when exposures were made on thin films and subsequently developed a normal image (less dense than surrounding film) were obtained. Images were readily obtained with ten-minute exposures on developed plates. Molecular chlorine did not produce an image.

The following explanation is offered for the reversal of the image on thick or thin films. The thin film is of approximate atomic thickness and tellurium tetrachloride is formed which evaporates. The thicker films are of several atom thickness and lower chlorides such as Te_2Cl_2 which contain more than one tellurium atom per

molecule are possible. These are both intensely colored and nonvolatile.

Bromine atoms

The introduction of bromine into the apparatus was done in the following manner. The capillary leak was replaced by a bulb of 1000 cc capacity which was joined to a small bulb containing liquid bromine. After the air had been exhausted from the apparatus the bromine was held at a temperature of −63.5°C in a bath of partially frozen chloroform. At this temperature the vapor pressure of solid bromine is about 0.2 mm. The buffer volume and the discharge bulb were filled with bromine at this pressure and then the small bulb containing the solid bromine was sealed from the system. Exposures with the discharge running were made as the pressure slowly decreased with the gas going through the slit system. The pressure in the collimating chamber decreased from 10^{-4} to 10^{-6} mm in one hour.

Four fifteen-minute exposures made on one plate in succession as the pressure decreased gave a slightly blurred first image due to excessive pressure in the collimating chamber. The second and third images were sharp and intense, and the last was sharp but faint. Although no detailed study of sensitivity was made, excellent images were obtained in a few minutes and the detector seems to be at least as sensitive for bromine atoms as for hydrogen atoms. A thick visible tellurium film did not give an observable image and no image was formed by molecular bromine.

In order to exclude the possibility that ions formed in the discharge were responsible for the images, the beam was passed through an electric field of sufficient strength to completely deflect all ions. No decrease in intensity of the image was observed.

Chemical detectors for atomic bromine and chlorine have not previously been reported. As these substances are very corrosive to metals, physical methods of detection are in general not satisfactory. The tellurium film detector using a thin plate subsequently developed should therefore find use whenever it is desired to study chlorine or bromine atomic beams.

Methyl radicals

When the discharge bulb was replaced with a device containing an electrically heated quartz tube, and lead tetramethyl or acetone thermally decomposed in it for the production of methyl radicals, very faint images on long exposure time could sometimes be obtained.

Possible Uses for This Detector

A number of uses for this detector are immediately obvious and we are submitting a list of them in the hopes that other investigators may find this technique useful.

1. The technique appears suitable for the investigation of the spreading of atomic beams.
2. Molecular moment studies particularly of the halogen atoms. Quantitative intensity measurements can quite probably be obtained.
3. Electric polarizability measurements of the halogen atoms.
4. In the mechanism of many thermal chemical reactions atomic hydrogen, oxygen, chlorine, or bromine are postulated as an intermediate. With having the first slit in the reaction zone detection of the particles on the plate would substantiate the postulated atomic species. Deflection of the beam through suitable magnetic fields would give positive identification from the known or measured magnetic properties of the particles.
5. If the detector can be made suitable for methyl or other organic radicals a number of important questions can be answered. Chemical evidence strongly indicates the existence of these radicals but positive proof that they are actually free radicals does not exist. By free radical is meant an uncharged, unactivated particle having an odd number of electrons and therefore an appreciable magnetic moment. Magnetic deflection measurements of a molecular beam of the active particles would give positive identification. Important questions relative to the magnetic and electric properties, special quantization, etc., of these particles could be studied. In addition, these radicals are postulated in the mechanisms of many chemical reactions. Magnetic deflection experiments with the source of the beam in the reaction zone could possibly give positive identification to the particles.

The Photogalvanic Effect

I. The Photochemical Properties of the Thionine-Iron System*

E. RABINOWITCH
Massachusetts Institute of Technology, Cambridge, Massachusetts

(Received February 23, 1940)

Solutions containing thionine and ferrous salts are bleached by illumination and recover their color in the dark. The kinetics of this reaction are investigated, by measuring photometrically the concentration of the dye in the photostationary state. Equations are derived for this state in terms of the initial concentrations and light intensity. At low thionine concentrations the extent of bleaching is proportional to the first power of light intensity and inversely proportional to the concentration of ferric ions. The bleaching reaches a maximum at a certain thionine concentrations and then decreases inversely proportional to the concentration of the dye. The bleaching increases strongly with increasing acidity. Kinetic mechanisms accounting for these relationships are discussed, and quantum yields and velocity constants are estimated. It is pointed out that the accumulation of free radicals ("semiquinones") and the occurrence of "circular" mechanisms maintaining the steady state are typical of photostationary states as distinguished from true equilibria.

THE term "photogalvanic effect" is used in the present series of papers to denote a special case of the so-called Becquerel effect, in which the influence of light on the electrode potential is due to a photochemical process in the body of the *electrolyte* (as distinct from photochemical or photoelectric processes in the surface layer of the *electrode*, which are the basis of the original Becquerel effect). A general kinetic theory of this effect will be given later.[1] The present two papers are concerned with one specific photogalvanic system of high efficiency, containing a reversibly reducible organic dyestuff (thionine) together with an inorganic oxidation-reduction pair (Fe^{3+}/Fe^{2+}). Paper I deals with the photochemistry of this system; Paper II, with its photogalvanic properties.

I. The Thionine-Iron System in the Dark

Thionine is a purple dye of the thiazine class. The commercial product is a monochloride; it probably[2] has the paraquinoid structure I:

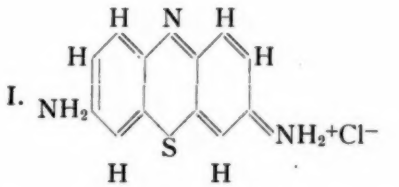

I. Thionine Chloride (Thio Cl)

The cation of (I) will be designated as $Thio^+$. At $p_H > 1$, the basicity of the two other nitrogen atoms begins to manifest itself, and the purple ions $Thio^+$ are crowded out, first by greenish-blue ions Thio H^{2+} and then by green ions Thio H_2^{3+}.

Thionine is reversibly reducible to leukothionine, by the addition of two hydrogen atoms. An intermediate form, which we will call *semithionine*, has been discovered by Granick, Michaelis and Schubert.[3] Table I shows the different ionic species of the three oxidation stages of thionine. According to Clark, Cohen and Gibbs,[4] the most abundant ionic species of leukothionine in the acid range ($p_H < 4$) is Thio H_2^{2+}; that of thionine, $Thio^+$. According to Michaelis and co-workers[3] the percentage of semithionine in the half-reduced state does not change appreciably between

* Contribution No. 447 from the Research Laboratory of Physical Chemistry, Massachusetts Institute of Technology. Publication No. 1, Solar Energy Conversion Research Project.

[1] E. Rabinowitch, See paper III of this series.

[2] A. Bernthsen, Ber. d. Chem. Ges. **16**, 1025, 2896 (1883); **13**, 611 (1884); Lieb. Ann. **230**, 73 (1885); **251**, 1 (1883).

[3] S. Granick, L. Michaelis and M. P. Schubert, Science **90**, 422 (1939); J. Am. Chem. Soc. **62**, 204 (1940).

[4] W. M. Clark, B. Cohen and H. D. Gibbs, *Studies on Oxidation-Reduction VIII*, Reprint No. 1017, Public Health Reports.

$p_H = 0$ and 7. The basicity of semithionine must stand therefore halfway between those of thionine and leukothionine; and its most abundant forms in the acid range probably are Thio H^+ and Thio H_2^{2+}.

The oxidation-reduction potential of the thionine-leukothionine system, $\epsilon_0^{T/L}$, is shown in Fig. 1 as function of p_H. Because of the predominance of the leukothionine species Thio H_3^{2+} in the range $p_H = 1$ to 4, ϵ_0 is in this range a linear function of p_H, with the slope $-3RT/2 \log e = 0.09$ (volt per p_H).

$\epsilon_0^{T/L}$ is the arithmetic mean of $\epsilon_0^{T/S}$ and $\epsilon_0^{S/L}$, the potentials corresponding to the two reduction steps thionine→semithionine and semithionine →leukothionine. The difference between them is related[5] to the "dismutation constant" K_d

$$\log K_d = \frac{\epsilon_0^{T/S} - \epsilon_0^{S/L}}{0.06}, \qquad (1)$$

$$K_d = \frac{[\text{semithionine}]^2}{[\text{leukothionine}] \times [\text{thionine}]}. \qquad (2)$$

According to Michaelis, from 5 percent to 10 percent of thionine is in the semiquinoid state at 50 percent reduction. Thus, $K_d \backsimeq 0.01$–0.05, and $\epsilon_0^{T/S} - \epsilon_0^{S/L} = -0.12$ to -0.18 volt. At $p_H \backsimeq 2$ (where most of our experiments have been carried out), $\epsilon_0^{T/L}$ is 0.38 volt and the two single potentials must be 0.44–0.47 volt ($\epsilon_0^{S/L}$) and 0.29–0.32 volt ($\epsilon_0^{T/S}$), respectively.

Semithionine is only a minor, although not negligible, component of partly reduced, moderately acid thionine solutions *in the stable state.* Larger concentrations may, however, accumulate in *illuminated* thionine solutions.

TABLE I. *The thionine ions (species which are most abundant at $p_H = 1$–4 in bold type).*

THIONINE	SEMITHIONINE	LEUKOTHIONINE	
Thio$^+$ (purple)	Thio	Thio$^-$	
Thio H^{2+} (blue)	**Thio H^+** (colorless ?)	Thio H (colorless)	↑ electrolytic dissociation
Thio H_2^{3+} (green)	**Thio H_2^{2+}** (yellow ?)	Thio H_2^+ (colorless)	
	Thio H_3^{3+} (yellow ?)	**Thio H_3^{2+}** (colorless)	
	Reduction →		

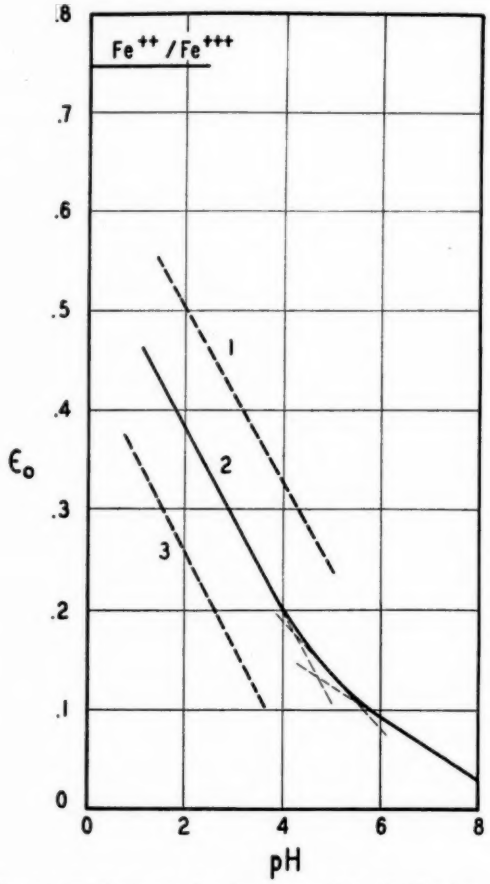

FIG. 1. Oxidation-reduction potentials of thionine and iron in relation to p_H 1: Curve 2: Mean redox potential of thionine, $\epsilon_0^{T/L}$; curves 1 and 3: probable values of the two single step potentials $\epsilon_0^{T/S}$ (lower curve) and $\epsilon_0^{S/L}$ (upper curve).

The oxidation-reduction potential of iron, $\epsilon_0^{Fe^{3+}/Fe^{2+}}$ is +0.77 volt (Schumb, Sherrill and Sweetser[6]). Ferric ions must therefore oxidize both leukothionine and semithionine practically completely. In other words, the equilibrium:

$$\text{thionine} + 2\,Fe^{2+} \rightleftharpoons \text{semithionine} + Fe^{3+} + Fe^{2+} \quad (3)$$
$$\rightleftharpoons \text{leukothionine} + 2\,Fe^{3+}$$

lies, in the dark, entirely on the left side.

II. THE THIONINE-IRON SYSTEM IN LIGHT

The thionine-iron equilibrium (3) is strongly affected by illumination with visible light. J.

[5] See, e.g., L. Michaelis, *Handbuch der Biologischen Arbeitsmethoden*, Vol. 5, Part 10 (1935), p. 712.

[6] W. C. Schumb, M. S. Sherrill and S. B. Sweetser, J. Am. Chem. Soc. **59**, 2360 (1937).

Weiss[7] has discovered that thionine-ferrous salt mixtures lose their color in light, and regain it in the dark. The primary photosensitive component is thionine, whose absorption maximum lies at 5970A. Of the other components of system (3), Fe^{2+} and Fe^{3+} are colorless in the concentrations used; and leukothionine does not absorb above 3800A. Semithionine, however, is a semiquinone and as such may have absorption bands in the visible. According to Granick, Michaelis and Schubert[3] the semiquinones of methylene blue and thionine are yellow in concentrated acid solutions and probably colorless in moderately acid and neutral solutions. Conceivably, the yellow form of semithionine may be Thio H_2^{2+} (Scheme II), or Thio H_3^{3+} and the colorless form, Thio H^+. Probably (although not certainly) the colorless form is the only one occurring in our experiments.

Illumination of system (3) leads to the establishment of a photostationary state.

$$\text{Thionine}+2\,Fe^{2+} \underset{\text{dark}}{\overset{\text{light}}{\rightleftharpoons}} \left\{\begin{matrix}(1-x)\text{ leukothionine}\\ x\text{ semithionine}\end{matrix}\right\} + \{(2-x)\,Fe^{3+}+xFe^{2+}\}. \quad (4)$$

Under favorable conditions, system (4) requires only a few seconds to reach both its stationary state in light and its stable state in the dark. In absence of oxygen, the bleaching is completely reversible; in presence of oxygen, the reduced dye is partly reoxidized by oxygen, with a resulting accumulation of ferric ions and a gradual weakening of the effect.

The thionine-iron system (4) is similar to the inorganic system

$$\tfrac{1}{2}I_2+Fe^{2+} \underset{\text{dark}}{\overset{\text{light}}{\rightleftharpoons}} I^-+Fe^{3+}. \quad (5)$$

(Rideal and Williams,[8] Sasaki and Nakamura,[9] Kistiakowsky[10]), but the latter requires minutes or even hours to reach the stationary state. The explanation lies in the much lower extinction coefficient of iodine (maximum extinction coefficient, of iodine $\alpha_{max}=8\times10^2$, Rabinowitch and Wood,[11] as compared to $\alpha_{max}\backsimeq5\times10^4$ for thionine).

Figure 2 illustrates the readiness with which the color of a thionine-iron salt solution follows the variations in the intensity of illumination, L. The top curve shows L as a function of time, measured by means of a thermopile; the middle curve shows the variations in the transmission I of the solution. The lower curve represents the simultaneous changes in the potential of a Pt-electrode placed in the solution—the "photogalvanic effect."

A similar reversible bleaching can be observed with other thiazine dyestuffs, e.g. methylene blue, calcozine (methylene green), toluidine blue, and thiocarmine. However, none of these dyes equals thionine in sensitivity. The sensitivity can be increased by addition of substances which form complexes with ferric ions. Thus the effect is stronger in sulphate than in chloride solutions, because SO_4^{2-}-ions form more stable complexes

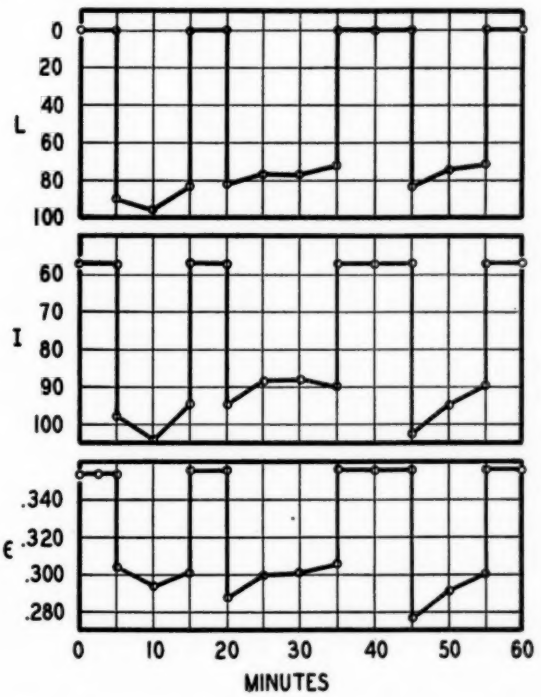

FIG. 2. Response of a thionine-iron solution to light. Upper curve: intensity of illumination (measured by a thermopile). Middle curve: reversible bleaching. Lower curve: photogalvanic potential.

[7] J. Weiss, Nature **136**, 794 (1935).
[8] E. K. Rideal and E. C. Williams, J. Chem. Soc. London **127**, 258 (1925).
[9] N. Sasaki and K. Nakamura, Sexag. Coll. of Papers dedicated to T. Osaka, Kyoto (1927).
[10] G. B. Kistiakowsky, J. Am. Chem. Soc. **49**, 976 (1927).
[11] E. Rabinowitch and W. C. Wood, Trans. Faraday Soc. **32**, 540 (1936).

with ferric ions. The bleaching is particularly enhanced by phosphate ions. In a sulphate solution, the most concentrated thionine solution which can be completely decolorized by the light of a 1000-watt lamp, (in the presence of 10^{-2} mole/l $FeSO_4$ and 0.1 mole/l H_2SO_4) is 10^{-4} molar. In the presence of 0.2 mole/l phosphoric acid, however, even a 1.5×10^{-3} molar thionine solution becomes colorless in the same light, in presence of 0.04 mole/l Fe^{2+}. If 0.01 mole/l Fe^{3+} are present, the color is restored in a few seconds in the dark.

The following experiments deal with the kinetic mechanism of the photostationary state (4). Simultaneously with the stationary composition of the illuminated solutions, we have measured their photogalvanic potentials; these will be discussed in paper II.

III. Experimental Procedure

Because of the speed with which the composition of a thionine-iron solution adjusts itself to the intensity of illumination (Fig. 2), no samples can be taken for analysis. We measured the stationary concentration of thionine photometrically, by means of the light beam I (Fig. 3) (from a 6-volt, 6-amp. automobile headlight bulb 6) made parallel by a microscope eyepiece lens 8 and filtered through infra-red-absorbing filter 7 and red filter 10 (Wratten, No. 25). The light beam traverses the reaction vessel 12 (rectangular glass cell $3\times1\times6$ cm) near its bottom. The broad side of the cell is illuminated uniformly by the light L from a 1000-watt projection lamp, filtered through running water 2, 10 cm of saturated $FeSO_4$ solution 3, and made parallel by a 12-cm condenser lens 5. The light intensity can be varied by Wratten gray filters and measured by a Moll large surface thermopile 13, calibrated against a standard lamp.

The beam I passes a second red filter 15 to reduce scattered light from L and falls on a barrier layer photo-cell 16, connected to a galvanometer 17. I_0 is controlled by a second photocell 11; the beam I_0' being split from I_0 by a Wollaston prism.

The electrode A is a bright platinum foil 1×1 cm placed parallel to the light beam L to avoid shadows and to minimize a direct photo-

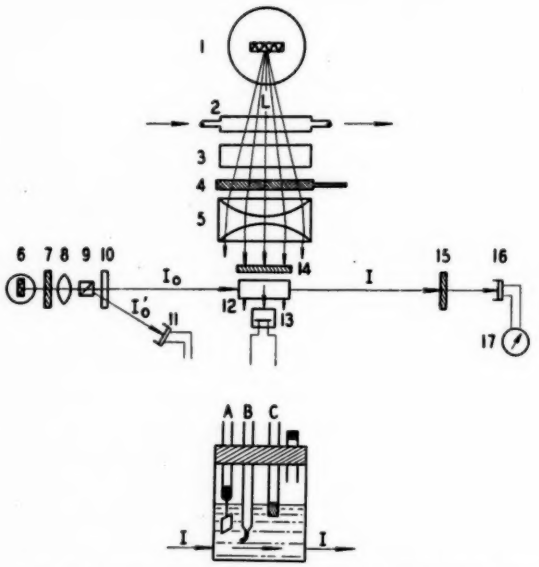

Fig. 3. Apparatus: 1. 1000-watt lamp. 2. Water filter. 3. $FeSO_4$-filter. 4. Shutter. 5. Condenser. 6. 6-volt, 6-amp. headlight lamp. 7. Infra-red absorbing filter. 8. Microscope eyepiece lens. 9. Wollaston prism. 10. Red filter. 11. Photo-cell. 12. Reaction vessel. 13. Thermopile. 14. Gray filter. 15. Red filter. 16. Photo-cell. 17. Galvanometer. *A*. Pt-electrode. *B*. Nitrogen supply. *C*. Syphon.

effect (Becquerel effect) on the electrode-electrolyte interface. Nitrogen is bubbled through B to remove oxygen and to stir the solution.

Since of all components of system (3), only thionine absorbs in the red, the system can be calibrated with thionine solutions of known concentrations. A similar curve can be constructed for determining absorption of the illuminating light L (assuming that the contribution of semithionine to the absorption is negligible). The number of quanta absorbed has been calculated by assuming a mean wave-length 6000A.

The potential of the electrode A was measured by a potentiometer against a calomel electrode in 1 m KCl. A was connected to the normal electrode by a syphon C with 1 molar KCl solution.

Since experiments are carried out in 0.001 to 1 normal acid, and the concentration of thionine is only about 10^{-5} mole/l, no buffering is necessary, although a shift in equilibrium (4) results in a certain change in p_H, because of the stronger basicity of the reduced dye.

The measurements give ΔI, the change in transmission. With the help of the calibration curve, $\Delta[Thio^+]$, the change in the concentration

of the dye can be calculated. If all reduced dye were in the form of leukothionine, the knowledge of $\Delta[\text{Thio}^+]$ (which will be further designated simply by Δ) would be sufficient to calculate the concentrations of all other components. An additional variable, x in Eq. (4), is introduced by the possible occurrence of semithionine. To eliminate it, it would be desirable to determine independently one more stationary concentration, e.g. that of Fe^{3+}, or semithionine. However, no simple methods are available for the estimation of the colorless components of the system.

IV. Results

We made about 150 measurements, of which Table II is a specimen. The values of $[Fe^{3+}]^*$ (asterisks are used to denote stationary concentrations in the illuminated state) were calculated upon the assumption that *two* Fe^{3+} are produced per each thionine molecule reduced, which is wrong if semithionine is the main product. This uncertainty is important only in experiments with low initial $[Fe^{3+}]$ concentrations.

The interpretation of the results is complicated by the fact that no set of measurements corresponds to the change in *one* variable only. E.g., if light intensity is varied, the stationary concentration of thionine is changed; the intensity of light absorption is therefore not proportional to the intensity of illumination. The reproducibility of the results was not very good (the largest error being introduced by the determination of Δ from the change in the color density, which change is often small); the best way of analyzing the results was found in arranging Δ-values in groups corresponding to similar, at random distributed values of all variables, with the exception of one, and determining the effect of this remaining variable on the group average of Δ. This treatment leads to the conclusion that for a constant p_H ($\backsimeq 2$), Δ is best represented by the following equations:

$$\Delta = K_1 \frac{N_{h\nu}\gamma}{[Fe^{3+}]^*}, \tag{6}$$

or

$$\Delta = K_2 \frac{N_{h\nu}\gamma}{[Fe^{3+}]^* \times [\text{Thio}]^*}. \tag{7}$$

Eq. (6) is the limiting formula for low thionine concentration, (7) the limiting formula for the higher values of $[\text{Thio}]^*$. (We use the abbreviation Thio for thionine, although it has been used in Table I for one ionic species of semithionine.) $N_{h\nu}$ is the number of Einsteins absorbed per second in 1 l. γ is the quantum yield of the reduction of Thio^+ by Fe^{2+}, and a function of $[Fe^{2+}]$. Most of the experiments used in the tables were carried out with a constant $[Fe^{2+}]$-value (5×10^{-3} mole/l). $[Fe^{2+}]^*$ is under these conditions, practically identical with $[Fe^{2+}]$.

Figure 4 shows why two different relations (6) and (7), must be used for different ranges of thionine concentrations.

$K_1\gamma$ is practically inversely proportional to $[\text{Thio}]^*$ above 4×10^{-5} mole/l, and approaches a constant value at low thionine concentrations; $K_2\gamma$ is constant at the higher values of $[\text{Thio}]^*$ and becomes proportional to $[\text{Thio}]^*$ when the thionine concentration approaches zero.

The proportionality of Δ with the first power of absorption intensity $N_{h\nu}$ is shown by Table III.

The last row in Table III shows only irregular fluctuations, whereas the top one exhibits a strong trend. Thus, Δ is proportional to $N_{h\nu}$, rather than to $N_{h\nu}^2$.

Table IV is the basis for the introduction of the factor $[Fe^{3+}]^{*-1}$ in the formulae (6) and (7).

At $[\text{Thio}]^* > 6\times10^{-5}$ measurements have been made with one $[Fe^{3+}]^*$-concentration only, so that there is no certainty that $[Fe^{3+}]^{*-1}$ must appear in (7), as well as in (6). However, it is difficult to imagine a mechanism which would

TABLE II. *Example of an experiment.* $[Thio]=6.25\times10^{-5}$ *mole/l,* $[Fe^{2+}]^* \backsimeq [Fe^{2+}]=447\times10^{-5}$ *mole/l,* $[Fe^{3+}]=33\times10^{-5}$ *mole/l,* $[HCl]=1.98\times10^{-2}$ *mole/l,* $\epsilon=0.380$ *volt (against 1 m* KCl *calomel electrode).*

Light Absorption $N_{h\nu}\times10^5$ (Einstein per 1 per sec.)	Stationary Concentrations in mole/l $\times10^5$			
	[Thio]	$[Fe^{3+}]^*$	Δ	ϵ^* Volt
11.0	3.6_0	39	2.65	0.213
11.2	3.7_0	38	2.55	0.221
5.3	5.4_6	35	0.80	0.303
5.3	5.4_5	35	0.80	0.304
2.7	6.0_5	33	0.20	0.346
11.3	3.8_0	38	2.45	0.222
11.4	3.9_0	38	2.35	0.223
11.6	4.1_0	37	2.15	0.237
5.4	5.6_5	34	0.60	0.310
11.6	4.1_0	37	2.15	0.237

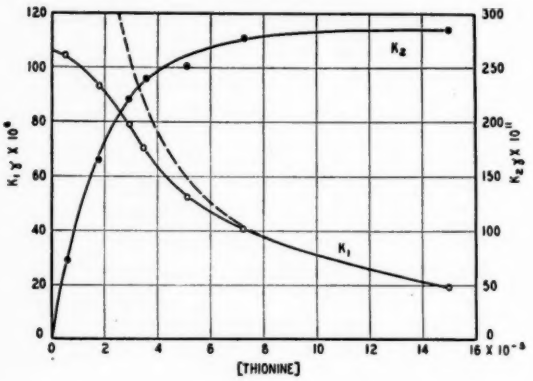

FIG. 4. Constants γK_1 and γK_2 in relation to thionine concentration.

make Δ proportional e.g. to $[Fe^{3+}]^{*-2}$, without making it at the same time proportional to $N_{h\nu}^2$, and the latter possibility appears excluded by the figures in Table III.

Our data provide no definite answer to the question of the dependence of Δ on $[Fe^{2+}]$. Table V gives an indication of a direct proportionality between Δ and $[Fe^{2+}]$.

The results relative to the two highest $[Fe^{2+}]$ values are taken from single measurements and therefore unreliable. Theoretically, the quantum yield γ should be a function of the type

$$\gamma = k_1^*[Fe^{2+}]/(k_{de}+k_1^*[Fe^{2+}])$$

(Stern-Volmer), where k_1^* is the velocity constant of the reaction of excited Thio*-molecules with ferrous ions, and k_{de} the velocity constant of their deactivation.

Table V makes it probable that "saturation" ($k_1^*[Fe^{2+}] \gg k_{de}$) does not occur below $[Fe^{2+}] = 2\times10^{-2}$ mole/l, and that in the region 1×10^{-2} mole/l, γ is almost linear with $[Fe^{2+}]$. Other arguments in favor of this conclusion will be found in the next paragraph.

Δ could remain dependent on $[Fe^{2+}]$ even after the photochemical reaction has become "saturated" in respect to ferrous ions, if ferrous ions would take part in another stage of the reaction, e.g. in the reduction of semithionine to leukothionine. However, thermochemical considerations make this participation improbable (see below).

V. Discussion of Results

The formulae (6) and (7) look very simple and it is easy to indicate mechanisms which would account for each of them. It is, however, more difficult to explain the transition from one to another with increasing thionine concentration.

The reactions which we have to consider include reduction and reoxidation of thionine by iron ions, dismutation of semithionine, its dimerization, and interaction with H^+-ions (Table I). We assume that ionization and ionic association are rapid compared to the reactions responsible for the photostationary state. (Velocity constants of the latter are of the order of sec.$^{-4}$.) Under these circumstances, thionine, semithionine and leukothionine represent, in the photostationary state, the same mixture of different ionic species which they would form in the stable state at the same p_H. Under these circumstances, Scheme III is sufficient to describe the interplay between all these species:

TABLE III. *Average values for different $N_{h\nu}$-ranges.*

	Low [Thio]*-region ($<3\times10^{-5}$)				High [Thio]*-region ($>5\times10^{-5}$)			
$N_{h\nu}$-range ($\times10^4$)	0.2	0.2 to 0.4	0.4 to 0.6	0.6	0.25	0.25 to 0.50	0.50 to 1.0	1.0
$\frac{\Delta\times[Fe^{3+}]^{*2}}{N_{h\nu}^2}(\times10^4)$†	32	8	6	4	10	4.5	2.8	1.4
$\frac{\Delta\times[Fe^{3+}]^*}{N_{h\nu}}(\times10^6)$	94	110	87	97	56	38	37	44

† Theoretically, proportionality with $N_{h\nu}^2$ should entail an inverse proportionality with $[Fe^{3+}]^{*2}$, see below.

TABLE IV. *Averages for different ranges of $[Fe^{3+}]^*$.*

$[Fe^{3+}]^*(\times10^5)$	10	10–25	25–50	50
$\frac{\Delta\times[Thio]^*\times[Fe^{3+}]^*}{N_{h\nu}}(\times10^6)$	63	72	71	70

TABLE V. *Averages for different ranges of $[Fe^{2+}]$. $[Thio]^* = 4\times10^{-5}$ mole/l.*

$[Fe^{2+}]\times10^5$ (mole/l)	100–200	200–400	500	1000	2000
$K_2\gamma\times10^{11}$	20	43	60	128	112

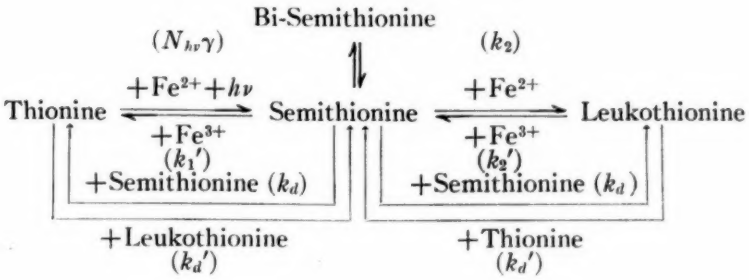

(III)

The horizontal arrows represent the oxidation-reduction reactions with iron ions; the broken arrows represent dismutation. The symbols in brackets are velocity constants. We neglect the possible photochemical contribution to the dismutation reaction, as well as the thermal reduction of thionine by ferrous ions, whose velocity constant k_1 should be properly added to the photochemical reaction velocity $N_{h\nu}\gamma$ in Scheme III. Velocity constants in (III) are *p_H-dependent*, since "thionine," "semithionine" and "leukothionine" stand for p_H-dependent distributions of different ionic species. We have to select from the possibilities presented by Scheme (III), those which will account for the relationships (6) and (7). Eq. (6) can be accounted for in two ways: either by reducing (III) to

$$\text{Thio} \underset{(k_1')}{\overset{(N_{h\nu}\gamma)}{\rightleftharpoons}} \text{Semi} \qquad \text{(IV)}$$

with semithionine as the only reduction product, or by assuming a circular mechanism

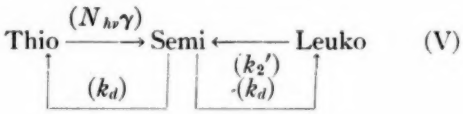

(V)

with leukothionine as the main reduction product. (Circular mechanisms are excluded in true equilibria by the principle of microscopic reversibility, but are allowed in the photostationary state.) Mechanism IV leads to the equation:

$$\Delta=[\text{Semi}]=\frac{N_{h\nu}\gamma}{k_1'[Fe^{3+}]^*} \qquad (8)$$

and mechanism V—to

$$[\text{Leuko}]=\frac{N_{h\nu}}{k_2'[\text{Fe}^{3+}]^*}. \qquad (9)$$

(8) and (9) become identical with (6), if K_1 is given either the meaning

$$K_1=1/k_1' \quad \text{or} \quad K_1=1/k_2', \quad \text{respectively.} \qquad (10)$$

It is to be noted, that the fact that semithionine does not occur in large quantities in the stable state of partially reduced thionine solutions, does not preclude the possibility of it being the main product of reduction in the photostationary state. Since the reaction primarily accelerated by light is the formation of semithionine, and the further reduction of semithionine to leukothionine by ferrous ions is precluded by the fact that the oxidation potential of ferric ions is much higher than that of semithionine, the only way in which semithionine can be further reduced is by dismutation. The ratio between semithionine and leukothionine in the photostationary state thus depends on the relative efficiency of dismutation as compared with the reoxidation of leukothionine by ferric ions. In (IV) dismutation is neglected, in (V) it is assumed to be sufficiently rapid to maintain most of the reduced thionine in the state of leukothionine.

Equation (6) can be also satisfied by an appropriate *combination* of (IV) and (V), producing a *mixture* of semithionine and leukothionine

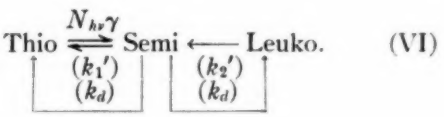

(VI)

E.g., if $k_1'=k_2'=k'$, (VI) gives

$$\Delta=[\text{Semi}]+[\text{Leuko}]=\frac{N_{h\nu}\gamma}{k'[\text{Fe}^{3+}]^*}. \qquad (11)$$

Transition to Eq. (7) at high [Thio]* values shows that reduction does not stop entirely at the semithionine stage, since the decrease in Δ

with increasing [Thio]* indicates that thionine accelerates the reoxidation. The only way in which thionine can participate in the back reaction is the reversal of the dismutation. The limiting case should be that represented by (VII)

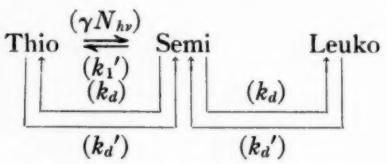

(VII)

in which leukothionine is both formed and destroyed exclusively by dismutation. Mechanism (VII) leads to the kinetic relationship (12)

$$[\text{Leuko}]=\frac{\gamma^2 N_{h\nu}{}^2 k_d}{k_1'^2 k_d'[\text{Fe}^{3+}]^*[\text{Thio}]^*}. \qquad (12)$$

(12) agrees with the empirical Eq. (7) in respect to the occurrence of a factor $[\text{Thio}]^{*-1}$, but requires a proportionality with the *square* of $(\gamma N_{h\nu}/[\text{Fe}^{3+}]^*)$. This discrepancy cannot be yet definitely explained. In single experiments, values of the exponent z in $x=\text{const.}\times N_{h\nu}{}^z$ up to $z=1.6$ were obtained.

Formally, there is a way to obtain an equation for [Leuko] containing the factor $[\text{Thio}]^{*-1}$ and retaining the first powers of $\gamma N_{h\nu}/[\text{Fe}^{3+}]^*$. This is to assume the circular mechanism (VIII),

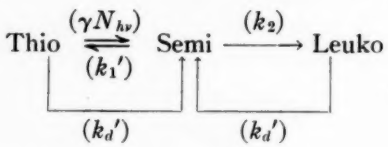

(VIII)

in which leukothionine is formed by reduction with Fe^{2+}, and disappears by dismutation. We have mentioned, however, that the equilibrium between Semithionine/Leukothionine and Ferri/Ferro must lie far on the side of semithionine. If, to the reactions (a) Leuko+Fe^{3+}→Semi+Fe^{2+}, we add the reaction (b) Leuko+Thio→2 Semi, with a velocity k_d' which, according to (VIII) should be even *larger* than that of (a), the result can be only a still more complete disappearance of the leukoform. Scheme (VIII) will be thus reduced to (IV), with semithionine as the only reduction product.

This discussion shows that in the region where Eq. (6) holds the reduced thionine is present either in the form of semithionine, or in that of a mixture of semithionine with leukothionine, with the latter being formed by dismutation of semithionine and reoxidized by Fe^{3+}-ions; and that in the region where Eq. (7) becomes valid, leukothionine is the chief reduction product, and is re-oxidized mainly by thionine.

VI. Quantum Yield and Velocity Constants

Table I shows that the absorption of $\sim 10^{-4}$ Einstein per second in a liter of a solution containing $\sim 5\times 10^{-5}$ mole/l thionine and 5×10^{-3} mole/l Fe^{2+} causes a bleaching of about 50 percent. Under these circumstances, each molecule absorbs $10^{-4}/5\times 10^{-5}=2$ times per second. It thus stays an average of 0.5 sec. in the reduced state. Visually, however, the return to the stable state is a reaction with a "half-period" of about 2–3 sec. This indicates that the quantum yield of bleaching is of the order of 0.25. That $\gamma<1$ is confirmed by the fact that bleaching can be made more complete by an increase in $[Fe^{2+}]$; Table IV shows that in the region $[Fe^{2+}]\leqq 5\times 10^{-3}$, γ is roughly proportional to $[Fe^{2+}]$.

The assumption $\gamma<1$ is further strengthened by the fact that it is possible, by addition of phosphoric acid, to increase Δ almost tenfold, without making the back reaction slower. According to Fig. 4, the limiting value of γK_1 for low $[\text{Thio}]^*$-values is about 1×10^{-4}. If we assume $\gamma=0.25$, this means $K_1=4\times 10^{-4}$, or, according to (10), k_1' (or k_2') $=2.5\times 10^3$. This must be the velocity constant of oxidation of semithionine (or leukothionine) by ferric ions; and it is noteworthy that this constant is comparatively small, despite the fact that this oxidation is an exothermal ionic reaction.

In the region where thionine begins to compete with Fe^{3+} in the reoxidation of leukothionine, $[\text{Thio}]^*$ is still ~ 10 times smaller than $[Fe^{3+}]^*$. This shows that k_d', the velocity constant of the reaction leukothionine+thionine→2 semithionine, must be of the order of 2.5×10^4 (which is more than a thousand times slower than the velocity of the corresponding reaction for cumoquinone, according to Kornfeld[12]). Since we have estimated that $K_d(=k_d'/k_d)\leqq 0.01$–0.05, the dis-

[12] G. Kornfeld, J. Chem. Phys. **7**, 274 (1939).

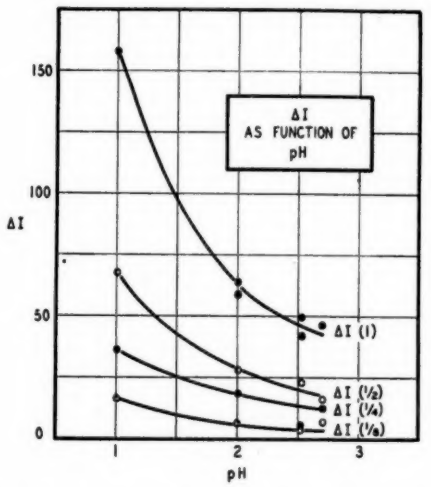

FIG. 5. Bleaching ΔI in relation to acidity, p_H.

mutation velocity constant k_d must be of the order of $5\times10^5-2.5\times10^6$.

VII. EFFECT OF p_H

Figure 5 shows the continuous decrease in the intensity of bleaching with the increase in p_H; Δ is found to be roughly proportional to $([H^+])^{\frac{1}{2}}$. The effect of acidity on bleaching is related to its effect on the thermodynamic equilibrium of the thionine-leukothionine system, but the relation is not a simple one, since the equilibrium depends on *ratios* of the velocity constants, whereas the photostationary state depends on the absolute values of certain of these constants. Applying, for instance, Scheme III to the equilibrium in the dark, (by substituting the thermal velocity constant k_1 for the photochemical reaction velocity $\gamma N_{h\nu}$), we recognize that the enhancing effect of increasing p_H on the extent of reduction (at a given ratio $[Fe^{3+}]/[Fe^{2+}]$, i.e., at a constant oxidation-reduction potential) can be traced to a decrease in the ratios k_1/k_1' and k_2/k_2'. Michaelis' observation that the dismutation constant $K_d=k_d'/k_d$ remains unchanged in the p_H range 1–7 indicates that in this region the two ratios k_1/k_1' and k_2/k_2' are affected by p_H in the same way. Referring to Scheme II, we find that these effects of p_H on the velocity ratios are due to the "stabilization" of the weak acids semithionine and leukothionine by H^+-ions, and that the acidity of semithionine must stand halfway between those of thionine and leukothionine.

Considering now the photostationary state, we have to discuss Scheme (III) with the *p_H-independent* photochemical reaction velocity constant $N_{h\nu}\gamma$ instead of k_1. The increase in bleaching with increasing p_H indicates that the *absolute* velocity constant k_1' (or k_2', or k_d, or all of them) are decreased by increasing acidity, which is a plausible (but not the only one possible), explanation of the decrease in the *ratios* k_1/k_1' and k_2/k_2'. What particular reaction velocity is responsible for the p_H-effect on bleaching, depends on the actual mechanism of the photostationary state. If mechanism IV, Eq. (8), or mechanism VII, Eq. (12) are correct, the effect is due to a change in k_1'; (the ratio k_d'/k_d is independent of p_H); if mechanism V, Eq. (9) is chosen, the p_H-effect must be due to a change in k_2'.

The proportionality between bleaching and $([H^+])^{\frac{1}{2}}$ is probably not to be interpreted as an exact kinetic relationship. We have to remember that k_1, k_1', etc., are composite constants; e.g. k_2' is defined as follows:

$$k_2'=k_2'_{(\text{Thio}^-)}\frac{[\text{Thio}^-]}{[\text{Leuko}]}+k_2'_{(\text{Thio H}^+)}\frac{[\text{Thio H}]}{[\text{Leuko}]}$$
$$+k_2'_{(\text{Thio H}_2^+)}+k_2'_{(\text{Thio H}_3^{2+})}\frac{[\text{Thio H}_3^{2+}]}{[\text{Leuko}]}, \quad (13)$$
$$([\text{Leuko}]=[\text{Thio}^-]+[\text{Thio H}]$$
$$+[\text{Thio H}_2^+]+[\text{Thio H}_3^{2+}]).$$

The first concentration factor on the right side is proportional to $[H^+]^3$, the second one to $[H^+]^2$, the third to $[H^+]$, and the fourth is practically independent of $[H^+]$ (in the p_H-region 1–4). An approximate proportionality of k_2' with $[H^+]^{\frac{1}{2}}$ can be explained by appropriate ratios between the values of the individual constants $k_2'_{(\text{Thio}^-)}$ etc. in (13).

The Photogalvanic Effect

II. The Photogalvanic Properties of the Thionine-Iron System*

E. RABINOWITCH
Massachusetts Institute of Technology, Cambridge, Massachusetts

(Received February 23, 1940)

The oxidation-reduction system thionine-iron, described in paper I, provides an extremely sensitive photogalvanic cell. The illuminated half-cell is negative in respect to the nonilluminated one. The photogalvanic potential ϵ^* is determined in relation to composition and light intensity. The results are in a qualitative (and partially quantitative) agreement with the kinetic theory of the photogalvanic effect. In strongly bleached solutions, the electrode potential is maintained by semithionine ions transferring electrons to the electrode, and ferric ions acquiring electrons from the electrode, whereas ferrous ions and leukothionine ions remain practically inactive. In weakly bleached solutions, the mechanism is more complicated.

I. PHOTOGALVANIC EFFECT IN THIONINE-IRON SOLUTIONS

THE photogalvanic effect was defined in paper I of this series[1] as the change in the electrode potential of a galvanic system, produced by illumination and traceable to a photochemical process in the body of the electrolyte. Shifts in oxidation-reduction equilibria are probably the cause of most photogalvanic effects, as this shall be discussed in more detail elsewhere.[2] The oxidation-reduction system thionine-ferrous iron,

$$\text{Thio}+\text{Fe}^{2+} \underset{\text{dark}}{\overset{\text{light}}{\rightleftharpoons}} (\text{Semi}+\text{Leuko})+\text{Fe}^{3+} \quad (1)$$

(Thio = Thionine, Semi = Semithionine, Leuko = Leukothionine) whose kinetics have been discussed in paper I, is probably the most highly light-sensitive oxidation-reduction equilibrium known; it was therefore to be expected that this system should possess a particularly high photogalvanic sensitivity.

To demonstrate this sensitivity we place two bright platinum electrodes at the two ends (or, better, at top and bottom) of a glass vessel (e.g. a rectangular cell 1 cm deep) containing 5×10^{-5} mole/l thionine and 5×10^{-3} mole/l $FeSO_4$, at $p_H=2-2.5$, and illuminate one-half of the cell with a strong light source. Within a few seconds, a sharp boundary is formed between the decolorized illuminated solution and the colored solution in the dark, and a potential difference $\Delta\epsilon$ is established between the two electrodes. When illumination ceases, the color returns and the potential difference disappears within 2–20 seconds. The presence of about one percent Fe^{III} in Fe^{II} accelerates the return to the normal state without affecting the photogalvanic effect.

Figure 2 in paper I shows how closely this potential follows changes in the intensity of illumination. We recognize that $\Delta\epsilon$ is closely parallel to the intensity of bleaching ΔI. However, this is only true for a given solution. The dependence of the two effects on composition is not always the same; the strongest photogalvanic effects are obtained in solutions which show hardly any bleaching at all. An explanation of this striking fact will be given below.

It was mentioned in I that, photochemically, the thionine-ferrous iron system is similar to the well-known iodine-iron system. The latter is, however, about 100 times slower in attaining both its steady state in light and its stable state in the dark. The iodine-iron system also shows a photogalvanic effect (Rideal, Williams,[3] Sasaki, Nakamura[4]), but apart from being more sluggish than the thionine-iron system, it is also considerably less sensitive, probably because the

* Contribution No. 448 from the Research Laboratory of Physical Chemistry, Massachusetts Institute of Technology. Publication No. 2, Solar Energy Conversion Research Project.

[1] E. Rabinowitch, preceding paper.

[2] E. Rabinowitch, paper III of this series.

[3] E. K. Rideal, E. C. Williams, J. Chem. Soc. London **127**, 258 (1925).

[4] N. Sasaki, K. Nakamura, Sexag. Coll. Papers dedicated to T. Osaka, Kyoto, 1927.

difference between the normal potentials of iodine and iron (0.14 volt) is much smaller than that between the potentials of iron and thionine (0.41 volt at $p_H=2$).

The above-mentioned simple arrangement is inadequate for quantitative work, because it does not allow stirring. We have, therefore, built the apparatus shown in Fig. 3 (paper I), which contains an uniformly illuminated thionine half-cell connected by a syphon to a calomel electrode. With this apparatus, photogalvanic effects of 10–250 mv have been measured in thionine-ferrous iron solutions upon illumination with a 1000-watt projection lamp, or a 20-amp. automatic carbon arc.

The illuminated half-cell is always negative as compared to the nonilluminated one; ($\Delta\epsilon<0$). The absolute value of the effect depends on the concentrations of iron and thionine, on p_H, and on light-intensity. Table I in paper I is a sample of the data; it shows the concentrations in the dark and in light, and the corresponding potentials ϵ and ϵ^* (measured against a calomel electrode in 1 m KCl; in the present paper, potentials will be referred to the normal H_2 electrode by the addition of 0.285 volt). Δ in this table is the concentration of decolorized (reduced) thionine, which may be semithionine, leukothionine or a mixture of both.

II. Theoretical Equations for $\Delta\epsilon$

According to a kinetic picture which shall be presented in more detail in another paper, the electrode potential of a redox system is the result of a dynamic equilibrium, determined by the velocities with which the electrons are transferred from the electrode to the oxidized ionic species in solution ("electron acceptor ions") and back to the electrode from the reduced ionic species in solution ("electron donor ions"). We further postulate—as a special assumption, subject to test by experience—that the rate of electron losses by the electrode is independent of the nature of the acceptor ions in solution, whereas the rate at which the electrons are acquired by the electrode depends on the properties of the donor ions. More specifically we assume that the activation energy of this last process is determined by the ionization potentials of the donor ions, or by their (closely related) normal oxidation potentials.

In the thionine-iron system, the acceptor ions are those of thionine and ferric iron, the donor ions—those of leukothionine and ferrous iron. Semithionine ions should be able to act both as electron acceptors and as electron donors. The effect of illumination is, according to (1), to substitute a certain number of leukothionine ions (or semithionine ions) as electron donors for an equivalent quantity of ferrous ions. Simultaneously, an equivalent number of ferric ions are substituted for thionine ions as electron acceptors. If the above-mentioned postulate applies to the thionine-iron system, only the first of these two substitutions must have an effect on the electrode potential (since all acceptor ions are supposed to have equal efficiency). The oxidation potentials of thionine are considerably lower than that of ferric iron; the leukothionine, as well as the semithionine, ions must be therefore *more efficient* electron donors than ferrous ions. The electrode in the illuminated solution will therefore acquire electrons at a higher rate, and reach a stationary state at a more negative potential than the one it had in darkness.

Our assumption thus leads to a correct prediction of the negative sign of the photogalvanic effect in the thionine-iron cell.

A simplified quantitative treatment of the steady state on the basis of the same postulate leads to the following equation representing ϵ in terms of concentrations and normal potentials ϵ_0 of all components of the system.

$$e^{\epsilon/RT}=\frac{[Fe^{3+}]+[Thio]+[Semi]}{[Fe^{2+}]e^{-\epsilon_0^{Fe}/RT}+[Semi]e^{-\epsilon_0^{T/S}/RT}+[Leuko]e^{-\epsilon_0^{S/L}/RT}}. \qquad (2)$$

In the denominator of (2), we have taken into consideration that ferrous iron, semithionine, and leukothionine can all serve as electron donors, with an efficiency determined by their normal potentials ($\epsilon_0^{T/S}$ and $\epsilon_0^{S/L}$ being the two single-step oxidation potentials of thionine); the numer-

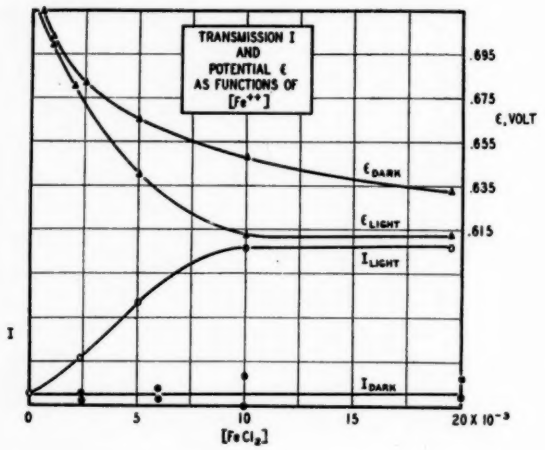

FIG. 1. I, I^*, ϵ and ϵ^* in relation to $[Fe^{2+}]$. $p_H=1.7$; $[Thio]=5\times10^{-5}$ mole/l; $[Fe^{3+}]=7\times10^{-4}$ mole/l; $N_{h\nu}=6\times10^{-5}$ (Einst./sec.).

ator expresses the assumption that semithionine can also serve as an electron acceptor with the same efficiency as thionine and ferric iron.

Since e.g. at $p_H=2$, $\epsilon_0^{Fe}=0.78$, $\epsilon_0^{T/S}=$ about 0.35 and $\epsilon_0^{S/L}=$ about 0.47 volt (Fig. 1 in paper I), the first term in the denominator disappears unless

$$\frac{[Fe^{2+}]}{[Semi]+[Leuko]}>2\times10^4.$$

In our *illuminated* solutions, this ratio is 10–100 and the neglect of the $[Fe^{2+}]$-term in (2) should be permissible, when this equation is applied to the calculation of ϵ^*. Furthermore, in most of our experiments, $[Thio]^*$ (the asterisks designate concentrations in the photostationary state) is small compared to $[Fe^{3+}]^*$, and $[Semi]^*$ is smaller than $[Thio]^*$. Thus, to the first approximation, we may neglect the two last terms in the numerator. Furthermore, because of the difference between $\epsilon_0^{T/S}$ and $\epsilon_0^{S/L}$ (about 0.12–0.18 volt), the semithionine term in the denominator of (2) must be much larger than the leukothionine term, if at least 5–10 percent of the reduced dye are in the form of semithionine. In this simplest case, the potential of the illuminated solution will be approximately

$$\epsilon^*=\epsilon_0^{T/S}+RT\ln\frac{[Fe^{3+}]}{[Semi]} \qquad ([Semi]>0.05\Delta). \quad (3)$$

On the other hand, if, under certain conditions, the reduced dye should consist of practically pure leukothionine, the electrode potential will be approximately

$$\epsilon^*=\epsilon_0^{S/L}+RT\ln\frac{[Fe^{3+}]}{[Leuko]} \qquad ([Leuko]=\Delta). \quad (4)$$

III. Discussion of the Results

With these theoretical concepts in mind, we will now examine the empirical relations between different independent variables and the photogalvanic potential. The task is complicated by the fact that the directly adjustable variables are the concentrations in the dark (and the light intensity), whereas the variables which determine the photogalvanic potential are the *photostationary* concentrations. (Paper I was devoted to the relations between these two sets of variables.) The problem of the photogalvanic effect is theoretically independent of the problem of the mechanism by which the photostationary state is maintained, but the two problems are inseparable in practice. By changing a certain concentration, e.g. $[Fe^{3+}]$, we affect the potential ϵ^* both directly (if it depends on the concentration of ferric ions) and indirectly, by changing the photostationary concentrations of other components.

Since, in our experiments $[Fe^{2+}]\gg[Thio]$, and

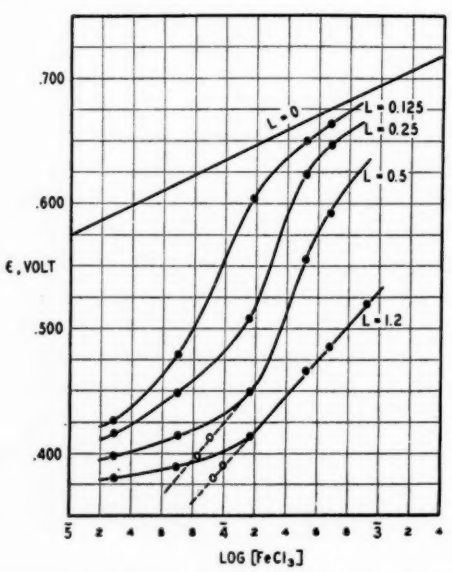

FIG. 2. ϵ and ϵ^* in relation to log $[Fe^{3+}]$ for four different intensities of illumination $[Thio]=4.5\times10^{-5}$ mole/l; $[Fe^{2+}]=5\times10^{-3}$ mole/l; $p_H=1.7$.

$[Fe^{3+}] \gg [Leuko]$, the "dark" potential ϵ is determined by the ratio $[Fe^{2+}] : [Fe^{3+}]$ in the reaction mixture, and practically independent of [Thio] and p_H. The "light" potential, ϵ^*, on the other hand, is essentially dependent on the concentration, Δ, of reduced thionine and on p_H. It is, therefore, convenient to consider primarily not the photogalvanic effect $\Delta\epsilon = \epsilon^* - \epsilon$, but the two potentials ϵ^* and ϵ separately; a small $|\Delta\epsilon|$, e.g., may be due either to a low dark potential ϵ or to a high light potential ϵ^*, and the two cases have nothing in common.

Effect of $[Fe^{2+}]$

Figure 1 shows how the bleaching increases with $[Fe^{2+}]$, to reach a constant value somewhere around 10^{-2} mole/l. (According to paper I, this curve expresses the dependence on Fe^{2+} of the quantum yield γ of bleaching.) Curve ϵ^* shows that the photogalvanic potential ceases to be affected by $[Fe^{2+}]$ as soon as the bleaching has become constant. In other words, $[Fe^{2+}]$ has *no direct effect* on ϵ^*. *The assumption that ferrous ions are practically ineffective as electron donors in presence of reduced thionine ions is thus confirmed.*

Since the dark potential ϵ decreases continuously with $[Fe^{2+}]$, $\Delta\epsilon$ reaches a maximum around $[Fe^{2+}] = 10^{-2}$ mole/l. Too much Fe^{2+} does not affect the bleaching, but can destroy the photogalvanic effect.

Effect of $[Fe^{3+}]$

Figure 2 shows that the light potential ϵ^* (shown for different illumination intensities $L = 0.125$ to 1.2) increases with $[Fe^{3+}]$ *faster* than the dark potential ϵ, $(L = 0)$, thus causing a rapid decrease in $|\Delta\epsilon|$. These curves include both a direct and an indirect effect of $[Fe^{3+}]$ on ϵ^*. The source of the indirect effect is obvious: it is the decrease in the extent of bleaching. According to Eqs. (6) and (7) in I, Δ is inversely proportional to $[Fe^{3+}]^*$. If we eliminate this indirect effect, by comparing results corresponding to equal values of Δ, but different values of $[Fe^{3+}]^*$ (this can be done by using measurements at different light intensities), we find that ferric ions have also a direct influence on ϵ^*. This agrees with our theoretical picture (comp. Eqs. (2), (3) and (4)). The exact form of the dependence of ϵ^* on $[Fe^{3+}]$ cannot be predicted theoretically, unless we know

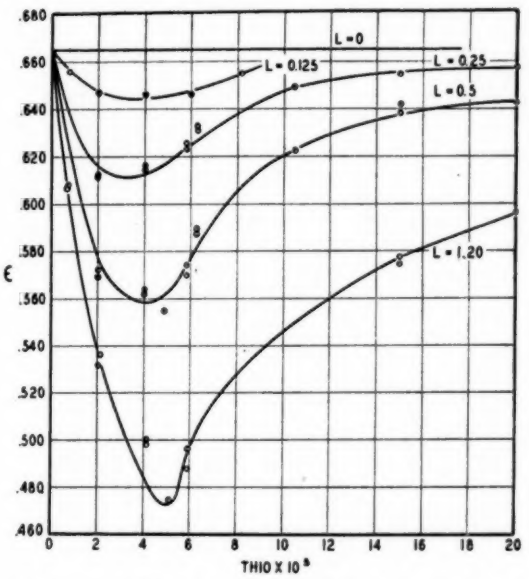

FIG. 3. ϵ and ϵ^* in relation to $[Thio]^*$ for four intensities of illumination. $[Fe^{2+}] = 4.5 \times 10^{-3}$ mole/l; $[Fe^{3+}] = 3 \times 10^{-4}$ mole/l; $p_H = 1.7$.

more about the parts played by semithionine and leukothionine, respectively. If we assume, e.g. that the semithionine ions are practically the only "electron donors," i.e., that formula (3) is correct, and that [Semi] is either equal to Δ, or at least proportional to Δ, and thus inversely proportional to $[Fe^{3+}]^*$, we find that ϵ^* must be a *linear* function of $[Fe^{3+}]$, with the slope $+2RT$. In other words, ϵ^* must increase with $[Fe^{3+}]$ *twice as rapidly as* ϵ. The lowest curve in Fig. 2 shows this behavior over a considerable range of $[Fe^{3+}]$-values. The other curves, however, are increasing much more steeply. This is a special example of a phenomenon which we will discuss later: In the region of strong effects (low $[Fe^{3+}]$, large Δ) the data can be represented by a single equation of the type (3); but in the region of larger $[Fe^{3+}]$-values and lower Δ-values, the photogalvanic effect decreases abruptly.

The deviation of the curves from linearity on the *left side* of Fig. 2 is more easily understandable. The abscissae in Fig. 2 are $[Fe^{3+}]$-values, i.e., the *initial* concentrations of ferric ions. When $[Fe^{3+}]$ is not much larger than [Thio], the ferric ions produced by bleaching begin to affect markedly $[Fe^{3+}]^*$, (which, on the *right* side of Fig. 2, is practically identical with $[Fe^{3+}]$). If we plot the potentials in Fig. 2 against the (calculated) values

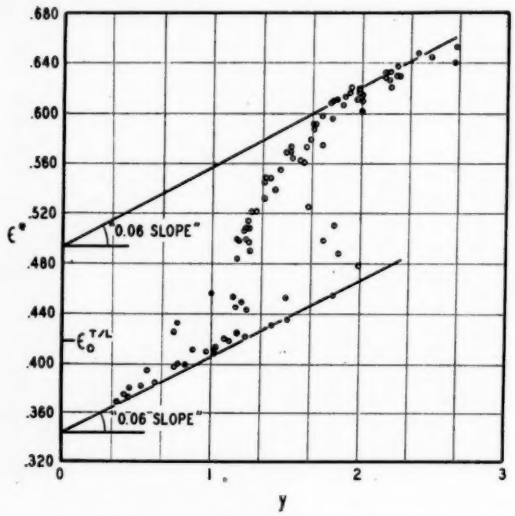

FIG. 4. ϵ^* in relation to y ($=\log [Fe^{3+}]/\Delta$); $p_H = 1.7$.

of $[Fe^{3+}]^*$ instead of against $[Fe^{3+}]$, the points are shifted in the way shown by the dotted continuation of the two lower curves in Fig. 2.

Because of this bending of the ϵ^*-curves at low $[Fe^{3+}]$-values, the photogalvanic effect $|\Delta\epsilon|$ reaches a maximum at a certain value of $[Fe^{3+}]$ and then decreases again. (Theoretically, it should even change its sign at extremely low Fe^{3+}-concentrations.) This is why we have stated at the beginning that it is not advisable to use extremely pure ferrous salt in the demonstration of the photogalvanic effect.

Sasaki and Nakamura[4] have suggested, in their investigation of nonequilibrium iodine-iron mixtures, that the potential of these systems is simply that of the iodine-iodide pair. In other words, they assumed both ferrous and ferric ions to be practically ineffective in the electrode process, in presence of iodine. In our case, the *ferrous* ions are inactive, but we are certainly not allowed to neglect the *ferric* ions. Having no access to the original paper, we cannot judge how exactly the data of Sasaki and Nakamura agree with their assumption. The similarity between the two cases is obvious, and we would expect the ferric ions to act as "electron acceptors" in iodine-iron mixtures as well, with an efficiency not much different from that of iodine.

Effect of [Thio]

Figure 3 shows that the largest photogalvanic effects are obtained at $[Thio] = 4$ to 5×10^{-5} mole/l. This effect of the thionine concentration on $\Delta\epsilon$ is closely parallel to its effect on the intensity of bleaching, as described in I, and explained there by the transition from relation (6) to relation (7), i.e., by the participation of thionine in the reoxidation of leukothionine. This shows that the influence of $[Thio]^*$ on ϵ^* is largely an *indirect* one. According to (2), we may expect also a *direct* influence of $[Thio]^*$ on ϵ^*. However, we have stated already in explaining the reduction of Eq. (2) to the simple forms (3) and (4), that our experiments are insufficient to identify the small term $[Thio]^*$ besides the usually much larger term $[Fe^{3+}]^*$; the question of a direct effect of $[Thio]^*$ on ϵ^* must be therefore left open.

Effect of Δ

The parallelism between $\Delta\epsilon$ and Δ in a given solution shows that reduced thionine ions are participating actively in the electron exchange between electrode and solution. Fig. 4 is a plot of ϵ^* against $y = \log([Fe^{3+}]/\Delta)$. If Eq. (3) or (4) were correct, the points should fall on a straight line with the slope 0.06. In fact, they lie on an S-shaped curve. However, at low y values (low $[Fe^{3+}]$, large Δ), the points define a "limiting" straight line, which has the expected slope 0.06 and cuts the ϵ-axis at 0.345 volt, a value significantly close to the normal potential $\epsilon_0^{T/S}$ (0.32–0.35 volt according to the estimate made in paper I). It thus looks as if Eq. (3) actually applies to *strongly bleached* thionine-iron solutions.

The sharp increase in ϵ^* at the higher y values, which we have already encountered, indicates that in this region (high $[Fe^{3+}]$-values, low Δ-values) another term in the denominator of (2) becomes important, besides the semithionine term. We cannot say definitely which one it is—the $[Fe^{2+}]$ term or the [Leuko] term. An argument in favor of the second assumption is that the ϵ^*-values in Fig. 4 apparently approach, at large y values, a *second limiting straight line*, also with the slope 0.06 and with an extrapolated intercept somewhere around 0.495 volt, i.e., close to the normal potential $\epsilon_0^{S/L}$, (estimated in I to 0.47–0.50 volt). However, this extrapolation is much wider than the first one. Furthermore, to accept the validity of Eq. (4) in the region of large y's, would mean to assume that practically

pure leukothionine is the product of reduction in this region, and that relatively more semithionine is formed when $[Fe^{3+}]$ is small and the bleaching strong. None of the kinetic mechanisms discussed in paper I seems to be able to account for such a relation. We found there that leukothionine is produced mainly by *dismutation* of semithionine. The rate of production of leukothionine is therefore proportional to $[\text{Semi}]^2$, and the ratio [Leuko]/[Semi] should *increase* and not decrease with the intensity of bleaching. The second alternative, the participation of Fe^{2+}-ions in the electron processes at the larger y values, also has its difficulties. We have estimated that a ratio $[Fe^{2+}] : \Delta = 2 \times 10^4$ must be reached in order that the $[Fe^{2+}]$-term in (2) should become noticeable beside the other two terms. Since the steep increase in ϵ^* happens under conditions when this ratio is of the order of only 10^2, ferrous ions can be made responsible for this increase only if we assume that the iron ions are *a priori* (i.e., apart from differences in the activation energy) at least 200 times more effective than the thionine ions in the electrode process. This assumption, although in itself not impossible, would bring us, however, into numerous difficulties. For instance, the limiting law for low y values should be not (3), but

$$\epsilon = \epsilon_0^{T/S} + RT \log \frac{[Fe^{3+}]}{[\text{Semi}]} + RT \log \frac{C_{Fe}}{C_{\text{Thio}}}. \quad (5)$$

where C_{Fe} and C_{Thio} are the "efficiency factors" of iron and thionine, respectively. With $C_{Fe}/C_{\text{Thio}} \geq 200$ the intercept in Fig. 4 must fall at least 0.140 volt *above* $\epsilon_0^{T/S}$, instead of coinciding with $\epsilon_0^{T/S}$, as we have found experimentally.

Thus, neither of the two suggested explanations of the steep increase in ϵ^* in the region of low Δ and high $[Fe^{3+}]$ is an entirely satisfactory one.

Effect of p_H

Figure 5 shows the strong influence of p_H on ϵ^*. We have discussed in paper I the effect of p_H on bleaching, and found Δ to decrease steadily with p_H (Fig. 5 in paper I). We would thus expect to find a corresponding *decrease* in the photogalvanic effect as well. Instead, Fig. 5 shows a very strong *decrease in* ϵ^* (and since ϵ remains constant, an *increase* in $|\Delta\epsilon|$), which continues up to $p_H = 2.5$. At p_H values above 2.5 the ϵ^* curves bend upwards, first those for weaker, then those for stronger illumination. However, in very strong light, no minimum of ϵ^* does occur below $p_H = 3$. In the region $p_H = 2.5$ and above the bleaching is no longer recognizable to the eye. This is the case which we had in mind when saying that the strongest photogalvanic effects can be observed in solutions which show almost no bleaching at all.

Since the increase in $\Delta\epsilon$ with p_H is not due to the change in Δ, it is natural to link it to the influence of p_H on the *normal potential* of thionine (that of iron is scarcely affected by p_H). The lowest straight line in Fig. 5 is the (mean) normal potential $\epsilon_0^{T/L}$ of thionine. (The single potentials $\epsilon_0^{T/S}$ and $\epsilon_0^{S/L}$ probably change with p_H in a similar way, see Fig. 1 in paper I.) The parallelism between the effect of p_H on $\epsilon_0^{T/L}$ and on ϵ^* is striking, and forms another confirmation of the fundamental correctness of assumptions underlying formulae (3) and (4).

In considering the upward bend of ϵ^* curves at the higher p_H's, the first suspicion is obviously that they may be due to the influence of decreasing Δ-values, which sooner or later ought to overbalance the effect of decreasing ϵ_0. However, the examination of the data shows that this explanation is insufficient. For instance, in the column relative to $p_H = 2.7$, the lowest point ($L = 1.2$) and the uppermost point ($L = \frac{1}{8}$) differ

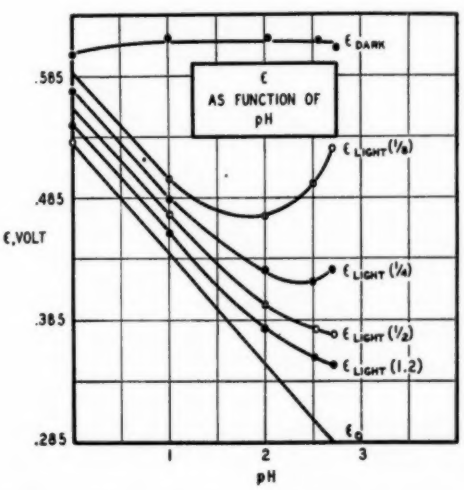

FIG. 5. ϵ and ϵ^* in relation to p_H. $[Fe^{2+}] = 2 \times 10^{-3}$ mole/l; $[\text{Thio}] = 5 \times 10^{-5}$ mole/l; $[Fe^{3+}] = 2.5 \times 10^{-5}$ mole/l.

by 0.18 volt. The ratios $[Fe^{3+}]/\Delta$ corresponding to these two points differ only by a factor 5. This could account for a shift of the upper curve by $0.06 \log 5 \backsimeq 0.04$ volt, but not more. Apparently, the divergence of the ϵ^*-curves is due mainly to the same effect which we have encountered (and not satisfactorily explained) already in discussing Figs. 2 and 4—namely, to the unexpectedly steep increase in ϵ^* which occurs when the bleaching becomes weak.

Effect of light intensity

From our general notion that the photogalvanic potential is the electrode potential of a nonequilibrated oxidation-reduction system, it follows that light intensity affects ϵ^* in an *indirect* way, by the intermediate of Δ, the extent of bleaching. In other words, illumination determines the composition of the solution; and the composition determines the potential. The effect of light intensity on Δ was discussed in I; Δ is usually proportional to $N_{h\nu}$ (the *intensity of absorption*, which is, because of the bleaching, not exactly proportional to the *intensity of illumination* L); sometimes to $N_{h\nu}^z$ with z up to 1.6. This relation should make ϵ^* a *linear function of* $\log N_{h\nu}$ (assuming that $[Fe^{3+}] \ll [\text{Thio}]$, so that $[Fe^{3+}]$ is practically unchanged by bleaching). No simple exact relation can be expected, however, between ϵ^* and $\log L$. Furthermore, the linear dependence of ϵ^* on the logarithm of absorption intensity can be only expected in the region where the constant term (e.g. ${\epsilon_0}^{T/S}$ in (3)) does not change. Sometimes, however, the change in light intensity causes a transition from the "high y" type of photogalvanic effect to the "low y" type. This is plainly shown by Fig. 5. On the left side, the points in each vertical column are approximately equidistant (the light intensities corresponding to the five curves increase approximately by powers of 2); on the right side, however, the change in L from $\frac{1}{8}$ to $\frac{1}{4}$ has a much stronger effect on ϵ^* than the change from $\frac{1}{4}$ to $\frac{1}{2}$, or that from $\frac{1}{2}$ to 1.2. Here, the upper curves have entered into the "low y" region, whereas the lower curves are still in the "high y" region.

The relation between photogalvanic effect and light intensity is thus a complicated one, and cannot be expressed by a simple formula. In a very general form, we can say that concentrations are algebraic functions of light intensity, whereas the potentials are logarithmic functions of concentrations.

SUMMARY

The reversible redox system thionine $\underset{\text{dark}}{\overset{\text{light}}{\rightleftharpoons}}$ reduced thionine $+ Fe^{III}$ has a high photogalvanic sensitivity. The electrode potential of the illuminated solution ϵ^*, is established after a few seconds of illumination. It is always lower than the "dark" potential ϵ; the photogalvanic effect $\Delta\epsilon = \epsilon^* - \epsilon$ may reach -250 mv. Measurements have been made of ϵ^* in relation to the concentrations $[Fe^{2+}]$, $[Fe^{3+}]$, [Thio] and Δ(=[Leukothionine]+[Semithionine]). ϵ^* does not depend on $[Fe^{2+}]$, but depends strongly on $[Fe^{3+}]$ and Δ; a possible dependence on [Thio] is obscured by the relation $[Fe^{3+}] \gg [\text{Thio}]$ prevailing in most of our experiments. Whereas the reversible bleaching decreases steadily with increasing p_H, $|\Delta\epsilon|$ increases at first with p_H, and the strongest photogalvanic effects are obtained in solutions with $p_H \backsimeq 3$, which show almost no bleaching.

All these facts are in qualitative agreement with a formula derived under very simplified assumptions.

$$\epsilon^* = {\epsilon_0}^{\text{Thio}} + RT \ln \frac{[Fe^{3+}](+\text{Thio})}{\Delta} = {\epsilon_0}^{\text{Thio}} + 0.06y,$$

where ${\epsilon_0}^{\text{Thio}}$ is the normal potential of thionine. Extrapolation of empirical data to $y=0$ gives for ${\epsilon_0}^{\text{Thio}}$ the value 0.35 volt, which coincides with the probable value of ${\epsilon_0}^{T/S}$ (normal potential of the first reduction step, thionine→semithionine). The dependence of ϵ^* on p_H is closely parallel to the known effect of p_H on ${\epsilon_0}^{\text{Thio}}$.

The formula, which apparently gives a correct limiting relationship for low y values, is not obeyed at the higher values of y (i.e., low Δ, high $[Fe^{3+}]$), where ϵ^* increases with y much steeper than linearly. This indicates that either the leukothionine ions or the ferrous ions begin to participate in the supply of electrons to the electrode, which was previously monopolized by the semithionine ions.

A Short Table of Quantities Used in Computations for Cubic Space Lattices

L. W. McKeehan
Sloane Physics Laboratory, Yale University, New Haven, Connecticut

(Received June 4, 1940)

EWALD'S use of three-argument theta-functions[1] in computations respecting crystal space lattices involves finding a series of functions, related to the error function and its derivatives. The argument in each case is the distance between one selected lattice point and others in the immediate neighborhood. The functions of interest are of the following form[2]

$$g_m(\alpha)=\alpha^{-2}[(2m-1)g_{m-1}(\alpha)+2^m\pi^{-\frac{1}{2}}\exp(-\alpha^2)],$$

wherein α is a number proportional to the distance between the lattice points considered,

[1] P. P. Ewald, Ann. d. Physik [4] **64**, 253–287 (1921).

[2] The notation is that which is explained in my paper, "Magnetic Dipole Fields in Unstrained Cubic Crystals," Phys. Rev. [2] **43**, 913–923 (1933), esp. p. 919.

TABLE I, PART 1. $\alpha^2=0.25$ *to* $\alpha^2=12.00$, *interval 0.25.*

α^2	$L(\alpha)$	$\alpha g_0(\alpha)$	$g_1(\alpha)$	$\alpha^2 g_2(\alpha)$	$\alpha^4 g_3(\alpha)$	$\alpha^6 g_4(\alpha)$	$\alpha^8 g_5(\alpha)$
0.25	0.54564136	0.47950012	7.3511313	23.810959	119.93358	839.97444	7559.9896
0.50	0.65567954	0.31731051	2.2662828	8.1676415	42.207000	296.81780	2672.7290
0.75	0.71708792	0.22067136	1.0504239	4.2172888	22.685470	161.19683	1454.3693
1.00	0.75787216	0.15729921	0.57240671	2.5474351	14.397605	104.10410	943.57861
1.25	0.78743907	0.11384630	0.34009062	1.6668439	9.9506499	73.695625	673.36331
1.50	0.81006948	0.083264520	0.21317375	1.1430721	7.2260130	55.114048	509.62231
1.75	0.82805111	0.061368829	0.13855621	0.80783443	5.4117525	42.686298	400.99079
2.00	0.84273846	0.045500264	0.092441529	0.58274361	4.1353942	33.834464	324.05699
2.25	0.85499296	0.033894853	0.062900826	0.42656306	3.2031879	27.238992	266.82597
2.50	0.86539259	0.025347319	0.043461622	0.31563087	2.5043844	22.161841	222.61232
2.75	0.87434151	0.019016473	0.030400811	0.23547217	1.9708444	18.160070	187.44351
3.00	0.88213192	0.014305878	0.021479398	0.17679557	1.5581222	14.951721	158.83468
3.25	0.88898094	0.010787449	0.015303326	0.13341399	1.2358461	12.347967	135.16250
3.50	0.89505356	0.0081509716	0.010980279	0.10108903	0.98248254	10.216639	115.32459
3.75	0.90047768	0.0061698994	0.0079261483	0.076852313	0.78231558	8.4616141	98.545065
4.00	0.90535410	0.0046777350	0.0057514632	0.058588360	0.62361356	7.0106691	84.259015
4.25	0.90976341	0.0035514649	0.0041925124	0.044768466	0.49746522	5.8080511	72.041715
4.50	0.91377090	0.0026997961	0.0030684125	0.034275558	0.39701067	4.8097707	61.564200
4.75	0.91743005	0.0020547189	0.0022537184	0.026285941	0.31691516	3.9805180	52.564725
5.00	0.92078514	0.0015654022	0.0016606057	0.020187735	0.25299785	3.2915768	44.830109
5.25	0.92387315	0.0011937454	0.0012270826	0.015523629	0.20196314	2.7193645	38.183317
5.50	0.92672521	0.0009111189	0.0009090782	0.011950090	0.16120186	2.2443785	32.475028
5.75	0.92936774	0.0006959619	0.0006750643	0.009207960	0.12864162	1.8504123	27.577802
6.00	0.93182333	0.0005320055	0.0005023604	0.007101026	0.10263247	1.5239553	23.381934
6.25	0.93411138	0.0004069520	0.0003745704	0.005480280	0.08185850	1.2537234	19.792433
6.50	0.93624868	0.0003114910	0.0002797887	0.004232265	0.06526901	1.0302830	16.726746
6.75	0.93824982	0.0002385635	0.0002093362	0.003270401	0.05202430	0.8457461	14.112991
7.00	0.94012756	0.0001828106	0.0001568635	0.002528488	0.04145300	0.6935189	11.888540
7.25	0.94189308	0.0001401595	0.0001177103	0.001955823	0.03301815	0.5680930	9.998844
7.50	0.94355625	0.0001075112	0.0000884462	0.001513516	0.02629025	0.4648717	8.396446
7.75	0.94512582	0.0000825053	0.0000665391	0.001171699	0.02092576	0.3800230	7.040118
8.00	0.94660953	0.0000633425	0.0000501155	0.000907405	0.01664995	0.3103565	5.894119
8.25	0.94801431	0.0000486501	0.0000377862	0.000702956	0.01324314	0.2532199	4.927524
8.50	0.94934634	0.0000373798	0.0000285189	0.000544736	0.01052972	0.2064108	4.113643
8.75	0.95061119	0.0000287308	0.0000215448	0.000422243	0.00836937	0.1681033	3.429490
9.00	0.95181384	0.0000220905	0.0000162907	0.000327378	0.00665000	0.1367860	2.855321
9.25	0.95295881	0.0000169904	0.0000123283	0.000253886	0.00528209	0.1112089	2.374215
9.50	0.95405018	0.0000130718	0.0000093371	0.000196934	0.00419420	0.0903404	1.971703
9.75	0.95509166	0.0000100600	0.0000070769	0.000152788	0.00332930	0.0733296	1.635445
10.00	0.95608661	0.0000077442	0.0000053677	0.000118560	0.00264193	0.0594762	1.354939
10.25	0.95703811	0.0000059631	0.0000040741	0.000092016	0.00209584	0.0482040	1.121266
10.50	0.95794895	0.0000045928	0.0000030942	0.000071426	0.00166213	0.0390400	0.926868
10.75	0.95882171	0.0000035383	0.0000023514	0.000055451	0.00131779	0.0315961	0.765354
11.00	0.95965874	0.0000027265	0.0000017880	0.000043056	0.00104450	0.0255543	0.631330
11.25	0.96046220	0.0000021014	0.0000013603	0.000033435	0.00082765	0.0206542	0.520252
11.50	0.96123408	0.0000016200	0.0000010355	0.000025968	0.00065565	0.0166831	0.428300
11.75	0.96197622	0.0000012491	0.0000007886	0.000020170	0.00051925	0.0134672	0.352267
12.00	0.96269032	0.0000009634	0.0000006009	0.000015669	0.00041113	0.0108647	0.289466

TABLE I, PART 2. $\alpha^2 = 12.0$ *to* $\alpha^2 = 30.0$, *interval 0.5.*

α^2	$L(\alpha)$	$10^{10}\alpha g_0(\alpha)$	$10^{10}g_1(\alpha)$	$10^9\alpha^2 g_2(\alpha)$	$10^8\alpha^4 g_3(\alpha)$	$10^7\alpha^6 g_4(\alpha)$	$10^6\alpha^8 g_5(\alpha)$
12.0	0.96269032	9634	6009	15669	41113	108647	289466
12.5	0.96404052	5733	3494	9458	25755	70592	194941
13.0	0.96529593	3414	2035	5711	16118	45766	130845
13.5	0.96646622	2035	1187	3450	10079	29610	87546
14.0	0.96755980	1213	693	2085	6297	19120	58402
14.5	0.96858401	724	406	1260	3931	12324	38851
15.0	0.96954527	432	238	762	2452	7929	25776
15.5	0.97044922	258	139	461	1528	5094	17058
16.0	0.97130086	154	82	278	952	3267	11262
16.5	0.97210463	92	48	168	593	2092	7419
17.0	0.97286445	55	28	102	369	1338	4876
17.5	0.97358384	34	17	62	229	855	3199
18.0	0.97426597	20	10	37	142	545	2094
18.5	0.97491365	12	6	23	88	347	1369
19.0	0.97552944	7	3	14	55	221	893
19.5	0.97611564	4	2	8	34	140	581
20.0	0.97667434	3	1	5	21	89	378
20.5	0.97720744	2	1	3	13	57	245
21.0	0.97771667	1	0	2	8	36	159
21.5	0.97820358	1		1	5	23	103
22.0	0.97866962	0		1	3	14	67
22.5	0.97911611			0	2	9	43
23.0	0.97954426				1	6	28
23.5	0.97995517				1	4	18
24.0	0.98034986				0	2	11
24.5	0.98072928					1	7
25.0	0.98109431					1	5
25.5	0.98144574					1	3
26.0	0.98178432					0	2
26.5	0.98211074						1
27.0	0.98242566						1
27.5	0.98272966						1
28.0	0.98302331						0
28.5	0.98330713						
29.0	0.98358160						
29.5	0.98384718						
30.0	0.98410429						

m is an integer greater than zero, and $g_0(\alpha) = \alpha^{-1}[1 - 2\pi^{-\frac{1}{2}}\int_0^\alpha \exp(-\beta^2)d\beta]$. More precisely, the quantities of principal interest are $\alpha^n g_m(\alpha)$ where $n = 2m-2$ in one series, $n = 2m-4$ in another, and $n = 2m-6$ in still another. These may very roughly be identified as related to monopoles, dipoles and quadrupoles in undistorted lattices.

In the case of cubic lattices, and even in others when particular axial ratios are selected, the square of the argument α may always be made an integer, or an integer multiplied by an arbitrary factor. The choice of an integer for this factor, or of the simple fractions $\frac{1}{2}$ or $\frac{1}{4}$, is generally permissible and greatly shortens the work, since it reduces the number of functions g_m which need to be computed. In the course of a number of calculations for different purposes a convenient set of $\alpha^n g_m(\alpha)$ have in this way been collected and are here presented (Table I) for more general use. An auxiliary quantity

$$L(\alpha) = \alpha^2 g_0(\alpha) e^{\alpha^2} \pi^{-\frac{1}{2}},$$

which was found first in each computation,[3] is also given. All tabulated quantities have been carefully checked and are thought to be correct within one unit in the last figure given.

[3] For a discussion of this quantity and its computation see James Burgess, Royal Society of Edinburgh, Trans. **39**, 257–321 (1898). Values of $L(\alpha)$ are there tabulated for $\alpha = 3$ to $\alpha = 5$, by tenths in α, and for $\alpha = 5.5$ and $\alpha = 6$.

LETTERS TO THE EDITOR

This section will accept reports of new work, provided these are terse and contain few figures, and especially few halftone cuts. The Editorial Board will not hold itself responsible for opinions expressed by the correspondents. Contributions to this section should not exceed 600 words in length and must reach the office of the Managing Editor not later than the 15th of the month preceding that of the issue in which the letter is to appear. No proof will be sent to the authors. The usual publication charge ($3.00 per page) will not be made and no reprints will be furnished free.

Note on the Solution of Secular Equations

It is frequently necessary in applications of the quantum mechanics to find one or more roots of a secular equation

$$D_N(\lambda) = |a_{ij} - b_{ij}\lambda| = 0,$$
$$a_{ij} = a_{ji}, \quad b_{ij} = b_{ji}; \quad i, j = 1, 2, 3 \cdots N. \quad (1)$$

In certain problems $b_{ij}=0$ for $i \neq j$, and in general it is possible to reduce Eq. (1) to this form by addition and subtraction of rows and columns.

Three of the many methods which may be used for solving Eq. (1) are: (i) The method of successive approximation,[1] (ii) the matrix method,[2] (iii) determine the polynomial $P_N(\lambda)$ equivalent to the determinant $D_N(\lambda)$ and find its zeros by any of the classical methods or by iteration.[3,4]

It is the purpose of this note to describe a convenient method for carrying through the polynomial technique of solution.[5] Suppose the determinant $D_N(\lambda)$ is computed for $(N+1)$ equally spaced numerical values of λ, $\lambda_r = \lambda_0 + rh$, $r = 0, 1, 2 \cdots N$. From these a table of differences for the determinantal function may be constructed, and by use of Newton's interpolation formula the polynomial $P_N(\lambda)$ equivalent to the determinantal function $D_N(\lambda)$ may be determined. In order to pass from the Newtonian form

$$P_N(\lambda_0 + nh) = D_N(\lambda_0) + \sum_{s=1}^{N} \Delta^s D_N(\lambda_0) \binom{n}{s} \quad (2)$$

to the power series form

$$R_N(\lambda - \lambda_0) = \sum_{t=0}^{N} p_t (\lambda - \lambda_0)^t = \sum_{t=0}^{N} p_t n^t h^t \quad (3)$$

it is convenient to use the quantities $a_i(s)$ where

$$(\alpha_s^n) = s! \binom{n}{s} = \sum_{i=1}^{s} a_i(s) n^i.$$

The $a_i(s)/s!$ may be computed once for all from the recursion relation $a_i(s+1) = a_{i-1}(s) - s a_i(s)$, and the resulting table checked by the identities

$$\sum_{t=1}^{s} \left| \frac{a_i(s)}{s!} \right| = 1, \quad \sum_{t=1}^{s} \frac{a_i(s)}{s!} = 0, \quad a_s(s) = 1,$$
$$a_{s-1}(s) = \frac{s(1-s)}{2}, \quad a_1(s+1) = (-)^s s! \text{ etc.}, \quad s \geq 1.$$

With these definitions the formula for p_t is

$$p_t = h^{-t} \sum_{s=t}^{N} \frac{\Delta^s D_N(\lambda_0) a_t(s)}{s!}, \quad t \geq 1, \quad p_0 = D_N(\lambda_0). \quad (4)$$

If the determinantal function is expanded algebraically into the polynomial form directly, the calculation of the coefficients of the powers of λ is found to be cumbersome, being unadaptable to machine calculation, subject to error and difficult to check. In the case of the difference technique described, the evaluation of the necessary symmetrical determinants, the formation of the difference table and the calculations of the sums of products from Eq. (4) are all well suited to machine computation. Furthermore, it is possible to check the evaluation of the determinants *independently* by computing more than $(N+1)$ values of $D_N(\lambda)$ and forming the $(N+1)$st differences which should vanish identically.

The solution of the polynomial equation found by the self-correcting process of iteration automatically gives roots in their correct order as to magnitude, a point involving some care in the successive approximation method. Likewise, the polynomial method is more straightforward than the matrix method in case there are nondiagonal terms in λ, for but little more labor is involved in computing determinants with off-diagonal λ terms than determinants with no such terms.

A graphic picture of the behavior of the determinantal function is supplied by plotting the successive values of $D_N(\lambda)$ which are computed in the difference method, thus giving at once a semi-quantitative idea of the location of the roots (all real).

BRUCE L. HICKS

Department of Physics,
University of Wyoming,
Laramie, Wyoming,
May 24, 1940.

[1] James and Coolidge, J. Chem. Phys. **1**, 825 (1933); J. Sherman, unpublished paper.
[2] Duncan and Collar, Phil. Mag. **17**, 865 (1934). See also *Elementary Matrices* by Frazer, Duncan and Collar (Macmillan, 1938).
[3] A. C. Aitken, Proc. Roy. Soc. Edinburgh **46**, 289 (1926).
[4] T. C. Fry, private communication.
[5] This technique was described briefly in the author's thesis, California Institute of Technology, 1939.

The Directional Catalytic Activity of a Single Crystal of Copper

Results recently reported[1] showed that the rate of oxidation of a single crystal of copper when heated in air at a reduced pressure varied with the crystal plane along which the surface was prepared. The oxygen caused a rearrangement of the metal atoms in the surface as shown by the development of microscopic facets parallel to certain crystal planes.

In order to study the influence of the crystal plane on the catalytic activity of a metal, a single crystal of copper in the form of a sphere and prepared by the method previously described[2] was heated in a glass tube through which a 3 : 1 (by volume) mixture of hydrogen and oxygen was passed at a rate of about 50 cc per minute. A small furnace was placed over the tube and the temperature of the air adjacent to the tube was measured with a thermometer. At about 200°C a slight pinkish tint appeared on the surface apparently due to oxidation. At about 260°C a very striking pattern appeared consisting of green and red colored areas. At about 300°C the pattern became quite irregular and soon disappeared apparently due to the reduction of the oxide film. At about 360°C the metal atoms in the surface seemed to rearrange themselves to produce a definite pattern composed of both smooth and roughened regions, and simultaneously the rate of the catalytic reaction became appreciable as shown by the condensation of water in the exit tube. The temperature was raised to 540°C over a period of an hour when the crystal was cooled, removed from the glass tube, and examined. Smooth shiny circular areas of about 4 mm in diameter and elliptical ones, 1×4 mm, remained at the (111) and (110) pole positions, respectively. The remainder of the surface had a frosty appearance apparently due to a slight roughening produced by the development of facets parallel to the (111) planes. When a beam of light was directed normally at a (111) pole position, a striking reflection was obtained from the surface in the octant located at this (111) pole. Under the microscope a large part of the roughened area showed definite step-like formations. This experiment has been repeated several times, and results similar to those described above have been obtained. A more detailed account of the experiment will be given later.

A freshly polished single crystal of copper was also heated to 450°C in a 1 : 1 mixture of ethylene and hydrogen. No appreciable reaction took place after a half-hour and no pattern or preferred crystal planes were developed. Heating the crystal to about 400°C in ethylene alone produced a highly colored pattern but produced no appreciable preferred facets. From these results the following conclusions have been drawn:

1. A catalytic reaction between hydrogen and oxygen may be initiated by a massive single crystal of copper whose surface is microscopically plane.

2. The reaction between hydrogen and oxygen renders the surface sufficiently mobile to develop certain crystal facets. In order to produce this rearrangement, the effective temperature at the surface of the metal where the reaction is taking place must be considerably above the measured temperature of the reaction vessel.

3. Since the catalytic reaction between hydrogen and oxygen becomes appreciable at the same temperature at which the development of the facets takes place, this experiment suggests that these facets may be related to the positions of enhanced catalytic activity for this particular reaction.

4. In the one case investigated where no facets were developed, i.e., in the heating of the crystal in ethylene and hydrogen, no appreciable reaction took place.

ALLAN T. GWATHMEY
ARTHUR F. BENTON

School of Chemistry,
University of Virginia,
Charlottesville, Virginia,
May 28, 1940.

[1] A. T. Gwathmey and A. F. Benton, J. Chem. Phys. **8**, 431 (1940).
[2] A. T. Gwathmey and A. F. Benton, J. Phys. Chem. **44**, 35 (1940). Trans. Electrochem. Soc., in press.